DIFFERENTIAL GENE EXPRESSION OF MURINE BLASTOCYST STAGE EMBRYOS AND MURINE EMBRYONIC STEM CELLS

By

SARAH E. MYER

Bachelor of Arts in Biology
Oral Roberts University
Tulsa, Oklahoma
1994

Masters of Education
Oral Roberts University
Tulsa, Oklahoma
1995

Submitted to the Faculty of the
Graduate College of the
Oklahoma State University
in partial fulfillment of
the requirements for
the Degree of
DOCTOR OF PHILOSOPHY
December, 2007

DIFFERENTIAL GENE EXPRESSION OF MURINE

BLASTOCYST STAGE EMBRYOS AND MURINE

EMBRYONIC STEM CELLS

Dissertation Approved:

Lee F. Rickords, Ph.D.
Dissertation Adviser

Robert W. Allen, Ph.D.

Kirby L. Jarolim, Ph.D.

Jerry R. Malayer, Ph.D.

A. Gordon Emslie, Ph.D.
Dean of the Graduate College

ACKNOWLEDGEMENTS

In the completion of a doctorate degree, there are invariable many people and organizations who deserve special thanks for their support and assistance. Thank you to Dr. Lee Rickords for the opportunity to work within your laboratory, for the willingness to work with a non-traditional research student, and for assistance over numerous years of graduate study. Thank you to my graduate committee, Dr. Rob Allen, Dr. Kirby Jarolim, and Dr. Jerry Malayer, for your assistance thoughout the research process and your thoughtful input into our study. Thank you to Dr. Ute Hochgeschwender at the Oklahoma Medical Research Foundation (OMRF) for the generous donation of the stem cell and feeder cell samples not only once, but twice.

Several individuals deserve special thanks for invaluable research support. I am so thankful to Crystal Shults for her willingness to answer my numerous lab questions, for sharing her research wisdom, and for numerous years of laughters, tears, and friendship! Diana Spencer, you have been a special friend as we have together learned research methods, as you got me started in real time PCR, and as we experienced the frustrations of lab closures. Thank you. I am also thankful to Tami Ross Sartashtour for her assistance in lab protocols and use of equipment in Dr. Blewett's lab.

Numerous additional faculty and staff members have my sincere gratitude for assistance throughout the years. Thank you Dr. David John and Dr. Stan Conrad for research support, especially in the tough time after the lab closed and funds were short.

Thank you to Dr. Earl Blewett, Dr. Greg Sawyer, and Dr. Rashmi Kaul for making your research space, equipment, and lab technicians available for the completion of this research project. And an additional thank you to Dr. Blewett and Dr. Jarolim who both assisted me in an advisor function when needed over the past several years. Thank you also to the administrative assistants who helped me with numerous issues. A special thank you also belongs to Dr. Julie Marino who assisted me with review and analysis of the real time data. Your assistance and encouragement were very appreciated.

Throughout my time as a graduate student, I have also taught as an Instructor in the Biology Department at Oral Roberts University. This would not have been possible without the numerous supportive and giving individuals there who helped in everyway possible. Thank you for switching class sections with me, for praying for me, for encouraging me continually, and for every other means of support!

My family has been an invaluable part of this process. Thank you for your understanding for all of the late birthday cards, Christmas presents, and phone calls! Thank you, mom and dad, for your support and encouragement, for giving me a love of learning and for teaching me that I could do anything I set my mind to through Christ. And thank you, Ross and Caroline, for your encouragement and all of the times you helped with the girls or the house!

I am also thankful to my two beautiful daughters, Hannah and Maggie. While at 28 and 11 months, you are too young to be aware of this momentous degree completion, your smiles, joy, and cuddles have been a great source of joy and motivation. You too have had to endure long hours at school while I pushed towards completion and it is with great anticipation of the time we will share together that I rejoice about being completed.

I love you and hope I will always make you proud.

Most of all, I have an immense gratitude for my husband, Brian Myer. For the almost 15 years of marriage, I've been in school for one degree or another for all but 4 years and yet your support and encouragement never waiver. Thank you for believing in me, for being willing to endure the sacrifices that this has entailed, and for always being a rock of encouragement. I could not have asked God for a better best friend and husband. I look forward to moving on into a new phase of life together with you and the girls.

Beyond those on this earth, I am also immensely thankful to my Father God for leading me though the process (Ps. 35:3-5) and being the rock on whom I stand.

TABLE OF CONTENTS

Chapter Page

Chapter Page

LIST OF TABLES

LIST OF FIGURES

Figure Page

Chapter II

Chapter IV

Figure Page

Figure Page

ABBREVIATIONS

AFS	Amniotic fluid-derived stem cells
AIF	Apoptosis inducing factor
ALBP	Adipocyte lipid-binding protein
ANOVA	Analysis of variance
ANT	Adenine nucleotide translocase/translocator
ASK1	Apoptosis signal regulated kinase 1
BAD	Bcl2-3 antagonist causing cell death protein or BCL-2/X_L associated death promoter
Bcl2	B-cell CLL/lymphoma 2 protein
bFGF	Basic fibroblast growth factor
Bim	BCL-2 interacting mediator of cell death
BLAST	Basic local alignment and search tool
BP	Base pair
BSA	Bovine serum albumin
BWW	Biggers, Whitten, Whittingham media
c-Abl	Abelson leukemia oncogene
CBP	Cruciform binding protein
Cdc2	Cell division cycle 2; also known as Cdk1
Cdk	Cyclin-dependent kinase
cDNA	Complementary deoxyribonucleic acid
CDS primer	SMART cDNA synthesis primer
CFTR	Cystic fibrosis transmembrane conductance regulator
Chk1	Checkpoint 1 kinase
CKIα	Casein kinase Iα
c-Myc	Myelocytomatosis oncogene
Cys-SOH	Cysteine sulfenic acid
DIA	Differentiation-inhibiting factor
DRF	Differentiation-retarding factor
EC cells	Embryonal carcinoma cells
EDTA	Ethylenediaminetetraacetic acid
EG cells	Embryonic germ cells
ERK	Extracellular signal-regulated kinase
ES cells	Embryonic stem cells
EST	Expressed sequence tag
FACS	Fluorescence-activated cell sorting
FAT	Fatty acid transporter
FBS	Fetal bovine serum

FGF2	Fibroblast growth factor 2
Fkhr	Forkhead in rhabdomyosarcoma transcription factor
Foxo	Forkhead box, subgroup O protein
G_0	Resting phase of the cell cycle
G_1	Gap 1 phase of the cell cycle
G3PDH	Glyceraldehyde-3-phosphate dehydrogenase
GAPDH	Glyceraldehyde-3-phosphate dehydrogenase
GDNF	Glial cell line-derived neurotrophic factor
gp130	Glycoprotein 130
hCG	Human chorionic gonadotrophin
hES	Human embryonic stem cells
HNF-4	Hepatocyte nuclear factor-4
H_2O_2	Hydrogen peroxide
ICM	Inner cell mass
IP	Intellectual property
IU	International units
IVF	*In vitro* fertilization
JNK	c-Jun N-terminal kinase
kDa	Kilodalton
KB	Kilobase pairs
LIF	Leukemia inhibitory factor
MEF	Murine embryonic fibroblast
MEK	Mitogen activated protein kinase kinase
mRNA	Messenger ribonucleic acid
MST2	Mammalian sterile 20-like kinase 2
MPT	Mitochondrial membrane permeability transition
NCBI	National Center for Biotechnology Information
NIA	National Institute on Aging
Nrf2	Nuclear factor (erythroid-derived-2)-related factor
Oct-4	Octamer-binding transcription factor 4
OMM	Outer mitochondrial membrane
ORCC	Outwardly rectifying chloride channel
Pax-6	Paired box gene 6
PBS	Phosphate buffered saline
PCR	Polymerase chain reaction
PGC	Primordial germ cells
Pka	Protein kinase A
PMSG	Pregnant mare serum gonadotrophin
POU	Pit-Oct-Unc - transcription factor family
Prdx1	Peroxiredoxin 1
Prdxs	Peroxiredoxin gene family
PTP	Permeability transition pore
PTP	Protein tyrosine phosphatases
ROS	Reactive oxygen species
RT	Reverse transcriptase
S phase	Synthesis phase of the cell cycle

Sdk1	Sphingosine-dependent kinase
SNP	Single nucleotide polymorphism
S.O.C. medium	Super Optimal Catabolite Repression Broth
SR	Sarcoplasmic reticulum
SSEA	Stage-specific embryonic antigen
SSH	Suppression subtraction hybridization
STAT-3	Transcription factor 3
TRX	Thioredoxin
Vdac	Voltage-dependent anion channel protein family
Vdac3	Voltage-dependent anion channel 3
WARF	Wisconsin Alumni Research Foundation
Yap	Yes-associated transcriptional activator protein
Ywhaz	Tyrosine 3-monooxygenase/tryptophan - 5-monooxygenase activation protein, zeta peptide or 14-3-3 zeta

CHAPTER I

INTRODUCTION

While there have been many notable research discoveries throughout history, few have gained the level of attention of stem cells. In the time since the first isolation of mouse stem cell cultures in 1981, human and mouse stem cell research has grown exponentially and has captured the interest of the public with promises of potential cures to medical conditions such as paralysis and Alzheimer's disease.

A review of stem cell research demonstrates the complexity of the subject as multiple types of stem cells have been described with varying characteristics and research potential. Stem cell types include embryonic stem cells, adult stem cells, embryonic germ cells, embryonic carcinoma stem cells, umbilical cord stem cells, and amniotic fluid-derived stem cells. In general, stem cells are undifferentiated cells that have the ability for self-renewal and the ability to form one or more specialized cell types. While multiple types of stem cells have been studied, the embryonic stem cell is believed to have the greatest potential for research and medical applications due mostly to its ability to form numerous cell types. Research with human embryonic stem cells has faced limitations however due to ethical concerns over the methods used for their generation.

While a reflection on the stem cell literature shows a great amount of work done to characterize the various types of stem cells and their potential, much less work has

been done to characterize the molecular transition that occurs in the formation of embryonic stem cells from blastocyst stage embryos. One project analyzed gene expression levels as determined by expressed sequence tag (EST) frequencies common to various cellular and developmental stages (pre-implantation embryos, pluripotent stem cells, adult stem cells, etc.), however, it failed to directly measure gene expression levels or to characterize the blastocyst to stem cell transition [1]. Having a greater understanding of this molecular transition will provide a more complete picture of general development processes, of embryonic stem cell characteristics, and of the requirements for embryonic stem cell development. Long term, having a greater understanding of this process may lead to the ability to produce better alternative stem cell sources.

Several techniques are available for characterizing variations in gene expression including microarrays and Northern Blots, however, with limited starting material and a lack of information about which genes would be significantly altered, the best technique for this project was suppression subtraction hybridization (SSH). SSH allows the researcher to compare small amounts of transcripts from two sources and the process combines normalization and subtraction. mRNA is used to produce cDNA for both sources which are subsequently hybridized in order to isolate unique unhybridized cDNA samples for analysis.

After unique transcripts are amplified from both sources, the transcripts are cloned, sequenced, and identified through databank comparison. Differential expression of genes identified through SSH should be confirmed and ultimately the differential expression can be quantified through real time polymerase chain reaction (PCR).

In this study, four SSH comparisons were performed using CD1 mice and 129SvEv murine embryonic stem cells (ESC) - blastocyst vs. blastocyst, trophectoderm vs. blastocyst, 129 SvEv ESC vs. fibroblast feeder cells, and blastocyst vs. 129 SvEv ESC – with the first three comparisons serving as control comparisons and the last comparison being the primary comparison of interest. From these four comparisons, sequences were obtained for 33 clones of uniquely expressed transcripts and identified through the National Center for Biotechnology Information (NCBI) Basic Local Alignment and Search Tool (BLAST). From the 33 unique clones identified through SSH, 10 had strong homologies to ribosomal subunits while 23 had either gene specific homologies or else were unknown.

The second objective was to quantify the rate of expression of three selected transcripts through real time PCR in blastocysts, 129SvEv ESC, C57BL/6 ESC, and fibroblast feeder cells. A second strain of murine stem cells (C57BL/6) was included to confirm that differences were stage specific (for example, stem cells or blastocyst) variations and were not related to species specific variations. The three genes, peroxiredoxin 1 (Prdx 1), tyrosine 3-monooxygenase/tryptophan 5-monooxygenase activation protein (Ywhaz), and voltage-dependent anion channel 3 (Vdacs3), were all found to be uniquely expressed in the blastocyst versus embryonic stem cell comparison, the main comparison of interest.

The real time PCR results were as follows. For Prdx1, fibroblast feeder cells had the lowest expression level, blastocysts had a 4.81 fold increase, 129SvEv ESC had a 7.51 fold increase, and the C57BL/6 ESC showed a 27.28 fold increase. Expression

levels were significantly different between the blastocyst and C57BL/6 samples as well as the fibroblast feeder cells and both ESC samples based on ΔC_T statistical analysis.

For Ywhaz, the fibroblast feeder sample showed the lowest expression level, blastocysts had a 7.65 fold increase, 129SvEv ESC showed a 6.49 fold increase, and C57BL/6 ESC showed a 16.56 fold difference. The two ESC values were significantly different as was the fibroblast feeder cell value from all other samples.

For Vdacs3, the blastocyst sample had the lowest level of expression, fibroblast feeder cells had a 2.16 fold difference, 129SvEv ESC had a 68.07 fold difference, and C57BL/6 ESC had a 161.04 fold difference. Statistically, the blastocyst sample was different from both of the ESC samples and the fibroblast sample from either ESC sample.

A review of research literature for the three genes specifically studied through real time PCR, Prdx1, Ywhaz, and Vdac3, suggests important roles in promoting cell survival and continued cell division. Alterations of expression levels of all three genes have been found in cancer lines which have similar characteristics of continued cell division without normal occurrence of differentiation. In addition, all three genes have been suggested as direct or downstream targets of Oct4, an essential gene known for its role in maintaining stem cell pluripotency [2]. While much research remains to fully understand the actions of each of these genes within the cell, especially in distinguishing differences in gene isoform actions within the cell, the overall focus on allowing continued stem cell growth is clear.

This current work identifies a small sample of the potential genes involved in the transition from blastocyst stage embryo to embryonic stem cell line and offers a valuable

first step in understanding the molecular alterations that occur during this essential time period. Peroxiredoxin 1 and Voltage dependent anion channel 3 both demonstrated significant upregulation in the comparison between blastocyst stage embryos and ESC and function to enhance cell survival and continued cell reproduction. The significant difference of expression combined with the complex involvement of these three genes in cellular regulation open the door to better understanding the blastocyst to ESC transition. Hopefully future research will continue to expand our understanding of this transitional period in order to identify key markers of stem cell development in embryonic sources with potential applications in the development of additional stem cell sources.

CHAPTER II

REVIEW OF LITERATURE

Introduction

The general term "stem cell" commonly refers to undifferentiated cells that have the ability for self-renewal and the ability to form one or more specialized cell types. Stem cells that are able to produce a range of differentiated cells that would normally arise from the three germ layers of a developing embryo are called pluripotent. The broadest term, totipotent, indicating a potential for forming all cell types, is generally reserved for the fertilized egg which forms cells composing all three germ layers plus extraembryonic tissue such as the placenta. Stem cells can also be multipotent, meaning they can form several types of differentiated cells, or unipotent, meaning they can form only one type of differentiated cell. Pluripotent stem cells provide the greatest medical research potential due to their diverse developmental potential.

Stem Cell Early History

Much of the early research with stem cells was done using mouse models as is evidenced by a review of stem cell research advances. In fact, long term cultures of mammalian embryonic stem cells have only been achieved so far in mice, monkeys, and humans [3]. The first mouse stem cell lines were first isolated in the 1960's and 1980's

with human stem cell line isolation not to follow until the late 1990's. Murine stem cell research is important since it has provided much of the basic knowledge about stem cells while much of the current research focuses on therapeutic applications with human stem cells.

Experimentation with pluripotent stem cells began with the research on teratocarcinomas in the mouse by Leroy Stevens in the late 1960's. Culture of cells from these tumors led to the isolation of the first embryonic carcinoma (EC) cells, which were later shown to be able to produce cells characteristic of all three germ layers [4, 5].

By the mid-1970's, the potential of using EC cells for therapeutic purposes was acknowledged, but with hesitation due to their aneuploidy, common among cancer cell lines [5]. Nevertheless, the possibilities prompted additional research in the field of murine and human stem cell biology. Researchers already knew that teratocarcinomas could be developed by placing post-implantion embryos into ectopic sites. This led to the idea that perhaps stem cells could be isolated directly from the blastocysts without going through the process of teratocarcinoma development [6].

This concept of isolating stem cells directly from blastocysts led researchers Martin J. Evans and Matt H. Kaufman of Cambridge and Gail Martin of the University of California to independently develop the first mouse embryonic stem (ES or ESC) cell lines in 1981 [5, 7, 8] Evans and Kaufmann isolated the ES cell line by directly culturing blastocyst stage murine embryos from 129SvEv mice. Blastocysts were forced to enter diapause via a maternal ovariectomy between fertilization and blastocyst collection in order to increase cell numbers without allowing development past the formation of the primary endoderm. The blastocysts were collected and placed in tissue culture media for

several days. After "egg cylinder-like structures" had developed from the inner cell mass, these structures were removed and placed in culture with a mitomycin C-inactivated STO fibroblast feeder layer. Colonies of cells resembling EC cells were further isolated and grown for more than 30 passages. The cell lines were found to have a normal karyotype, to be able to produce embryoid bodies when passaged without feeder layers, and to be able to produce teratocarcinomas when injected subcutaneously [7].

The research by Gail Martin used slightly different techniques to achieve a stem cell line directly from early stage embryos. Early blastocysts were flushed from plugged superovulated ICR females that had been bred with SWR/J males. The cells were cultured until late blastocysts were obtained. Immunosurgery was used to isolate inner cell mass (ICM) which were grown on a feeder layer of mitomycin C-treated STO fibroblast in media that had been previously conditioned by growth of a PSA-1 embryonal carcinoma cell line. Stem cells formed from the ICM and after five passages, conditioned media was no longer required for proliferation. The stem cell line demonstrated the ability to form teratocarcinomas *in vivo* as well as the ability to differentiate into a variety of tissue types *in vitro* [8].

The first human stem cells were isolated in 1994 from embryos donated by patients undergoing *in vitro* fertilization (IVF) treatment. Twenty-one fertilized eggs were grown to the blastocyst stage, "healthy" ICM were isolated and cultured from 19 blastocysts, and 17 produced growths with "stem cell-like morphology" for up to two passages [9].

Subsequently, a human pluripotent stem cell line was first established in 1998. James A. Thomson from the University of Wisconsin also cultured donated IVF embryos

in order to obtained human embryonic stem (hES) cells. Five stem cell lines were produced, three that had XY karyotypes and two that had XX. In addition to having normal karyotypes, the cells had high telomerase activity, were able to be cultured for several months, and were shown to maintain pluripotency [10].

At about the same time, researchers at John Hopkins University led by John Gearhart, isolated the first human embryonic germ (EG) cell line from the primordial germ cells of aborted fetuses (5-9 weeks old). The cultures were karyotypically normal (both XX and XY) and were able to produce embryoid bodies containing differentiated tissue belonging to all three germ layers. This provided a second source of human pluripotent stem cells for research [11].

Since this early research, a great deal of national and international research has focused on stem cell characteristics, growth requirements, and differentiation potential for both mouse and human stem cells. While many believe embryonic stem cells have the greatest scientific and medical applications, several factors have limited human embryonic stem cell research within the United States. In 2001, due to ethical concerns about the derivation of human embryonic stem cells from early embryos, President Bush limited the use of federal research funds to those stem cell lines already created from surplus IVF embryos. At the present, there are 78 eligible human embryonic cell lines listed on the National Institute of Health's Human Embryonic Stem Cell Registry (http://stemcells.nih.gov/research/registry/defaultpage.asp), however not all of these lines have proven to be viable for research and only 21 lines are currently listed as available for use [12].

In addition, patent issues have arisen. The Wisconsin Alumni Research Foundation (WARF) at the University of Wisconsin, Madison, site of James Thomason's human ESC line discovery, holds two intellectual property (IP) patents on human embryonic stem cells, the only such patent in the world. (They also hold 5 of the 21 available human ESC lines on the NIH registry.) Within the two patents, claims include methods of primate and human ESC derivation in addition to the actual stem cells as well as all derivatives of human embryonic stem cells. WARF has required licenses for both academic and commercial institutions and has charged per cell line, per investigator rather than the customary one-charge per institution. While some institutions have chosen to infringe on the IP patent rather than pay the numerous fees, others have challenged the patent in court, and some have chosen to move their research outside of the United States [13].

Stem Cell Types and Source

Despite the common usage of the term "stem cell", much confusion still remains about the various stem cell types and sources. Stem cells are often divided based on the source – adult, fetal, or embryonic tissue. The two types of stem cells isolated from fetal and embryonic tissue are both pluripotent. Fetal derived stem cells are called embryonic germ (EG or EGC) cells while stem cells derived from the embryonic blastocysts are called embryonic stem (ES or ESC) cells.

Adult stem cells are isolated from adult body tissue and generally function in normal body maintenance. While these cells are valuable in normal body function, most are not naturally pluripotent. The unique pluripotent stem cells derived from adult tissue

is the embryonal carcinoma (EC) stem cell line. Other types of stem cells often discussed include umbilical cord stem cells and most recently, amniotic fluid-derived stem cells.

Embryonal Carcinoma Cells

Embryonal carcinoma (EC) stem cell lines are isolated from testicular teratomas, also called teratocarcinomas. This type of tumor is composed of a mixture of tissue, not characteristic of the testis, but rather a conglomerate of those derived from the three germ layers of the developing embryo [14, 15]. A large variety of tissue may be included such as cartilage, bone, muscle, and epithelia. They originate from primordial germ cells (PGCs) which during development normally lead to the production of eggs or sperm [4].

When these EC cells within the tumor are isolated from the teratocarcinomas and cultured *in vitro*, long term pluripotent cultures of EC stem cells can be produced. One difference in EC cells from other types of stem cells is that they often exhibit heteroploidy or abnormal chromosome numbers [4]. This is not surprising considering their carcinoma origin and even though EC cells are pluripotent like EG and ES cells, their research potential is limited by their chromosomal abnormalities and therefore are not utilized or discussed as frequently as the other forms of stem cells.

Embryonal Germ Cells

Like the embryonal carcinoma stem cells, embryonal germ (EG) cells also originate from PGCs. However, while EC cells are obtained from abnormal growth of PGCs in adult tissue, EG cells are obtained from developing fetal tissue. In the

developing human embryo, PGCs migrate from the yolk sac to a region of the posterior body wall forming the gonadal ridge which will eventually lead to the formation of ovaries or testis [16]. If the PGCs are isolated from the gonadal ridge within the fifth to tenth week of development and cultured in vitro with feeder layers, colonies of pluripotent EG cells are developed [4, 14].

In the mouse, the PGCs are first identifiable around day 8 after which these few cells (10-100) migrate to the genital ridge. During the migration, the cells replicate so that by day 13.5, the genital ridge is populated by approximately 25,000 PGCs. Isolation of murine PGCs occurs from about day 11.5 and later [17].

Embryonic Stem Cells

Both embryonal germ cells and embryonic stem (ES) cells are isolated from the early developing embryo; however the embryonal germ cells are isolated at a post-implantation stage while the embryonal stem cells are isolated from the pre-implantation blastocyst stage embryo. In the mouse, the blastocyst stage embryo is composed of about 150 cells divided into regions. The outer layer of cells is called the trophectoderm, an inner cluster of cells is called the inner cell mass, and the two are mostly divided by a fluid-filled cavity called the blastocoel. When the blastocyst stage embryos are cultured *in vitro*, some colonies develop that are stem-cell like. These cells are subcultured on feeder layers leading to the formation of ES cell lines [4].

When stem cells are referenced in general, often the reference may be to ES cells. Currently ES cell lines have only been isolated from three mammalian species – mice, humans, and monkeys [3, 4, 14]. (EC and EG cells have only been isolated from mice

and humans.) Research on murine ES cells first became possible about 20 years ago and since that time they have been involved in a great deal of research. Characteristics that make them valuable in research include their ability to replicate indefinitely, their normal chromosome number, and their pluripotency.

Adult Stem Cells

Adult stem cells in general are considered relatively rare and were not originally believed to be distributed throughout the adult human body. They have, however, been found naturally occurring in many body tissues and have now been isolated from tissues that originated from all three embryonic germ layers, including the bone marrow, blood, brain, cornea, gastrointestinal tract, liver, pancrease, retina, tooth dental pulp, skeletal muscles, and skin [14]. A common example is the multipotent hematopoietic stem cells which form the erythrocytes and the leukocytes of the blood.

Adult stem cells are undifferentiated and function in normal body maintenance to replace damaged or dying cells. The stem cells divide producing both a new stem cell and a second cell that develops to become the needed differentiated cell. However, unlike ES cells, most adult stem cells are not naturally pluripotent. As exceptions, murine spermatogonial stem cells and multipotent adult progenitor cells (MAPCs) obtained from the culture of human bone marrow have been reported to demonstrate pluripotency [18, 19].

Researchers though have questioned the plasticity or the ability of one type of adult stem cell to form a different type of tissue through “genetic reprogramming” via altered growth or differentiation conditions and the belief that the developmental

potential of adult stem cells is unchangeable has been contradicted by numerous research findings [4, 19]. One concern, however, about some of the early experiments was that the researchers often used a heterogenous pool of cells rather than demonstrate plasticity with a clonal pool of identical stem cells [14].

While other types of stem cells are often encompassed with ethical debates about their origins, adult stem cells have been proposed by some as an equal alternative. Several problems, however, currently exist with the widespread use of adult stem cells for research and therapeutic applications such as the limited availability of pluripotent adult stem cells as well as the difficulty in locating and isolating the adult stem cells.

In addition, while adult stem cells are able to continue to replicate *in vivo*, researchers have had difficulty in maintaining long term cultures *in vitro*. Adult stem cells have not been shown to replicate indefinitely like ES cells but often undergo differentiation in culture instead. This is problematic since researchers need large numbers of stem cells for experimentation and therapeutic procedures but are unable to grow them *in vitro* [4].

Other Types of Stem Cells

There are several other types of stem cells that may be utilized in research. Umbilical cord stem cells are multipotent cells taken from the umbilical cord at time of birth. Since they are genetically identical to the child, they hold great research promise for patient specific therapy [3]. In addition, isolation of a new type of stem cell from human, mouse, and rat amniotic fluid with both embryonic and adult stem cell markers was recently published. These amniotic fluid-derived stem (AFS) cells avoid the ethical

debate associated with embryonic stem cells, grow without a feeder layer, and are pluripotent, having been induced to form tissue characteristic of each germ layer ("adipogenic, osteogenic, myogenic, endothelial, neurogenic, and hepatic"). In addition to isolation from fluids collected via amniocentesis, these cells have also been isolated from prenatal chorionic villi and placental biopsies proving they are very accessible. Unlike ES cells, the AFS cells also proved to be nontumorigenic when implanted *in vivo* which may prove extremely useful in future therapeutic applications [20, 21].

General Stem Cell Characteristics

Much of the stem cell research within the last decade has focused on discovering stem cell characteristics. While each type of stem cell has some unique characteristics, there are also some common traits among most types including the ability for self-renewal in a pluripotent/multipotent state, maintenance of a normal karyotype, telomerase activity in maintaining full length telomeres, and expression of characteristic cell surface markers.

Pluripotency and Self-Renewal

Culture Dish

One basic characteristic is the ability for *in vitro* self-renewal in an undifferentiated state. This is a pluripotent/multipotent state for all stem cells other than adult stem cells. While researchers are still determining the factors required for maintaining an undifferentiated state, several factors have been discovered. One basic

determinant is the type of culture dish that is used. Dishes that have an adherent surface discourage differentiation while non-adherant surfaces allow embryoid body formation and differentiation [4].

Leukemia Inhibitory Factor

Secreted factors such as leukemia inhibitory factor (LIF) also play an important role in the maintenance of an undifferentiated state. LIF is a 45 kDa cytokine which has also been known as differentiation-inhibiting factor (DIA) and differentiation-retarding factor (DRF). It is normally secreted from numerous cell types including T cells, fibroblasts, the liver, and the heart [22]. It's secretion by the mitotically-inactivated murine embryonic fibroblast (MEF) cells upon which stem cells are normally grown is essential for the maintenance of the undifferentiated state. In murine ES cell cultures however, addition of LIF can actually replace the need for MEF feeder cells [4]. In addition to LIF, EG cell isolation requires two additional factors, Kit ligand and basic fibroblast growth factor (bFGF or FGF2) [4].

While LIF has numerous actions within the body including promoting bone resorption, causing a decrease in body fat, and promoting hematopoiesis, LIF promotes maintenance of the undifferentiated state and continued division in stem cell cultures [22]. LIF works within the stem cells by activating glycoprotein 130 (gp 130) which affects the signal transducer and activation of transcription-3 (STAT-3) molecule as well as other molecules such as mitogen-activated protein kinase. The activation of the mitogen-activated protein kinase however has been reported to be a counter-balance in

that it seems to inhibit the ability for continued self-renewal [4].

In contrast to murine ES cells, while human ES cultures generally do require feeder cells (with the exception of the AFS cells), they do not require LIF. Since the feeder cells are also secreting other factors, it has been proposed that perhaps the same downstream signaling molecules are being activated [4]. MEF feeder cells are the most common, however due to concern about the potential transfer of animal pathogens and in attempts to improve stem cell growth and differentiation, numerous other types of feeder layers have also been tried including human placenta-derived feeders, human bone marrow-derived feeders, and human glioblastoma feeders [3, 23, 24].

Cell Cycle Alterations

Alterations in the cell cycle also play an important role in the maintenance of pluripotency and self-renewal. Researchers have found that stem cells seem to lack the gap 1 (G_1) checkpoint in the cell cycle. External stimuli are not required for replication to begin and ES cells spend the majority of their time in the synthesis (S) phase of the cell cycle replicating DNA in preparation for cell division [14].

In a normal eukaryotic somatic cell cycle, the G_1 phase is preparation for the S phase and contains a regulated checkpoint that determines whether the cell enters the S phase or a G_0 resting phase. The checkpoint is regulated by a delicate balance of factors including cell to cell contact, cell differentiation, and anti-mitogenic factors that all promote transition to G_0 and mitogens (extracellular growth factors) and nutrients which promote continued transition through the restriction checkpoint and into the S phase. The

presence or absence of these various factors influences a cascade of biochemical events involving cyclin-dependent kinases that control the transition. Without this checkpoint in somatic cells, uncontrolled cell division can lead to the development of cancer [25]. In stem cells, the lack of the checkpoint allows the cells to continue dividing without entering a differentiation stage.

Transcription Factors

In addition to secreted factors, culture dishes, and cell cycle alterations, transcription factors also play a large role in the pluripotent self-renewal capacity of stem cells. Certain transcription factors are characteristic of undifferentiated pluripotent stem cells in both humans and mice such as Sox2, genesis (also known as FoxD3), germ cell nuclear factor, nanog, fibroblast growth factor (Fgf4), undifferentiated embryonic cell transcription factor (Utf1), reduced expression (Rex-1), and octamer-binding transcription factor 4 (Oct-4; also known as Oct-3 and Oct-3/4) [14, 26]. In fact, many of these identified transcription factors have been shown to be directly influenced by Oct-4 as they work together to prevent cellular differentiation [26].

Oct-4 is a POU-domain transcription factor that is key for the maintenance of an undifferentiated state. Recently Oct-4 has also been renamed as POU domain class 5 transcription factor 1 (Pou5f1) [2]. Researchers have found that Oct-4 is essential in early embryonic development for pluripotency and that embryos lacking Oct-4 fail to develop an ICM in a blastocyst stage embryo [27]. When Oct-4 is downregulated in ES cells, differentiation begins [4]. Oct-4 was also found to be expressed in over 90% of the

AFS stem cells recently described [20] and in numerous types of adult stem cells [28]. In contrast however to the majority of research indicating Oct-4 expression as an important characteristic of undifferentiated cells (i.e. embryonic and stem cells), one recent study found Oct-4 expression in human peripheral blood mononuclear cells bringing to question its use as a marker of pluripotency [28].

Other transcription factors are characteristic in the differentiation of stem cells. For example, Pax6 is expressed as ES cells form neuroepithelium, hepatocyte nuclear factor-4 (HNF-4) is expressed as endoderm is formed, and brachyury is expressed as mesoderm is formed [14]. The presence of these transcription factors can therefore be used to identify cells in the process of differentiation.

Pluripotency Verification

The pluripotency of ES, EC, and EG cells have been verified by various experiments. When the pluripotent stem cells are injected into the blastocoel of a blastocyst stage embryo and implanted into the uterus of a surrogate mouse, a chimeric mouse develops which contains a mixture of tissue derived from both the original blastocyst and the stem cells. The ES and EG cells contribute to all cell types, including the germ line. The EC cells, however, failed to contribute to the germline in most instances which could be due to their abnormal chromosome numbers [4].

A second similar test involves injection of ES cells into a blastocyst devoid of its ICM. When allowed to develop, the recreated blastocyst successfully develops into a

complete embryo [14]. These experiments alone verify the ability of the ES cells to form tissue derived from all three germ layers.

A third test involved the injection of pluripotent stem cells either under the skin or into the kidney of an immunocompromised or genetically identical mouse. The stem cells form a teratoma containing a mixture of differentiated or partially differentiated tissue as is in a normal teratoma. Teratomas formed by hES included tissues such as gut epithelia, cartilage, smooth muscle, neural epithelial, and stratified squamous epithelium [10]. This random differentiation however causes concern about using undifferentiated stem cells in therapeutic treatment [4, 14].

A fourth demonstration of pluripotency involves spontaneous or directed in vitro differentiation that can occur in culture. If the cell culture conditions are altered, such as in removal of the feeder layer or LIF, differentiation into a variety of tissue types may occur [4]. If the cells are allowed to overgrow past confluency, spontaneous differentiation may also occur [10]. In addition, if factors are changed or the cells are grown in suspension, the stem cells can clump and form embryoid bodies similar to early stage embryos or teratomas which contain a random mixture of differentiated or partially differentiated cells that can be further cultured [14].

Karyotype

Maintenance of a normal karyotype is another important characteristic of most stem cell types and is essential if they are to be used for therapeutic applications and for most experimental applications. Only the embryonal carcinoma cell line which is derived from the teratocarcinoma generally contains abnormal chromosome numbers [4].

Telomerase Activity

High telomerase activity is an additional common characteristic among the stem cell types, including mouse and human ES cells [4, 10, 14, 26]. Eukaryotic chromosomes are composed of linear, anti-parallel strands of DNA which contain special ends containing long arrays of repeating sequences called telomeres. During normal chromosome replication, DNA is copied in the 5' to 3' direction with one side being copied in a long continuous strand towards the replication fork, called the leading strand, and the other strand copied in short segments away from the replication fork, called the lagging strand. Because the polymerase used to copy DNA requires a primer enzyme to initiate the DNA replication, a problem occurs for the lagging strand as it reaches the end of the DNA where there is no DNA upstream to which the primer may bind. Replication ceases and the newly replicated chromosome from the lagging strand is shorter than the original chromosome and continues to become shorter in the telomere region with each successive replication [25].

Throughout the life of the organism, these chromosomes continue to loose base pairs in the telomeric regions and this shortening has been associated with cell death and aging. Research has shown an inverse relationship between the length of the telomeres and the age of the individual [25]. If this situation were never corrected, the chromosomes of each successive division would be smaller than those of the generation before, leading to the potential for increased numbers of genetic abnormalities and accelerated aging. This shortening of the telomeres is a probable explanation for the Hayflick limit, which refers to the observation that normally somatic cells will only

divide a limited number of times before entering into senescence [10]. For example, in culture, human somatic cells only replicate approximately 50 times [15].

The activation of the enzyme telomerase corrects for this situation, providing cellular "immortality". Telomerase is a modified reverse transcriptase which acts by extending the length of the original or template strand of DNA at its 3' end. The telomerase enzyme has a RNA associated with it that base pairs with the telomeric sequences on the end of the template strand. Telomerase then extends the template by reverse transcription complementary to the RNA template. The RNA template slips to the end of the newly extended segment and the process is repeated. As this process is repeated over and over, a large number of repeating sequences are added to the chromosome and the telomeric length is restored [25].

Telomerase, however, is not active in all stages of the normal cell cycle. In normal differentiated somatic cells, telomerase is inactive, thus providing the association between shortening of the telomeres and aging. Rather, telomerase activity is generally associated with early development and germ line tissue which allows the new individual to begin life with normal length chromosomes. Stem cell research has shown however, that telomerase is also active in these cells. This activity is important in preserving the chromosome integrity in these rapidly replicating cells. Should the stem cells be used in therapeutic treatments, it would be important to know that cells from each division were identical to normal chromosome composition.

Variety of Cell Surface Markers

All cell surfaces have a variety of cell receptors that can be identified and used to characterize the cell type. For example, adipocytes are characterized by adipocyte lipid-binding protein (ALBP) and fatty acid transporter (FAT). Stem cells also often display patterns of surface markers or receptors that are characteristic of the cell type. For example, the first human ES cell lines isolated by James A. Thomson displayed cell markers that were similar to those expressed in human EC and primate ES cell lines. These markers included stage-specific embryonic antigen-3 (SSEA-3), SSEA-4, and alkaline phosphatase [10]. The stage-specific embryonic antigens are glycoproteins which are normally expressed during embryonic development [14]. While alkaline phosphatase is also expressed in murine ESC, SSEA-3 and SSEA-4 are not expressed in mice past the early cleavage stage embryo [26]. A variety of other cell surface markers have been found to be expressed in both human and murine ESC, including CD9, CD81, and osteopontin [26].

The amniotic cells isolated to produce AFS cells all expressed c-Kit (CD117), the stem cell factor receptor. Examination of cultures of these cells also found a mixture of adult and embryonic cell surface markers, including Class I major histocompatibility (MHC) antigens, sometimes MHC II antigens, mesenchymal and/or neural stem cell markers (CD29, CD44, CD73, CD90, CD105), and embryonic SSEA-4 (in human AFS cells) [20].

The differences in cell surface markers allow researchers to sort cell types based on these markers. Fluorescent labeled monoclonal antibodies specific for the various cell

surface markers can be used to label the cells which can then be separated by fluorescence-activated cell sorting (FACS).

Potential Stem Cell Applications

Developmental Understanding

With the broad range of possible applications, stem cell research has received a great deal of focus both within and outside of the scientific community. One of the most basic goals of stem cell research is to increase basic science knowledge of what occurs in embryonic development. Stem cells offer the opportunity to discover the various genes and associated factors that play important roles in early development. This research could potentially lead to the development of gene expression maps that would aid in the understanding of how the genes influence cell function [4].

Stem cells also provide an opportunity to discover the effects of atypical alterations such as in heteroploidy [14]. The affects of teratogens which normally cause fetal abnormalities can also be studied with the help of stem cells [4]. These may result in discoveries not only concerning birth defects, but also infertility and loss of pregnancy [10]. Since many childhood tumors originate from early stages of development, developmental stem cell research may also be able to provide insight into the mechanisms involved [14].

Repair of Damage Tissue/Organ Transplantation

The greatest proposed application is for the repair or replacement of damaged tissue. Research with stem cells may reveal new growth and differentiation factors that will be key in the progress towards directed differentiation or regeneration for medical applications [6]. Researchers have been able to manipulate the pluripotent ES cells to form at least 20 different tissue types *in vitro* including adipocytes, cardiomyocytes, dendritic cells, endothelial cells, mast cells, neurons, pancreatic islets, and striated muscle cells. The range of tissue types produced has provoked speculation about cures for a number of diseases including, but not limited to Parkinson's disease, diabetes, chronic heart disease, cancer, liver failure, multiple sclerosis, spinal cord injuries, and Alzheimer's disease [3, 14].

An additional potential medical application for stem cells is for organs for transplantation. The current supplies of donated organs for those in need are insufficient to meet the demand. The ability to induce differentiation of ES cells has led to the hope that researchers will deduce the culture conditions needed to lead to the production not only of specific tissues but also organs for transplantation [14]. For example, AFS cells have been shown to be able to form tissue-engineered bone within mice with immune deficiencies as well as hepatic cells secreting urea [20].

Small changes in culture conditions can influence the differentiation process. These changes can involve using different types of feeder cells, different types of culture containers, adding growth factors, growth in highly concentrated environments, or removal of inhibiting factors such as LIF or feeder cells. Differentiated cells may also be

produced in embryoid bodies and then separated based on surface markers by FACS or selected by the use of special culture conditions or drugs [3, 4].

Besides of the lack of available organs, the other greatest problem in tissue transplantation is organ compatibility. Transplantation patients must follow a strict drug regiment to prevent immunological rejection of the transplanted tissue despite the medical doctor's best attempt to match tissue types. With the aid of stem cells, these limitations could potentially be overcome.

With the developing nuclear transfer cloning technology, it could be possible to create a cell line that would be compatible with the tissue type of the patient, an idea called "therapeutic cloning" [5]. In nuclear transfer cloning, the nucleus of a normal somatic body cell is placed inside of an oocyte that has had the nucleus removed. The environment of the nucleus "reprograms" the somatic nucleus to create a more embryonic-like gene expression pattern and can lead to the development of an embryo. If the patient's own somatic cells were used to create the nuclear transfer clone, ES cells could be isolated from the developing blastocyst and used to create immunologically matched tissue [29].

There are several problems currently associated with the use of stem cells and nuclear transfer technology for the production of immunologically compatible cell lines. One major problem is that nuclear transfer is successful in only a small percentage of attempts [29]. This could potentially be due to a lack of reprogramming of the Oct-4 transcription factor gene [27]. In addition, it could be very expensive to create a cell line for each patient, in addition to the fact that depending on the urgency of the medical condition, there may not be sufficient time.

An alternative solution that is being explored for both general stem cell generation and patient specific stem cell production is parthenogentic blastocyst generation. Unfertilized eggs activated through chemical treatment rather than through fertilization by sperm have been grown to the blastocyst stage so that stem cells could be generated in both human and murine samples. This could be used to create patient specific matches (females), closely related matches (family members), or banks of cells for the various immunological groups [30, 31].

An alternative might be to create multiple cell lines through traditional methods that would closely match the major histocompatibility profiles of multiple patients and would adequately meet the needs of most patients. In addition, there may be ways to alter the stem cells to make them more immunologically compatible and less likely to be rejected [10].

Drug Development and Other Applications

Molecular techniques that would allow for genetic manipulation of the stem cells also open additional doors of research potential. For example, stem cells could be designed that would transport specific DNA segments that would help or completely destroy the targeted tissue [6, 14]. In addition, the ability of stem cells to contribute to the germ line in chimeric organisms creates the possibility of designing new tailored model research organisms which could be useful not only in basic disease research but also in drug development [6, 10].

Specific stem cell lines or differentiated tissue, especially from hES cells, could be developed and treated to demonstrate the effects or toxicology of the drugs on human

tissue rather than only on research animals [14]. Treated differentiated tissue could reveal the specific gene effects in a target tissue and identify future gene targets [10].

Current Obstacles

One major issue that will have to be solved before stem cells can be used in large scale clinical applications is how to grow large quantities of identical stem cells. This is made even more difficult by the fact that human stem cell lines grow more slowly than the animal models that are currently used in much of research [4]. One possible answer to this problem would be to allow the stem cells to partially differentiate into the needed progenitor cells and then grow large quantities of the progenitor cells. Research by Shamblott, et al, has shown that the progenitor cells are able to grow well *in vitro* [32].

An additional problem is that the controlled conditions for the directed differentiation of stem cells still need to be determined for most tissue types. Since undifferentiated stem cells can form teratomas when injected into immunocompromised research animals, undifferentiated stem cells could also create tumors in immunocompromised patients [14].

Comparison of Stem Cells and Blastocyst

While this brief review of literature reflects that much research has focused on the development potential of embryonic stem cells and general stem cell characteristics, much less research has been done to characterize the transition from the source cell, the inner cell mass, to the resulting cell line, the embryonic stem cell. A National Institute on

Aging (NIA) project published in 2003 created cDNA libraries for murine early embryos, embryonic and adult stem cells using expressed sequence tags (EST) which were subsequently released as clone sets for microarray analysis [33]. Later NIA work analyzing gene expression levels as determined by EST frequencies revealed key genes common to various cellular and developmental stages (pre-implantation embryos, pluripotent stem cells, adult stem cells, etc.), however it failed to directly measure gene expression levels or to characterize the blastocyst to stem cell transition [1]. Other research did show that the ICM and the ES cells share many common cell surface markers [14].

So while research has focused on characterizing both the blastocyst stage embryos and embryonic stem cells, a more extensive analysis of the developmental transition from blastocyst to stem cells has not been performed to our knowledge, despite the wide-spread use of embryonic stem cells.

Potential Techniques

For a comparison of differential gene transcription between two sources, a variety of methods are available. With the advent of microarray technology, much research has benefited from the vast information provided by this analysis. The utilization of microarrays was prohibited in this research due to procedural costs and quantity of RNA required for effective hybridization and analysis. Standard microarray protocols require a minimum of 10-50 ug of total RNA and even the newer improved kits, such as Perkin Elmer's MICROMAX^{TM} TSA Labeling and Detection Kit, required at least 0.5-1 ug of

total RNA. The difficulty and cost in obtaining adequate numbers of embryos made microarrays impractical for the proposed research.

Northern Blots can also be useful for the comparison of isolated RNA between samples for specific genes. However the low levels of RNA made this technique difficult and since a broad comparison of gene expression was needed without gene specific knowledge, an alternative technique was required.

Alternative techniques such as the polymerase chain reaction (PCR) or real time PCR can also be extremely valuable tools for comparing gene expression between samples, however once again for a broad gene expression analysis without specific knowledge of which genes should be analyzed, other initial techniques were needed.

Suppression Subtraction Hybridization

An alternative method for differential gene transcription analysis is suppression subtraction hybridization (SSH) through the use of the CLONTECH PCR-Select^{TM} cDNA Subtraction Kit (Mountain View, CA). This method compares transcription from two sources and combines normalization and subtraction. It converts source mRNA to cDNA, ligating an adaptor to one of the cDNA samples, hybridizing the two cDNA samples, removing the hybridized cDNAs, and amplifying the unhybridized cDNA samples containing the adaptor. The procedure is repeated, switching the sample that contains the adaptor, so that all uniquely expressed genes in either sample may be identified (Figure 2.1).

First described in 1996 by Diatchenko, et al [34], SSH has proven effective in numerous other research projects and has demonstrated its ability to identify uniquely

expressed genes between samples. For example, it has been used to study gene expression within the mouse oviduct during the preimplantation period [35], within maturing bovine oocytes [36], within murine oocytes and early embryos in order to characterize the maternal-to zygotic transition [37, 38], and to study the effect of differential gene expression, such as with Oct-4 [39].

The CLONTECH PCR-Select^{TM} cDNA Subtraction Kit requires 0.5-2 μg of poly A^+ RNA, an amount that can still be difficult to obtain from embryos. The limitation of RNA required can be overcome by the utilization of CLONTECH's Super SMART^{TM} PCR cDNA Synthesis Kit, which has been designed to use small amounts of RNA in a PCR based process to produce high quality cDNA which can then be used with the CLONTECH PCR-Select^{TM} cDNA Subtraction Kit. The Super SMART^{TM} PCR cDNA Synthesis Kit requires only 2 ng of total RNA, making this an effective procedure for differential gene expression analysis of murine blastocyst and embryonic stem cells [40].

In the production of the cDNA samples, special techniques must be used. One problem that has typically occurred in cDNA production is the under representation of sequence on the 5' end of the RNA due to the difficulty in transcribing the entire sequence by reverse transcriptase (RT). In this process, a modified oligo(dT) primer (the CDS primer), primes the synthesis of the first strand and as the RT reaches the 5' end of the mRNA, it adds an extra 3-5 nucleotides, typically deoxycytidine. The SMART^{TM} oligonucleotide primer contains an oligo(G) sequence which allows it to bind to the oligo(C) stretch providing opportunity for full strand replication. The RT switches strands and completes the double-stranded molecule. The poly(A) sequence and the SMART anchor sequence are then valuable primer sites for total cDNA amplification.

The CDS primer and SMART oligonucleotide primer both contain a Rsa I site so that these sequences may later be removed (Figure 2.2) [41].

In general PCR (which is not subtractive), the products are often produced in proportion to the original amount of cDNA present in the sample. This makes it difficult to identify genes that are differentially expressed in low quantities. The normalization that occurs in suppression subtraction removes the cDNAs that are more commonly expressed in higher quantities, allowing better identification of weakly expressed genes [42].

The first hybridization accomplishes equalization and enrichment of differentially expressed sequences (Figure 2.1). The procedure begins with two cDNA samples from the same source, called the tester samples (experimental samples), but with a different adaptor molecule annealed to each sample. An excess of driver (control sample) is added to each sample separately and the samples are heat denatured and allowed to anneal. More abundant molecules anneal faster which causes equalization or normalization in the "a" type molecule of high and low abundance sequences. Products are:

"a" – Unique high and low abundance tester sequences

"b" – High abundance tester sequences with the same adaptor

"c" – Common tester and driver sequences – only 1 adaptor

"d" – Driver cDNA with no adaptor

The second hybridization generates templates for PCR amplification from differentially expressed sequences. The two hybridized samples are mixed together without denaturing, which produces a new "e" molecule, which consists of the joining of the type "a" molecule from both samples having different adaptors. DNA polymerase

fills in the ends and the type "e" molecules have different annealing sites for nested primers on the 5' and 3' ends.

"e" – Differentially expressed tester sequences

The first PCR amplification is suppression PCR so that only differentially expressed sequences are amplified.

"a" – Missing primer annealing sites and can't be amplified.

"b" – Most form pan-like structures so that they can't be exponentially amplified.

"c" – Have only one primer site allowing only linear amplification.

"d" – Missing primer annealing sites and can't be amplified.

"e" – Has two different adaptors and is exponentially amplified.

In the second PCR amplification, the background is reduced and differentially expressed sequences are further enriched through the use of the nested primers (Figure 2.1) [42].

Subsequent Techniques

Once suppression subtraction hybridization is used to isolate the differentially expressed gene fragments, the unique fragments must be cloned, sequenced, and identified through online database searches. Since SSH has been found to generate about 2% false positives, the unique expression of sequenced genes needs to also be subsequently confirmed [43]. While Northern blots can be used for conformational analysis, it is prohibited once again by limited sample availability. Reverse-transcriptase polymerase chain reaction (RT-PCR) is possible with small test samples and will be used to first confirm differential expression of the isolated sequences between the original test

samples. Subsequently, selected confirmed differentially expressed segments will be quantified between samples through use of the real time polymerase chain reaction.

Research Focus

While the stem cell literature reflects a great deal of focus on stem cell characteristics as well as potential research and therapeutic applications, little has been done to characterize the transition from blastocyst stage embryo to embryonic stem cell. With the current limitations on available hES cell research and the limited number of viable stem cell lines, avenues to alternative sources of pluripotent stem cells need to be explored. Characterizing the blastocyst to ESC transition will provide basic developmental information on key stem cell genes that will give greater understanding to this transitional process and may aid both in monitoring the quality of new stem cell lines as well as in the potential development of future stem cell lines.

Murine embryos and embryonic stem cell lines were used for this project as they are readily available and have proved to be useful research models in numerous stem cell experiments. While murine stem cells are not identical to human stem cells and perfect correlations can't always be made, they do share a great number of basic characteristics and murine samples lack the ethical and availability concerns of human samples [26].

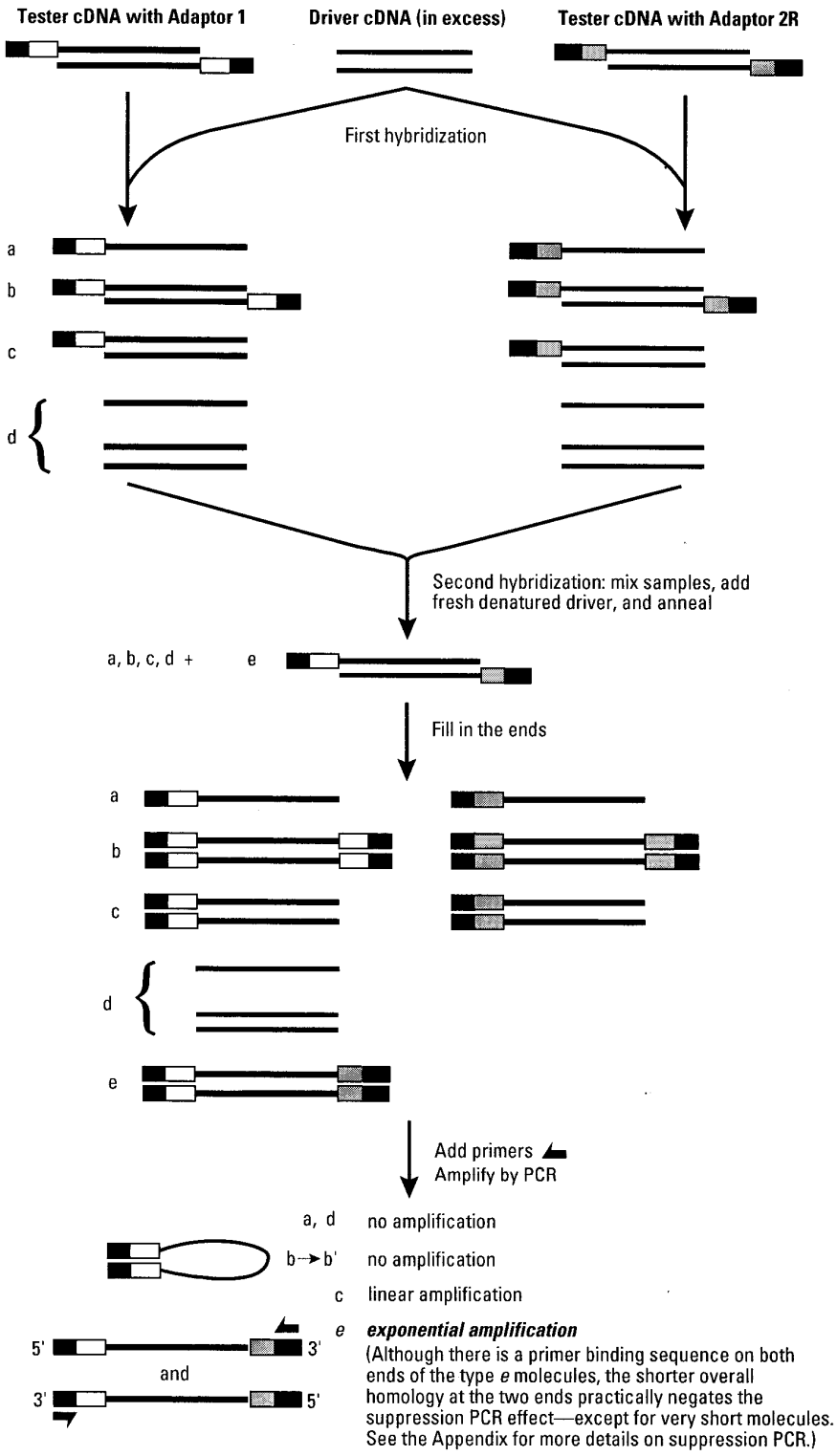

Figure 2.1 Suppression Subtraction Hybridization Differential Gene Amplification. Taken from [42].

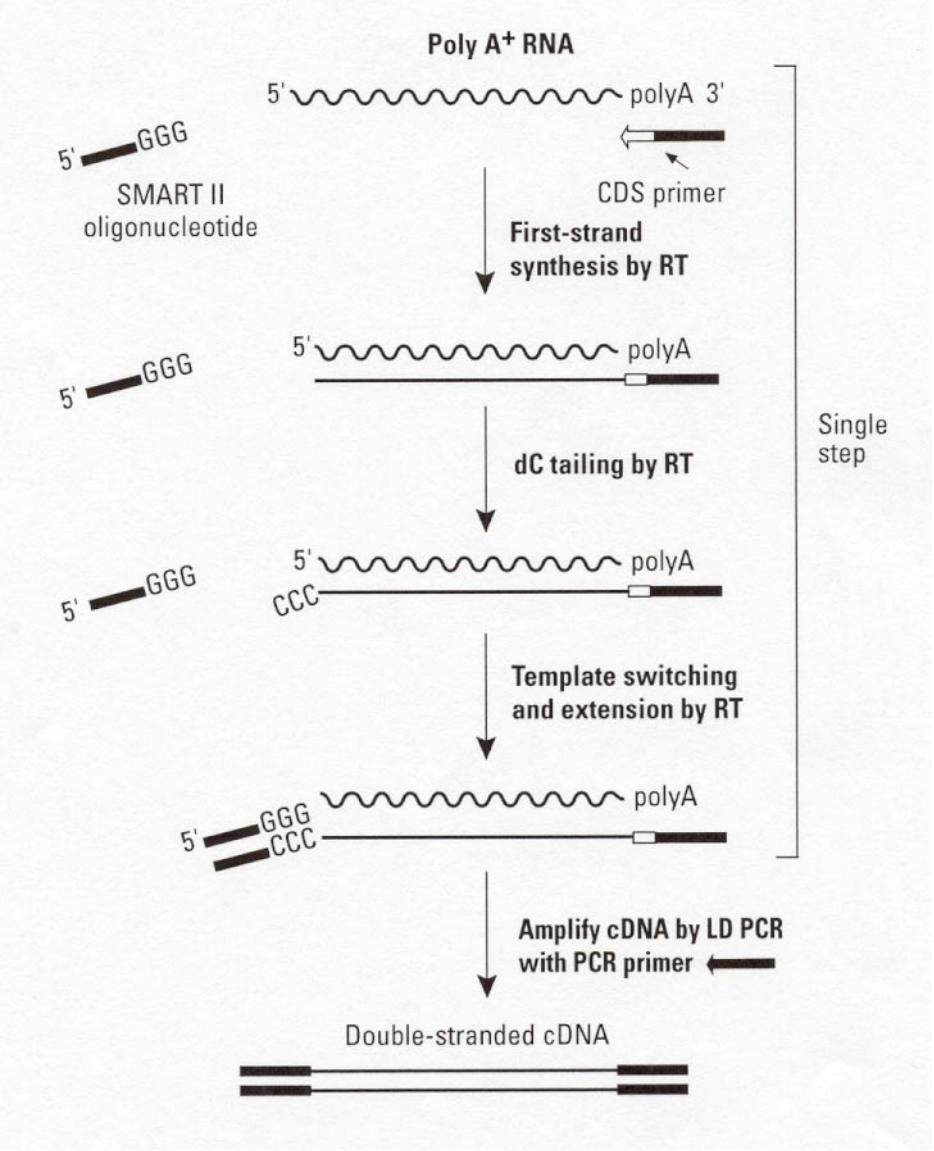

Figure 2.2 Suppression Subtraction Hybridization cDNA Production.
Taken from [40].

CHAPTER III

METHODOLOGY

In this study, four SSH comparisons were made - blastocyst vs. blastocyst, trophectoderm vs. blastocyst, 129SvEv stem cells vs. fibroblast feeder cells, and blastocyst vs. 129SvEv stem cells. The first three comparisons served as control comparisons while the last comparison was the primary comparison of interest.

Blastocyst vs. blastocyst was a control on the SSH procedure since in a comparison between the same source samples, one should not expect to see any genes amplified as uniquely expressed. The 129SvEv ESC vs. fibroblast feeder cell comparison served as a control as few unique transcripts should be identifiable in the fibroblast sample since these cells had been irradiated and should be generally inactive. However since the ESC sample would naturally be contaminated with small amounts of fibroblast due to common culturing techniques, the possibility of identifying unique transcripts in the ECS which had originated from the fibroblast contamination needed to be eliminated.

Similarly, the comparison of trophectoderm vs. blastocyst served to identify whether or not there were any major differences in gene expression in the trophectoderm in comparison to the blastocyst. Since embryonic stem cells are produced from the inner cell mass cells of the cultured blastocyst, the goal of the research was to identify genes

directly involved in ESC formation and differential expression originating from the trophectoderm needed to be eliminated.

Sample Collection

Blastocyts

Four week old female CD1 mice were superovulated with injections of 7.51 international units (IU) pregnant mare serum gonadotrophin (PMSG; Sigma, St. Louis, MO) followed two days later with 7.51 IU human chorionic gonadotrophin (hCG; Sigma) and overnight placement with CD1 breeder males. Oviducts of females who showed evidence of copulation by the presence of vaginal plugs the following morning were collected and flushed at 3.5 days post-copulation into a 37^{o}C solution of phosphate buffered saline (PBS) with 3 mg/ml bovine serum albumin (BSA; Irvine Scientific, Santa Ana, CA).

The blastocysts were washed in 37^{o}C PBS/BSA followed by the removal of the zona pellucidas in acid Tyrodes medium at 37^{o}C (pH 2.5; Sigma). A second washing in 37^{o}C PBS/BSA (40 µl drop) was followed by washes in serum free BWW (Biggers, Whitten, and Whittingham; Irvine Scientific) and a 40 µl drop of BWW/Hepes with RNasin (SUPERase-In, 1U/µl; Ambion, Austin, TX). A total of 176 blastocysts were obtained from 15 mice and processed immediately for RNA as a group. Following RNA isolation, the pool was divided into 6 samples for the remainder of the experiment.

Trophectoderm

Blastocysts were collected from 10 CD1 mice superovulated as previously described. Once the blastocysts were flushed from the oviducts, they were immediately placed in BWW Hepes medium (50 μl drop) and manually bisected at 50X magnification by use of a stereomicroscope to remove the portion containing the inner cell mass. A total of 47 trophectoderm samples were obtained from a pool of 78 blastocysts. Fetal bovine serum (FBS; 5 μl; HyClone, Logan, UT) was added to the drop to release the electrostatic charge and the pure trophectoderm portions were removed and immediately processed for RNA.

Stem Cells and Feeder Cells

Samples in the form of frozen cell pellets of 129 SvEv murine embryonic stem cells (1.1×10^7 cells) and irradiated embryonic murine fibroblast feeder cells (2×10^6 cells) were obtained from Ute Hochgeschwender at the Oklahoma Medical Research Foundation. The pellets were resuspended in 200 μl of PBS and processed for RNA.

RNA Extraction

Blastocysts and Trophectoderm

RNA was isolated from the blastocyst and trophectoderm samples using the NucleoSpin RNA and Virus Purification Kit (Clontech, Mountain View, CA). Samples to be processed were placed in 175 μl of cell lysis buffer. 1.75 μl of β-mercaptoethanol

was added and the samples were mixed by pipetting and vortexing. 175 µl of 70% ethanol was added to the samples and the tubes were again vortexed. The samples were placed in a NucleoSpin column (Clontech) and centrifuged at 8,000 g for 30 seconds. Once the flowthrough was discarded, 175 µl of membrane desalting buffer was added to the column, and the tube was centrifuged at 11,000 g for 1 minute. After discarding the flowthrough, DNase I (50 µl; Clontech) was added to the column and incubated for 15 minutes at room temperature. 100 µl of wash buffer I was added and the column was centrifuged at 8,000 g for 30 seconds. The flowthrough was discarded, 300 µl of wash buffer II was added, and the column was centrifuged at 8,000 g for 30 seconds. A second wash was performed using 125 µl of wash buffer II followed by centrifugation at 11,000 g for 2 minutes. The sample RNA was eluted by adding 30 µl of nuclease-free water, centrifuging at 11,000 g for 1 minute, and repeating a second time. RNA concentrations were determined by UV spectroscopy and the samples were frozen at -80^{o}C.

Stem Cells and Feeder Cells

The stem cell samples and feeder cells were processed using the same NucleoSpin RNA Kit. Cell lysis buffer (700 µl) was added directly to the samples which had been resuspended in PBS. After β-mercaptoethanol (7 µl) was added to the samples and vortexed, the samples were split in half and centrifuged in NucleoSpin Filter units (Clontech) at 11,000 g for 1 minute in order to reduce the viscosity. Each sample was then processed as previously described from the addition of the 70% ethanol to the final rinse with wash buffer II with the exception that the volumes of all added reagents were

doubled due to the increased cell concentrations. The samples were then eluted with 2 washes of 40 μl of water. Concentrations were once again determined by UV spectroscopy and the samples were frozen at -80^{o}C.

Sample cDNA Synthesis

Blastocysts and Trophectoderm

The blastocyst and trophectoderm samples had limited availability and therefore were processed from RNA to cDNA using the SuperSMART PCR cDNA Synthesis Kit (Clontech) according to the manufacturer's protocol. This kit allows SSH users to begin with as little as 10 ng of total RNA, however the blastocyst samples began with approximately 230 ng of total RNA and the trophectoderm sample began with 300 ng of total RNA. In brief, a 2 minute denaturation at 65^{o}C was followed by first strand synthesis at 42^{o}C for 90 minutes. The reaction primer, 3' SMART cDNA synthesis (CDS) primer, is an oligo-dT primer which only allows for mRNA amplification. A SMART II A oligonucleotide is also included which pairs with additional cytosine nucleotides added to the 5' end of the mRNA by the terminal transferase action of the reverse transcriptase (RT). This allows the RT to switch templates providing for total replication of the mRNA 5' end. In addition, both the CDS primer and the SMART II A oligonucleotide contain a primer amplification site that allows for future exponential amplification. Following first strand cDNA synthesis, the products are purified in a NucleoSpin Extraction Spin Column (Clontech) to remove cDNA fragments less that 100

base pairs as well as unincorporated nucleotides. The samples were eluted in 80-85 μl of water.

The cDNA synthesis was completed by an optimized PCR protocol in continuance of the SuperSMART protocol using the Advantage 2 PCR Kit (Clontech). Three tubes containing 27 μl of first strand cDNA product were set up for each sample and one of the tubes was used to determine the optimal number of amplification cycles. Aliquots were pulled every three cycles from cycle 15 through 30 and analyzed on a 1.2% TAE agarose gel. The blastocyst sample was optimized at 23 cycles while the trophectoderm was optimized at 27 cycles. The remaining two samples were amplified for the optimized number of cycles in the Perkin-Elmer 9600 thermal cycler (Applied Biosystems, Foster City, CA). Parameters were an intial denaturation of 95^{o}C for 1 minute followed by the optimized number of cycles of 95^{o}C for 5 seconds, 65^{o}C for 5 seconds, and 68^{o}C for 6 minutes. Aliquots (5 μl) of each sample were analyzed on a 1.2% TAE agarose gel and the tubes were combined for each sample.

Following PCR, the amplified products were purified with an equal volume of phenol:choloroform:isoamyl alcohol (25:24:1) and concentrated with 700 μl of n-butanol. The samples were further purified using the Clontech CHROMA SPIN-1000 columns according to the Super SMART PCR cDNA Synthesis Kit protocol. The columns are optimized for purifying fragments greater than 1,350 bases while remove proteins, enzymes, primers, excess dNTPs, and small nucleotide fragments. Presence of the PCR product was confirmed in the final sample by analyzing aliquots on a 1.2% TAE agarose gel.

In preparation for the subtraction protocol, the purified PCR product was digested with *Rsa I* at 37°C for 3+ hours to create short, blunt-ended DNA fragments. During the subtraction protocol, the blunt ends are needed for adaptor ligation and subsequent subtraction. In addition, the digestion removed the SMART II A oligonucleotide and the 3' SMART CDS Primer II A from the amplicons since each contains an *Rsa I* site. The reaction was analyzed with 10 µl aliquots on a 1.2% TAE agarose gel and subsequently stopped with the addition of 8 µl of 0.5 M ethylenediaminetetraacetic acid (EDTA).

Digested samples were purified using the QIAquick PCR Purification Kit (Qiagen, Valencia, CA) according to the manufacturer's protocol. Briefly, Buffer PB and the digested samples were combined in a 5:1 ratio, mixed, and filtered through a QIAquick spin column (750 µl at a time) by centrifugation at approximately 10,000 g for 60 seconds. Flow-through was discarded and the column filter was washed with 0.75 ml of Buffer PE and centrifuged at 10,000 g for 60 seconds. The flow-through was discarded and the column centrifuged for an additional minute at 10,000 g. Purified, digested DNA samples were eluted by applying 50 µl of TE (10 mM Tris-Cl, 1 mM EDTA, pH 8.0) to the center of the membranes, allowing them to stand for 1 minute, and centrifuging at 10,000 g for 1 minute. Subsequently, the purified samples were processed according to the Super SMART PCR Synthesis Kit User Manual.

Eluted samples were applied to a microfiltration column (Clontech) and centrifuged for 5 minutes at 10,000 g. Precipitation of the collected sample was performed with the addition of 50 µl of 4 M ammonium acetate (Clontech) and 375 µl of 95% ethanol followed by vortexing and centrifugation at 16,000 g for 10 minutes. The supernatant was discarded, 500 µl of 80% ethanol was added, and the tube was

centrifuged for 10 minutes at 16,000 g. Once again, the supernatant was discarded and dried pellets were resuspended in 6.7 μl of 1X TNE buffer (10 mM Tris-HCl [pH 8], 10 mM NaCl, 0.1 mM EDTA).

Aliquots of the DNA samples (1.2 μl in 11 μl of water) were used to determine the DNA concentration by UV spectrophotometry. The two blastocysts samples for the blastocyst versus blastocyst comparison had high concentrations and were diluted to the maximum protocol concentration of 300 ng/μl. The third blastocyst sample had a concentration of 290.3 ng/μl and the trophectoderm sample had a concentration of 297.6 ng/μl and therefore neither was diluted. The final samples were then ready for adaptor ligation.

Stem Cells and Feeder Cells

The stem cells and feeder cells were available in larger quantities than the embryonic cells and therefore were processed to cDNA using the Clontech PCR-Select^{TM} cDNA Subtraction Kit according to the provided protocol. As directed in the protocol, a supplied control Poly A^+ RNA sample from human skeletal muscle was processed along with the experimental samples to verify protocol success.

In brief, 2 μg of RNA from each sample was combined with cDNA Synthesis Primer (10 μM; Clontech) and incubated at 70^{o}C for 2 minutes, followed by 2 minutes on ice. Following brief centrifugation, 5X First-Strand Buffer (Clontech), dNTP mix (10 mM each; Clontech), water, and AMV Reverse Transcriptase (20 units/μl; Clontech)

were added to each sample and incubated at 42°C for 1.5 hours to complete first strand cDNA synthesis.

The samples were placed on ice to terminate the first strand synthesis and were immediately processed for second strand synthesis. Water, 5X Second-Strand Buffer (Clontech), dNTP mix (10 mM; Clontech), and 20X Second-Strand Enzyme Cocktail (Clontech) were added to the tubes for a total volume of 80 µl. Following incubation at 16°C for 2 hours, T4 DNA Polymerase (6 units; Clontech) was added to each sample and incubated at 16°C for an additional 30 minutes. Second strand synthesis was terminated with the addition of 4 µl of 20X EDTA/Glycogen mix (0.2 M EDTA; 1 mg/ml glycogen; Clontech).

The samples were extracted with 100 µl of phenol:chloroform:isoamyl alcohol (25:24:1) followed by two cycles of 100 µl of cholorform:isoamyl alcohol (24:1). Sample precipitation was obtained with the addition of 40 µl of 4M ammonium acetate and 300 µl of 100% ethanol. Following 20 minutes of centrifugation at 16,000 g, the pellet was washed twice with the addition of 500 µl of 70% ethanol and centrifugation for 10 minutes at 16,000 g. The pellets were dissolved in 50 µl of water and then proceeded to an *Rsa I* digestion.

Each DNA sample was digested with *Rsa I* (10 units/µl; Promega, Madison, WI) for 1.5 hours at 37°C. Addition of 2.5 µl of 20X EDTA/Glycogen mix terminated the reaction and the digested samples were extracted twice each with the addition of 50 µl of phenol:chloroform:isoamyl alcohol (25:24:1) followed by the addition of 50 µl of chloroform:isoamyl alcohol (24:1). Extracted samples were precipitated by the addition of 25 µl of 4M ammonium acetate and 187.5 µl of 100% ethanol and centrifugation for

20 minutes at 16,000 g. The pellets were washed with the addition of 200 µl of 70% ethanol and centrifugation followed by 100 µl of 70% ethanol. DNA samples were resuspended in 5.5 µl of water and were then ready for adaptor ligation.

Suppression Subtraction Hybridization

The cDNA samples prepared for the blastocyst, trophectoderm, stem cells, and feeder cells through the Super SMART™ PCR cDNA Synthesis Kit and the Clontech PCR-Select™ cDNA Subtraction Kit were processed in a pair-wise fashion beginning with the adaptor ligation step of the Clontech PCR-Select™ cDNA Subtraction Kit. The four comparisons being performed were blastocyst versus blastocyst, trophectoderm versus blastocysts, blastocyst versus stem cell, and stem cell versus feeder cell. Both the blastocysts versus blastocyst and the stem cell versus the feeder cells served as control comparisons.

For each pair, the comparison was performed twice. First one of the comparison samples served as the "tester" or experimental sample while the second sample served as the "driver" or control sample. A second comparison with the tester and driver samples reversed was then performed allowing for identification of uniquely expressed genes in both samples.

In the adaptor ligation protocol, the tester cDNA sample was divided into two aliquots. Each aliquot was ligated to either the adaptor with the forward primer site (Adaptor 1) or the adaptor with the reverse primer (Adaptor 2R). A control tester sample ligated to both adaptors was also created. The ligation protocol in brief was as follows.

Each experimental tester cDNA sample was diluted by adding 1 μl to 5 μl of water. A ligation master mix was made with the following reagents for each reaction: water (3 μl), 5X Ligation buffer (2 μl; Clontech), and T3 DNA Ligase (1 μl of 400 units/μl; Clontech). Each tester cDNA was then ligated to each adaptor. For Adaptor 1, 2 μl of diluted cDNA was mixed with 2 μl of Adaptor 1 (10 μM; Clontech) and 6 μl of the Master Mix. For Adaptor 2R, 2 μl of the diluted cDNA was mixed with 2 μl of Adaptor 2R and 6 μl of the Master Mix. A third ligation tube was then set up combining 2 μl of each of the adaptor reaction mixtures in order to serve as the unsubtracted tester control.

Following mixing, each adaptor ligation tube was incubated at 16^{o}C overnight (~ 12 hours). The reactions were stopped with the addition of 1 μl of 20X EDTA/Glycogen mix and the ligase was heat inactivated by incubation at 72^{o}C for 5 minutes.

The ligation efficiency was analyzed for each reaction through PCR using G3PDH (glyceraldehyde-3-phosphate dehydrogenase; also known as GAPDH) primers and gel electrophoresis. G3PDH is considered a housekeeping gene that is constitutively expressed in all tissues and therefore should be present in each test sample. Four tubes were set up for each experimental and control cDNA sample. Tube 1 contained 1 μl of the tester ligated to Adaptor 1, 1 μl of the G3PDH 3' Primer (10 μM; Clontech), and 1 μl of the PCR Primer 1 (10 μM; Clontech). Tube 2 contained 1 μl of the tester ligated to Adaptor 1, 1 μl of the G3PDH 3' primer, and 1 μl of the G3PDH 5' primer. Tube 3 contained 1 μl of the tester ligated to Adaptor 2R, 1 μl of G3PDH 3' Primer, and 1 μl of PCR Primer 1. Tube 4 contained 1 μl of the tester ligated to Adaptor 2R, 1 μl of G3PDH 3' Primer, and 1 μl of G3PDH 5' Primer. A master mix was made for each reaction

containing 18.5 µl of water, 2.5 µl of 10X PCR reaction buffer, 0.5 µl dNTP mix (10 mM), and 50X Advantage cDNA Polymerase mix (Clontech). The 22 µl of master mix was added to each of the previous four tubes and incubated for 5 minutes at 75°C to extend both adaptors. PCR was begun by 30 seconds at 94°C followed by 25 cycles of 10 seconds at 94°C, 30 seconds at 65°C, and 2.5 minutes at 68°C. Gel electrophoresis was subsequently performed on a 2.0% TAE agarose gel with 5 µl aliquots from each reaction.

Following verification of successful ligation, the first pair-wise hybridization was performed for each comparison in two separate tubes. In this protocol, driver and tester samples are mixed, heat denatured, and allowed to mix. The single stranded cDNAs that remain at the end of the reaction contain increased concentrations of differentially expressed genes and are available for binding in the second hybridization.

For the first hybridization, the first tube contained 1.5 µl of driver cDNA, 1.5 µl of adaptor 1 ligated tester cDNA, and 1 µl of 4X Hybridization Buffer (Clontech). A second tube contained 1.5 µl of driver cDNA, 1.5 µl of adaptor 2R ligated tester cDNA, and 1 µl of 4 X Hybridization Buffer. Both sample tubes were incubated at 98°C for 1.5 minutes followed by 8-12 hours of incubation at 68°C. Upon completion of the first hybridization, the samples were immediately processed for the second hybridization.

In the second hybridization, additional driver was denatured by mixing 1 µl of driver cDNA, with 1 µl of 4X Hybridization Buffer and 2 µl of water followed by incubation for 1.5 minutes at 98°C. Denatured driver and the two samples from the first hybridization were mixed simultaneously together and incubated at 68°C overnight. Following the incubation, 200 µl of the dilution buffer was added and the sample was

incubated at 68°C for an additional 7 minutes. The resulting hybridized molecules contained the differentially expressed cDNAs with different adaptors (Adaptor 1 and Adaptor 2R) on each end. These samples were then amplified through PCR.

PCR was performed for each hybridized sample, the unsubtracted tester control, and the PCR control subtracted cDNA provided in the kit. A master mix for each reaction was made containing 19.5 µl of water, 2.5 µl of 10X PCR reaction buffer (Clontech), 0.5 µl dNTP mix (10 mM; Clontech), 1.0 µl PCR Primer 1 (10 µM; Clontech), and 0.5 µl 50X Advantage cDNA polymerase mix. 24 µl of the master mix was added to 1 µl of each reaction sample and incubated at 75°C for 5 minutes in order to complete the missing adaptor strands. PCR was then performed in the Perkin-Elmer GeneAmp PCR System 9600 with 25 seconds at 94°C followed by 27 cycles of 10 seconds at 94°C, 30 seconds at 66°C, and 1.5 minutes at 72°C. The final products were analyzed on a 2.0% TAE agarose gel.

Product from the primary PCR was diluted by adding 3 µl to 27 µl of water. The diluted PCR product was then used in a secondary PCR reaction using nested primers in order to further select for the differentially expressed cDNAs while also decreasing any background product. A master mix for each reaction was mixed containing 18.5 µl water, 2.5 µl of 10 PCR reaction buffer, 1.0 µl of Nested PCR primer 1 (10 µM; Clontech), 1.0 µl of Nested PCR primer 2R (10 µM; Clontech), 0.5 µl dNTP mix (10 mM), and 0.5 µl of 50X Advantage cDNA polymerase mix. 24 µl of the master mix was added to 1 µl of the diluted primary PCR product and amplified in the Perkin-Elmer 9600 for 10 cycles of 94°C for 10 seconds, 68°C for 30 seconds, and 72°C for 1.5 minutes. The final products were analyzed on a 2.0% TAE agarose gel.

A final subtraction efficiency PCR was performed to analyze the resulting PCR products using the G3PDH housekeeping gene previously used in the ligation efficiency test. Subtracted and unsubtracted PCR products were diluted 10 fold based on DNA concentration. A reaction tube for each diluted product was mixed containing 1 μl of diluted cDNA, 1.2 μl of G3PDH 3' Primer (10 μM), 1.2 μl of G3PDH 5' Primer (10 μM), 22.4 μl water, 3.0 μl 10X PCR reaction buffer, 0.6 μl dNTP mix (10 mM), and 0.6 μl 50X Advantage cDNA Polymerase mix. The reaction was amplified in the Genemate Genius Thermal Cycler for 33 cycles of 30 seconds at 94^{o}C, 30 seconds at 60^{o}C, and 2 minutes at 68^{o}C. After cycles 18, 23, 28, and 33, 5 μl of each amplified product was removed from the reaction tube. Following completion of the PCR, each 5 μl sample was analyzed on a 2.0 % TAE agarose gel for evidence of a decrease of G3PDH in subtracted products in comparison to the unsubtracted samples.

Cloning and Sequencing of Subtracted cDNA

Upon amplification of the uniquely expressed cDNA sequences through the suppression subtraction hybridization protocol, the secondary PCR products were cloned using one of two methods. Initially, amplified products from the blastocyst and stem cell comparison were cloned into pBluescript II SK (+) (Stratagene, La Jolla, CA) and placed into TOP 10F' *E. coli* (Stratagene). In brief, the amplified cDNA and the plasmid were restriction digested with both *Sma I* and *Eag I* (New England Biolabs, Ipswich, MA) to produce complementary DNA ends. Subsequently the plasmid and digested cDNA were ligated in reactions set up in 1:1, 1:2, and 1:3 ratios, placed into the TOP 10F' cells, and

plated on 2YT (Amp 100) agar plates. (The plasmid contained an ampicillin resistance gene.) Following overnight incubation at 37°C, colonies were picked, grown overnight in 2YT broth, and miniprepped using a standard plasmid isolation protocol.

Subsequently, additional products from all of the comparisons except for blastocyst versus blastocyst (which as a control reaction wasn't cloned) were cloned into the TOPO TA Cloning Kit for Sequencing (Invitrogen, Carlsbad, CA) according to the manufacturer's protocol. The included vector, pCR®4-TOPO®, contained a 3' thymidine overhang making it compatible for ligation with PCR products produced with *Taq* polymerase which adds a deoxyadenosine overhang to its PCR amplicons. Insertion of the DNA segment into the vector disrupts the expression of a lethal *ccd*B gene, so that only the TOP10 *E. coli* cells containing recombinant vectors are allowed to grow, eliminating the need for blue-white screening as in other protocols.

The TOPO cloning procedure in brief is as follows. The cloning reaction was mixed containing 4 µl of fresh secondary PCR product, 1 µl of salt solution (1.2 M NaCl, 0.06 M $MgCl_2$; Invitrogen), and 1 µl of the TOPO vector (10 ng/µl; Invitrogen) and incubated for 30 minutes at room temperature followed with placement on ice. For the transformation, 2 µl of the cloning reaction was gently mixed with one vial (50 µl) of the One Shot® Chemically Competent *E. coli* (Invitrogen) and placed on ice for 5 minutes. The tube was subsequently heat-shocked for 30 seconds at 42°C followed by placement on ice. 250 µl of S.O.C. (Super Optimal Catabolite Repression Broth) medium (2% tryptone, 0.5% yeast extract, 10 mM NaCl, 2.5 mM KCl, 10 mM $MgCl_2$, 10 mM $MgSO_4$, 20 mM glucose; Invitrogen) was added to the reaction and the tube was shaken horizontally (200 rpm) for 1 hour at 37°C. Colonies were grown overnight on LB (Luria-

Bertani) agar plates containing 100 μg/ml of ampicillin. Selected colonies were subsequently grown overnight in LB broth containing 100 μg/ml of ampicillin. The plasmids were extracted from the cultures using a standard min-prep protocol and quantified by UV spectrophotometry.

Plasmid inserts were then sequenced by the Oklahoma State University Recombinant DNA/Protein Resources Facility and the sequences were analyzed using BioEdit 5.0.9 [44]. The identity of each sequence was obtained through use of the National Center for Biotechnology Information (NCBI) Basic Local Alignment Search Tool (BLAST) which compares the given nucleotide sequence with those of known sequences within their GenBank database (Bethesda, MD) and determines the statistical significance of any matches.

Confirmation Through PCR

From the identified cloned inserts, primers were designed for 22 sequences (Table 3.1) that were of non-ribosomal origin using the Primer Select portion of the Lasergene sequence analysis software [45] and obtained from Invitrogen. RNA from the original samples was converted to cDNA in a reverse transcriptase reaction. In addition, a second type of stem cell, C57BL/6, was also used as a PCR sample in order to verify the validity of the results in other strains of murine stem cells.

For the reverse transcriptase reactions, 1.5 μl of random decamer primer (150 ng/μl; Invitrogen), 5-6 μl of RNA (5 μg), and water were mixed in an 11 μl reaction and incubated at 70^{o}C for 10 minutes. Following placement on ice and a brief centrifuge, 4

μl of 5X First Strand Buffer (Clontech), 2 μl of dNTP mix (10 mM each; Clontech), 2 μl of DTT (dithiothreitol; 100 mM; Clontech), and 1 μl of PowerScript RT (Clontech) were added. The reaction was incubated at 42°C for 90 minutes followed by heating at 70°C for 15 minutes.

PCR and agarose gel electrophoresis was subsequently performed to confirm expression patterns for the 22 DNA sequences. The reactions consisted of 0.5 μl cDNA (0.25 μg/μl), 17.0 μl of water, 2.5 μl 10X Advantage 2 PCR Buffer (Clontech), 0.5 μl 50X dNTPs (10 mM each; Clontech), 2.0 μl of each primer (10 μM; Invitrogen), and 0.5 μl 50X Advantage 2 Polymerase (Clontech). The cycling parameters in general were an initial denaturation at 95°C for 1 minute, followed by 30 cycles of 95°C for 30 seconds, 58°C for 30 seconds, and 68°C for 1 minute. A final extension was performed at 68°C for 1 minute.

Quantification with Real Time Polymerase Chain Reaction

From the identified uniquely expressed DNA segments, three genes of interest were selected for additional quantitative study of the expression patterns through the real time polymerase chain reaction (qPCR). The three genes, peroxiredoxin 1 (Prdx 1), tyrosine 3-monooxygenase/tryptophan 5-monooxygenase activation protein (Ywhaz), and voltage-dependent anion channel 3 (Vdacs3), were all three found to be uniquely expressed in the blastocyst versus embryonic stem cell comparison, the main comparison of interest.

In addition to the three genes of interest, reactions were also run from each sample for ribosomal 18s (r18s), a housekeeping gene used as a standard of comparison

for relative quantification. The real time reactions were semi-quantitative rather than quantitative in that the original number of transcripts for each gene was not absolutely measured but was measured in comparison to the expression of the r18s gene.

For the real time PCR, new stem cell, feeder cell, and blastocyst samples were collected and processed to RNA as previously described. Initial quantities of cells were 1 x 10^7 for the 129 SvEv stem cells, 1.8 x 10^6 for the irradiated mouse embryonic fibroblast feeder cells, and 20 blastocysts. The gene expression levels were also analyzed in a second strain of murine stem cell, C57BL/6, whose initial quantity was 1.25 x 10^7. Following RNA isolation, cDNA was produced using the reverse transcriptase procedure previously described.

For the qPRC reaction, primers were designed for the three genes using Primer Select and obtained from Invitrogen (Table 3.2). The r18s primers utilized were originally designed by Dr. Marino in the lab of Dr. Miller at the University of Tulsa [46]. The specificity of all four sets of primers was checked through NCBI Blast searches. Real time PCR was subsequently performed using the DyNAmo^{TM} HS SYBR Green qPCR Kit (Finnzymes, Finland) in the DNA Engine Opticon 2 (BioRad, Hercules, CA). In the DyNAmo HS SYBR Green kit, SYBR Green 1 fluorescent dye emits fluorescence when bound to the double-stranded amplicons and therefore produces increasing fluorescence with each additional PCR cycle.

For each reaction, 1 μl of template cDNA (0.25 μg/ul), 0.75 μl of each primer (10 μM; Invitrogen), 12.5 μl 2X Master Mix (Finnzymes), and 10 μl of water were used. The 2X Master Mix contained modified DyNAmo hot start DNA polymerase, SYBR Green 1, optimized PCR buffer, 5 mM $MgCl_2$, and a dNTP mix. General reaction parameters were

95°C for 15 minutes followed by 43 cycles of 94°C for 20 seconds, 53-55°C for 45 seconds, 72°C for 45 seconds, 76°C for 1 second with plate read, and 78°C for 1 second with plate read. A melting curve from 50°C to 90°C was also performed for each reaction. Reactions were performed twice with duplicate wells (for a total of 4 data sets for each gene per sample) and with control reactions in each amplification run. The control reactions included no reverse transcriptase samples and no template reactions.

Following completion of the real time PCR reactions, the threshold (C_T) number was determined for each sample reading of the four genes. The C_T number for each of the three genes of interest in each sample was compared with the C_T number for the r18s housekeeping gene in that sample in order to calculate the fold difference of expression. Specifically, the delta C_T (ΔC_T) was calculated by subtracting the control r18s C_T from the experimental gene C_T value for each reading. These ΔC_T values were averaged for each gene in each sample. The expression of each gene across the samples was compared by subtracting the largest average ΔC_T for each gene from the other ΔC_T gene values to determine the $\Delta\Delta C_T$ for each sample tested for that specific gene. The fold difference of relative gene expression was calculated for each gene sample using the formula $2^{-\Delta\Delta C_T}$.

Statistical Analysis

The ΔC_T values for each sample tested within each gene were analyzed using the SPSS (Statistical Package for the Social Sciences; SPSS Inc, Chicago, IL). Homogeneity of variance was confirmed using the Levene's statistic with a P value of 0.05 for each gene data set followed by an ANOVA (Analysis of Variance) with a P value significance level of 0.05. Following a determination of significant difference of relative gene

expression levels with the ANOVA, Tukey's honestly significance difference (Tukey's HSD) multiple comparison test was performed with a P value of 0.05 to determine specifically which changes in gene expression were significant.

Table 3.1: Primer Sequences Used in Confirmation PCR Reactions.

Clone Number:	Primer Sequences:	Ta: (^{o}C)	Product Size: (bp)
129-1-C1	5' - CGTGAATCGGGGGACCTTG - 3'	58.0	503
	5' - CCCGACGGCATCTTTATTACACAG - 3'		
129-1-C3	5'- CTGGCGAAAGGGGGATGTG -3'	56.3	488
	5' - GCAGTAACAGCAAGGGTGAAAAG - 3'		
129-1-C4	5' - CGGGCCTCTTCGCTATTACG - 3'	57.5	488
	5' - ACCCCCTCCTCTCAGTCTCCATC - 3'		
129-1-C6	5' - GGCGGCCAAGCAGTTCATAG - 3'	57.9	568
	5' - CAGCCCCAGCACAGGACAAC - 3'		
129-1-C7	5' - GCCCCTTAGCTGACCTCTGG - 3'	55.9	397
	5' - GCTTCCGGCTCGTATGTTGTG - 3'		
129-2-C11	5' - CGGGCCTCTTCGCTATTACG - 3'	58.5	592
	5' - GCTTTTGCCCTTCTGCTCCAC - 3'		
B5A-C2	5' - CGGGCCTCTTCGCTATTACG - 3'	58.4	591
	5' - GACACCCCAGAAGAGGACATCAG - 3'		
B5B-C8	5' - CAGGGAAATAACTTGAGATGACGGC - 3'	54.0	317
	5' - GTGGGAGGTGGCTGAGGATGG - 3'		
B5B-C10	5' - CATGACACTACGTTGTTGCTGAGG - 3'	53.6	304
	5' - GTTGGATTGGGATTTGAACTGGAG - 3'		
B5B-C12	5' - CGCCATCGGAGAGCATCAG - 3'	60.1	353
	5' - TGGGGGAGGGTTCATCAATC - 3'		
B5B-C13	5' - CCCTCCTGTATGTTTTCGTCTTGC - 3'	57.3	416
	5' - CGTTTGCCCGGCCCACTCTC - 3'		
B5B-C14	5' - TTAAGCTCCATAGGGTCTTCTCGTC - 3'	54.5	280
	5' - GATAAAAGGAACTCGGCAAACAAG - 3'		
B5B-C15	5' - GACCCCAAGACATGTGAGCAACTG - 3'	56.3	581
	5' - GACCAAAACCGCCTGACACCTG - 3'		
B5B-C16	5' - CTAGGGAGGCACAGCAATCACTTC - 3'	55.9	496
	5' - TGAGGCCAGGCACCAAGG - 3'		
B5B-C17	5' - CTGGCAAACAGGACTGAGGTAGC - 3'	55.2	496
	5' - GTGTGGAATTGTGAGCGGATAAC - 3'		
B5B-C18	5' - CACAGAGCGGCCAACGGG - 3'	56.1	535
	5' - GGGCGACCTCTTCCTGCG - 3'		
F1-C1	5' - CATTTTCAGGGGACAGACAGACTTG - 3'	55.6	512
	5' - CCGACGAACCCTCCAGAATAG - 3'		
F1-C2	5' - CCCGTTCTTTGGTTTATTGTTCAG - 3'	54.1	194
	5' - CTCCATAATTATAAGAGCCGTTGTGC - 3'		
F1-C4	5' - CTATAATCATGGCCCGAGGACTTC - 3'	52.6	274
	5' - CGTGTGTGTGAGGGTTGGAGG - 3'		
F1-C5	5' - CTGTGCAATGAATAGTTTAAAAATCTCTG - 3'	52.1	269
	5' - GATCTGGCCATAGGATAAAGGATACC - 3'		
F1-C6	5' - GTTGGGGGAGGTGATGACTTG - 3'	55.7	287
	5' - ACAGCGGGAAGGATGGAAAC - 3'		
T - C1	5' - GGCCCACTTAGATATTGATTTGTTG - 3'	51.6	204
	5' - GGGTTGCCATTTCCTTCTCCAG - 3'		

Table 3.2: Primer Sequences Used in Real Time PCR reactions.

Gene:	Primers:	Ta: (^{o}C)	Product Size: (bp)
Prdx1	5' - TGAATACAAAGGAAAATATGTTGTGTTCTTC - 3'	52.8	175
	5' - TGTGTTAATCCATGCCAGATGACA - 3'		
Vdacs	5' - ATTTGTACCAAACACAGGAAAGAAGAG - 3'	54.7	267
	5' - CCAAACTCAGTGCCATCATTCAC - 3'		
Ywhaz	5' - CATCTGCAACGATGTACTGTCTCTT - 3'	53.2	161
	5' - GTGACTGGTCCACAATTCCTTTC - 3'		
r18s	5' - TCAAGAACGAAAGTCGGAGGTT - 3'	61.0	488
	5' - GGACATCTAAGGGCATCACAG - 3'		

CHAPTER IV

FINDINGS

Sample cDNA Synthesis

Blastocyst and Trophectoderm

The blastocyst and trophectoderm samples both began the suppression subtraction hybridization (SSH) process with the Super SMART^{TM} PCR cDNA Synthesis Kit which allows for starting total RNA concentrations of 10 ng to 1000 ng. Each of the 5 blastocyst samples began with 232.4 ng of total RNA while the trophectoderm sample began with 301.5 ng.

Following the 33 PCR cycles of the second strand synthesis optimization protocol, cDNA products were observed on the agarose gels for the blastocysts and trophectoderm ranging from .4 kb to over 4 kb (Figure 4.1 – blastocyst gel). The gels revealed the optimum number of PCR cycles for the blastocyst to be 23 while the trophectoderm sample required 27 cycles. The optimum number of cycles was one cycle less than the number required to reach plateau amplification.

Once the cDNA products were amplified, they were purified by column chromatography. Subsequent agarose gel electrophoresis analysis revealed that both the first and the second elution fractions contained a significant portion of the cDNA samples

for both the blastocyst and trophectoderm samples, so for each sample, the two elution fractions were combined for the rest of the experiment (data not shown).

Following the *Rsa I* digestion and purification of the blastocyst and trophectoderm cDNA samples, UV spectrophotometry was used for sample quantification. All samples ranged from 2-4 ug of cDNA which was within the expected quantities of 2-6 ug. Several of the blastocysts samples had higher concentrations than what was allowed for adaptor ligation (300 ng/µl) so each was diluted to the allowable concentration. The trophectoderm was slightly below this concentration (~297 ng/µl) and therefore was not diluted.

Stem Cells and Feeder Cells

The 129 SvEv stem cells and fibroblast feeder cells began the SSH process with the PCR-Select cDNA Subtraction Kit due to their increased number of available cells. Following the cDNA synthesis, purification, and *Rsa I* digestion, the products were analyzed by agarose gel electrophoresis. As in the blastocyst and trophectoderm samples, cDNA products ranged from .4 kb to over 4 kb (data not shown).

Suppression Subtraction Hybridization

For each of the samples being compared in SSH, Adaptor 1 and Adaptor 2R were ligated to aliquots of the tester sample. To confirm ligation success, a ligation efficiency PCR was performed using two different sets of primers. One set of primers was specific for the G3PDH housekeeping gene and produced an amplicon approximately 500 bp

(base pairs). The second set of primers contained one primer for the 3' end of the G3PDH gene and a second primer that is specific for the adaptor region that produced a band approximately 1.2 kb. A sample gel is shown for the blastocyst versus blastocyst comparison in Figure 4.2.

The final control reaction of the SSH procedure was a PCR of the G3PDH housekeeping gene in the subtracted and the unsubtracted tester samples of each comparison. Samples were pulled from each of the reaction tubes every 5 PCR cycles from cycle 18 through cycle 33 and analyzed on an agarose gel. The G3PDH product appeared in the unsubtracted samples 5-10 cycles before it appeared in the subtracted samples giving evidence that the gene levels were indeed decreased in the subtracted sample (Figure 4.3).

For each pair of comparisons, a final agarose gel was run showing the amplified subtracted product from the secondary PCR reaction and the control unsubtracted product. For the blastocysts versus blastocyst control comparison, a single discrete band was visible in the subtracted lanes as compared to general product smearing in the unsubtracted lanes (Figure 4.4). In the trophectoderm and blastocyst comparison, both the forward and reverse subtractions showed a general decrease of product in comparison to the unsubtracted products, however both subtracted samples showed a general smearing of numerous products rather than a limited number of discrete product bands (Figure 4.5). In the stem cell and blastocyst comparison, both subtracted products showed a decrease in product as compared to the unsubtracted samples, however the stem cell sample especially showed a substantial decrease in product bands (Figure 4.6). In the

final comparison, stem cell and feeder cell, a significant decrease of product was also visible in the subtracted versus the unsubtracted lanes (Figure 4.7).

Cloning and Sequencing of Subtracted cDNA

From the amplified subtracted products, approximately 300 clones were selected for analysis. Since the blastocyst versus the stem cell comparison was of the greatest interest, most of the clones came from this comparison, however some clones came from all comparisons except for the blastocyst versus blastocyst comparison. From those 300 analyzed clones, 44 clones were sent for sequencing to the OSU Core Facility. Of the sequenced clones, 8 were from pBluescript II SK+ and the remaining 36 were from pCR4-TOPO. The obtained sequences were compared to known sequences in the NCBI GenBank through a BLAST search. Of the sequenced clones, 11 contained only plasmids, 7 of which were pBluescript II SK+ and 4 were pCR4-TOPO. From the remaining 33 sequences, 10 were of ribosomal origin while the other 23 were of a gene specific origin or else unknown. Table 4.1 summarizes the clone sequences for those other than plasmid only.

Confirmation Through PCR

For the 22 sequences that were of non-ribosomal origin, primers were designed and confirmation PCR reactions were run. All PCR products were examined by agarose gel electrophoresis.

In general, the agarose gels could be visually examined to see evidence of the differential expression of the genes by comparison of the intensity of the PCR product between the two samples. An example of this can be seen in the gel picture for clone 129-1-C1 (Figure 4.8). In a few gels however, such as for F1-C4 and F1-C6, the bands appeared visually equal and the differential expression was not visually evident (data not shown). In other gels, such as B5B-C12, the differential expression was very evident by band intensity, however faint additional bands were evident, giving evidence of the need to optimize the PCR reaction (Figure 4.9).

Since the confirmation PCRs were not quantitative, the research progressed to the real time PCR reactions for quantitative results. However, based on the evidence of differential expression in the confirmation PCR reactions in combination with the identity of the clones based on the GenBank search (Table 4.1), three genes of interest were selected for the subsequent reactions.

Quantification with the Real Time Polymerase Chain Reaction

The gene expression levels of Prdx1, Ywhaz, and Vdacs3 were quantified in comparison to r18s through the real time polymerase chain reaction using the DyNAmo HS SYBR Green qPCR Kit (Finnzymes) in the DNA Engine Opticon 2 (MJ Research) (Figures 4.10 – 4.13). Each gene was tested twice in two different reactions for a total of four data sets for each gene in each sample. Melting curve analysis was also performed for each amplification run to ensure purity of amplification product since the DyNAmo HS SYBR Green binds to any double-stranded DNA product and is not gene specific (Figures 4.14 – 4.17).

The ribosomal 18s C_T values varied across the four different test samples from 11.85 to 22.21 with the highest in the blastocyst sample. It was expected however that the r18s value would be the highest within the blastocyst sample due to the high transcriptional activity associated with development. The real time PCR C_T value and fold difference calculation values can be seen in Table 4.2.

For the gene Prdx1, the lowest level of expression was seen in the feeder cells as expected with the levels of expression in the two stem cell samples surpassing that of the blastocyst sample. The great variation however between fold differences for the two stem cell samples however was an interesting note as the 129 SvEv stem cells had a 7.51 fold difference of expression and the C57BL/6 stem cells had a calculated 27.28 fold difference (Figure 4.18).

In the Ywhaz gene samples, the feeder cells once again expressed the lowest levels of transcript, however the blastocyst sample had a higher fold difference (7.65) of expression than the 129 SvEv stem cells (6.49) but lower level than the C57BL/6 stem cells (16.56) (Figure 4.19).

The blastocyst sample expressed the lowest level of the final gene, Vdacs3, followed by the feeder cells (2.16). The stem cells had a much higher level of fold difference of expression as seen in the 129 SvEv stem cell calculation of 68.07 and C57BL/6 stem cell value of 161.04 (Figure 4.20).

Statistical Analysis

The ΔC_T values for each sample within each gene were analyzed for statistical differences. Levene's Test of Homogeneity (Table 4.3) first confirmed that the group

variances were equal based on p = 0.05 in order to allow further testing by an ANOVA. An ANOVA for each gene confirmed that differences did exist within each comparison with a significance level at p = 0.05 (Table 4.4).

Tukey's HSD analysis was used to confirm the specific significant differences within each gene group with p=0.05 (Table 4.5). The data was also analyzed with the Least Significant Difference (LSD) multiple comparison test (data not shown) which showed a greater number of significant comparisons however since this test is not as stringent as Tukey's HSD and not as widely accepted, presented significance was based only on the Tukey's HSD results.

For Prdx1, the blastocyst sample was significantly different from the C57BL/6 stem cells at a significance of p = 0.034. In addition, the feeder cells were significantly different from the 129 SvEv stem cells (p = 0.014) and the C57BL/6 stem cells (p = 0.000). In the Ywhaz sample, the 129 SvEv stem cells and C57BL/6 stem cells showed significant differences at p = 0.045. The feeder cells also showed significant differences from all other samples (p = 0.000 for all).

The final sample, Vdacs3, showed four significant differences, all at a p = 0.000 value. The first two were between the blastocyst sample and each of the stem cell samples, 129 SvEv and C57BL/6. The second two significant differences existed between the feeder cells and the two stem cell samples.

In summary, the feeder cells showed significantly lower expression of each of these genes from either of the stem cell samples, therefore allowing that any significant differences between the stem cells and the blastocyst sample can be attributed more to the stem cells expression levels and not to any unavoidable feeder cell contamination. When

comparing the stem cell samples, they showed significant differences of expression for the Ywhaz gene but not Prdx1 or Vdacs3. For the blastocyst sample, it showed significant differences from the C57BL/6 stem cells for Prdx1 and from both stem cell samples for Vdacs3.

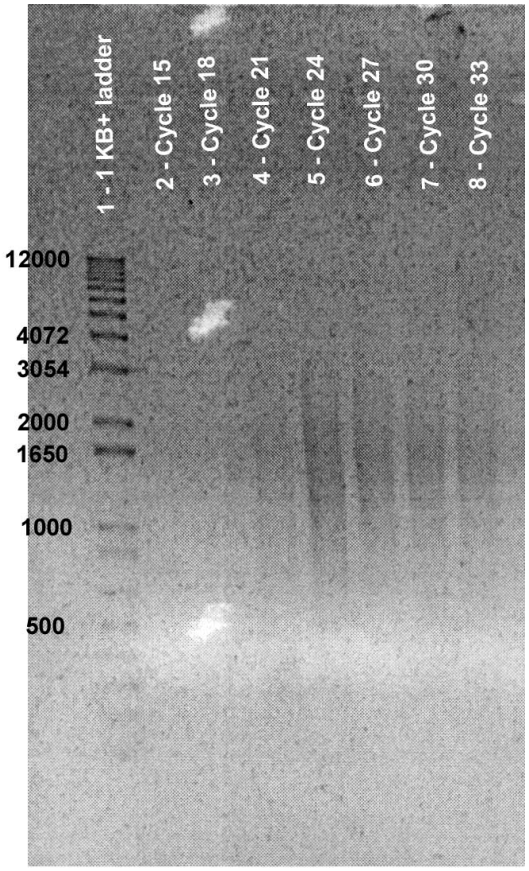

Figure 4.1 PCR Optimization of Blastocyst Sample. Aliquots were pulled from a PCR reaction of a blastocyst sample, every three cycles from cycle 15 through cycle 33 (Lanes 2-8) and analyzed by agarose gel electrophoresis. The optimum number of cycles was determined to be one cycle less than the number required to reach plateau amplification. The optimum number of cycles was determined to be 23. Lane 1 has a 1 KB+ ladder.

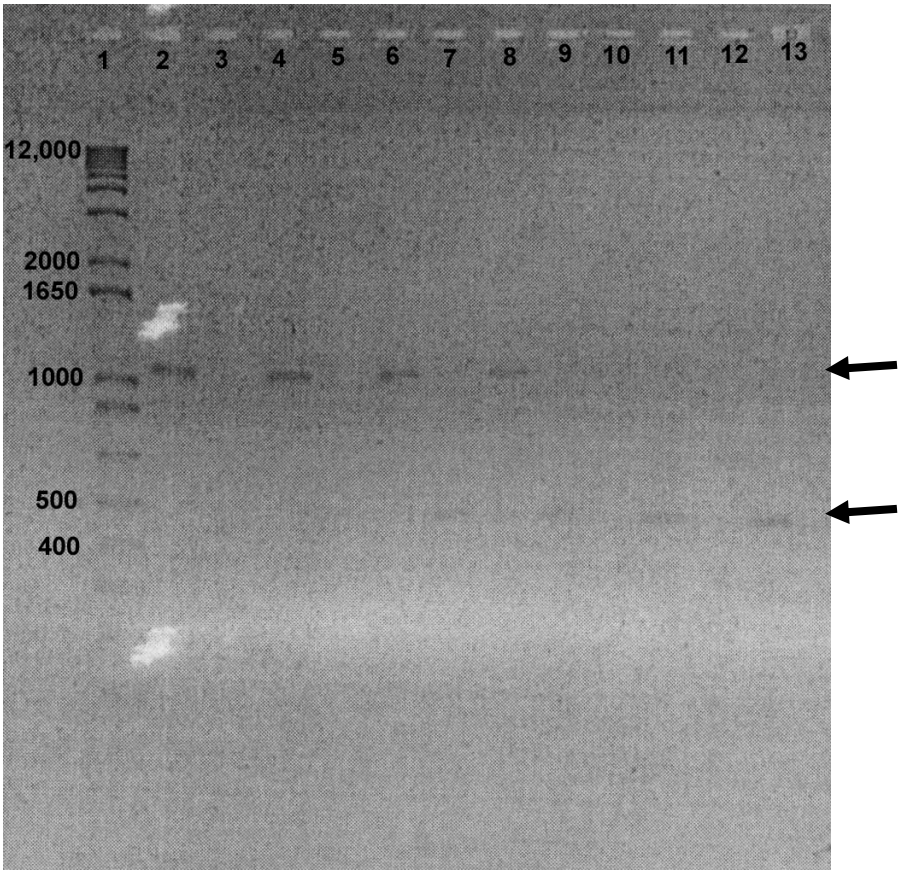

Figure 4.2 Ligation Efficiency PCR for Blastocyst vs. Blastocyst. For each sample tested by SSH, a ligation efficiency PCR was done with primers for the G3PDH gene producing a 500 bp amplicon and an approximately 1.2 kb adaptor region amplicon. This gel shows the bands after 25 cycles as per the kit protocol but due to the faint appearance, the PCR was extended for another 7 cycles and analyzed by gel electrophoresis a second time which showed the bands with greater intensity but also some non-specific smearing due to over-amplification. The product visible on the graph verifies that sufficient adaptor ligation has occurred for the experiment to continue with adequate subtraction efficiency.

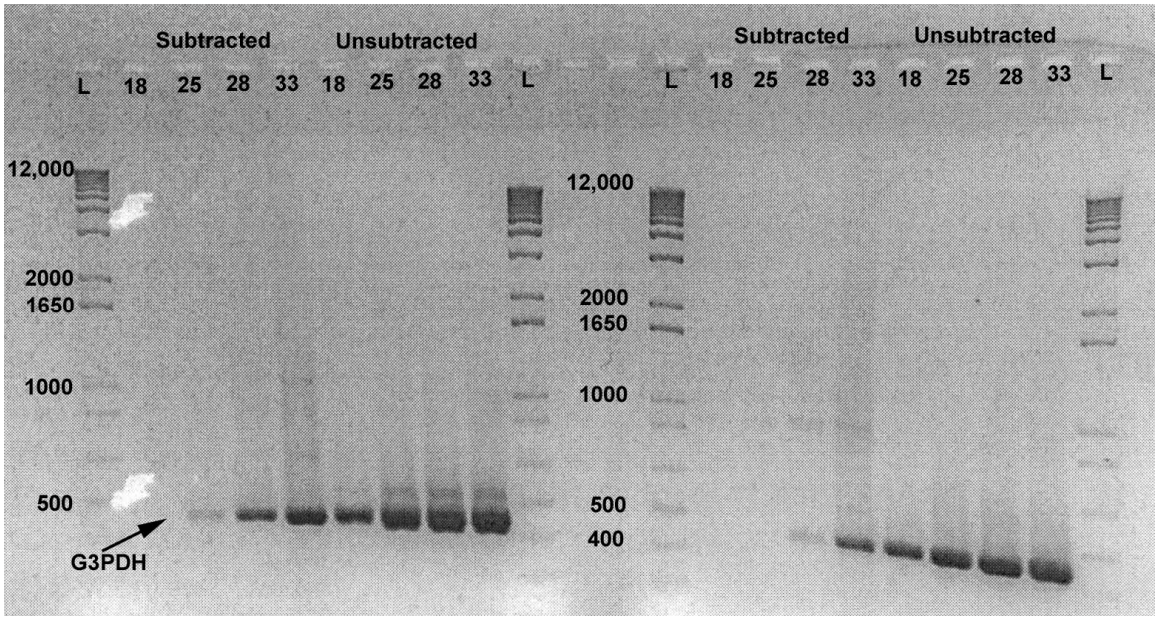

Figure 4.3 Subtraction Efficiency PCR for Blastocyst vs. Blastocyst. For each SSH comparison, a final control PCR amplified the G3PDH gene in both the subtracted and the control unsubtracted sample. In each PCR, samples were pulled at cycles 18, 25, 28, and 33 for analysis by agarose gel electrophoresis. The left side of the gel shows the samples for the subtracted followed by the unsubtracted samples for the first blastocyst sample and the right side has the same layout for the second blastocyst sample. The four lanes of ladder are all 1 KB+ ladder. For the first blastocyst sample, the first faint product band appears after 25 cycles in the subtracted product, but for the unsubtracted control, a significant band is apparent after 18 cycles. For the second blastocyst sample (right), the first faint band appears after 28 cycles for the subtracted sample but once again has a dark band in the unsubtracted control after 18 cycles. These results confirm that the gene levels were indeed decreased in the subtracted products through SSH.

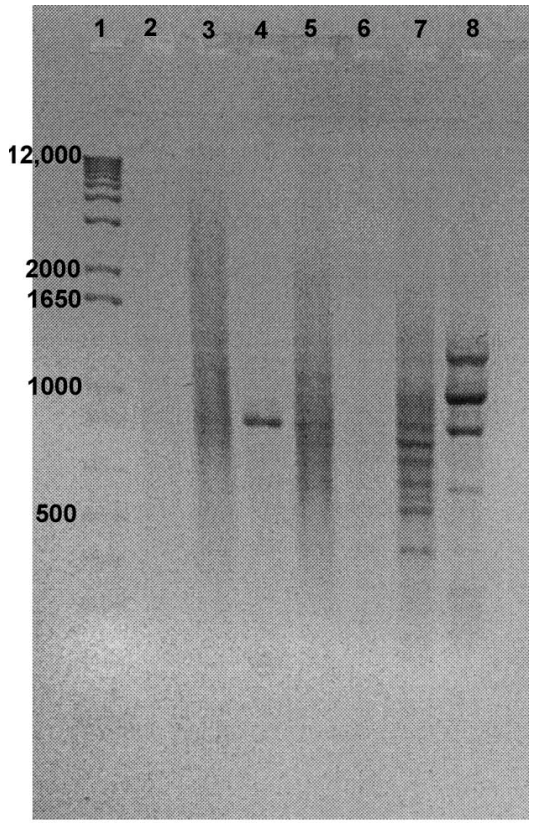

Figure 4.4 Blastocyst vs. Blastocyst Secondary Subtraction PCR Product. For each pair of comparisons, the amplified subtracted product from the secondary PCR reaction and the control unsubtracted product were analyzed by agarose gel electrophoresis. The lanes are as follows: 1 – 1 KB+ ladder, 2 – subtracted blastocyst sample 1, 3- control unsubtracted blastocyst sample 1, 4 – subtracted blastocyst sample 2, 5 – control unsubtracted blastocyst sample 2, 6 – control subtracted human skeletal muscle sample, 7 – control unsubtracted human skeletal muscle sample, and 8 – kit control subtracted product. From the subtracted lanes, a single discrete band is visible as compared to the general product smearing seen in the unsubtracted lanes.

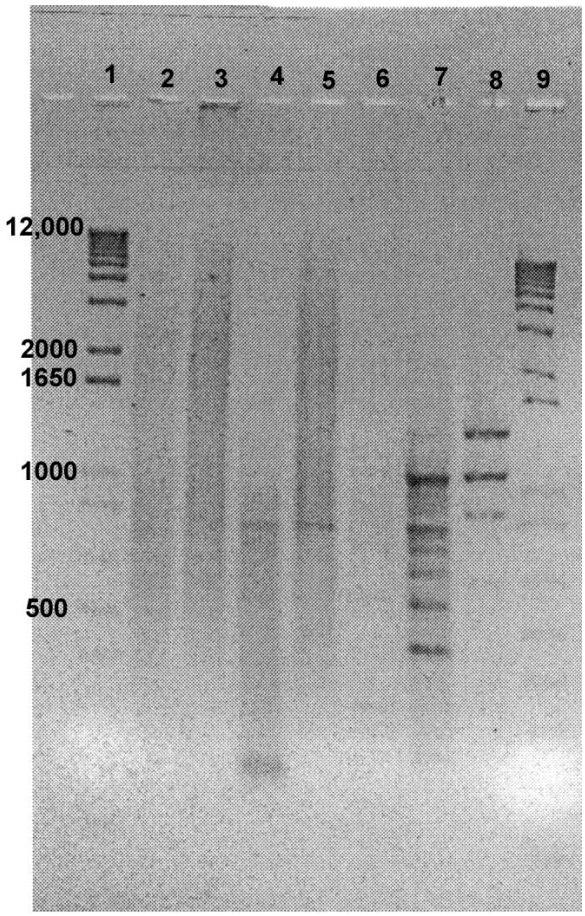

Figure 4.5 Trophectoderm vs. Blastocyst Secondary Subtraction PCR Product. For each pair of comparisons, the amplified subtracted product from the secondary PCR reaction and the control unsubtracted product were analyzed by agarose gel electrophoresis. The lanes are as follows: 1 – 1 KB+ ladder, 2 – subtracted trophectoderm sample, 3- control unsubtracted trophectoderm sample, 4 – subtracted blastocyst sample, 5 – control unsubtracted blastocyst sample, 6 – control subtracted human skeletal muscle sample, 7 – control unsubtracted human skeletal muscle sample, 8 – kit control subtracted product, and 9 – 1 KB+ ladder. Both the forward and reverse subtraction samples show a general decrease of product in comparison to the unsubtracted product, however they still show a general smearing of numerous products rather than a limited number of discrete product bands.

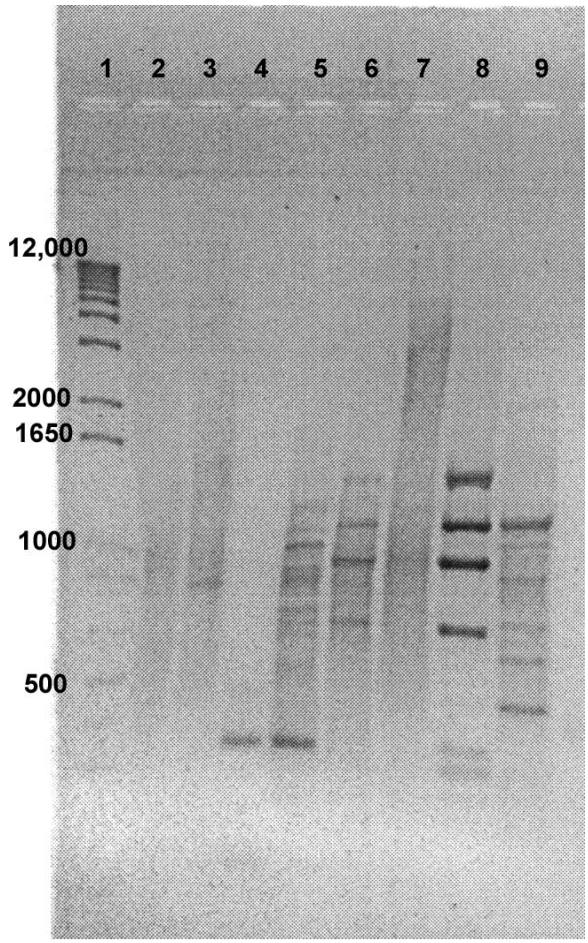

Figure 4.6 129SvEv Stem Cell vs. Blastocyst Secondary Subtraction PCR Product. For each pair of comparisons, the amplified subtracted product from the secondary PCR reaction and the control unsubtracted product were analyzed by agarose gel electrophoresis. The lanes are as follows: 1 – 1 KB+ ladder, 2 – subtracted blastocyst sample, 3- control unsubtracted blastocyst sample, 4 – subtracted stem cells sample, 5 – control unsubtracted stem cell sample, 6 – control subtracted human placenta sample, 7 – control unsubtracted human placenta sample, 8 – control subtracted human skeletal muscle sample, and 9 – control unsubtracted human skeletal muscle sample. Both the forward and reverse subtraction samples show a general decrease in number of transcript products in comparison to the unsubtracted product; however the stem cell sample showed a substantial decrease of product.

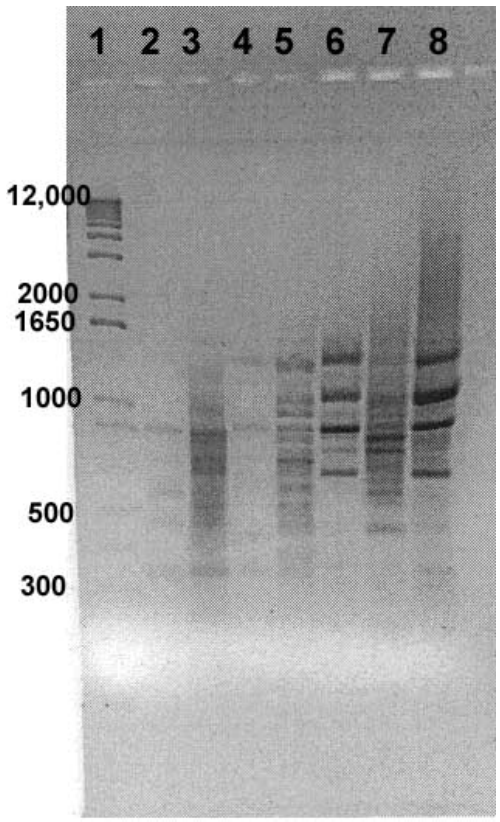

Figure 4.7 129SvEv Stem Cell vs. Fibroblast Feeder Cells Secondary Subtraction PCR Product. For each pair of comparisons, the amplified subtracted product from the secondary PCR reaction and the control unsubtracted product were analyzed by agarose gel electrophoresis. The lanes are as follows: 1 – 1 KB+ ladder, 2 – subtracted stem cells sample, 3 – control unsubtracted stem cell sample, 4 – subtracted fibroblast sample, 5- control unsubtracted fibroblast sample, 6 – control subtracted human skeletal muscle sample, 7 – control unsubtracted human skeletal muscle sample, and 8 – kit control subtracted product. All of the subtracted samples showed a visible decrease in product.

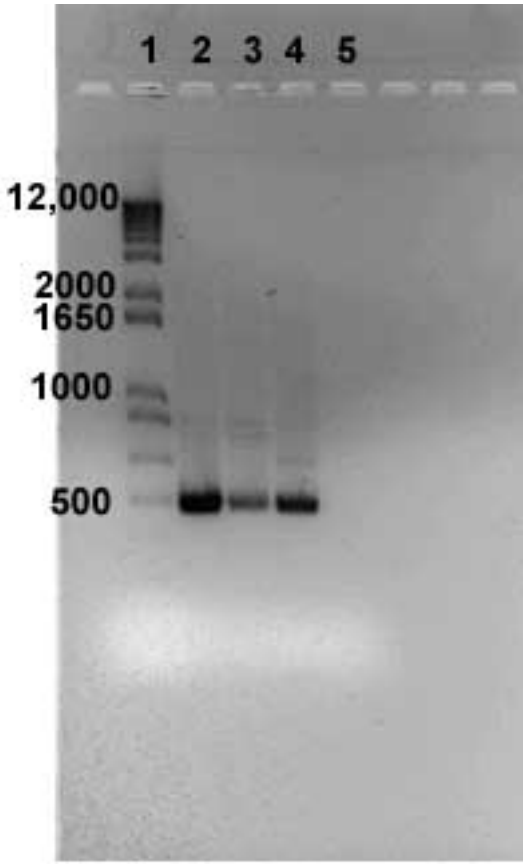

Figure 4.8 Confirmation PCR of Clone 129-1-C1. DNA sequences identified as differentially expressed through Suppression Subtraction Hybridization and isolated for cloning were visually confirmed as differentially expressed through PCR in the original samples used for comparison. The lanes are as follows: 1 – 1 KB+ ladder, 2 – 129SvEv Stem Cells, 3 – Fibroblast Feeder Cells, 4 – C57BL/6 Stem Cells, and 5 – Negative Control. An increase in product is visible in both stem cell samples as in comparison to the fibroblast sample, confirming the results of the SSH.

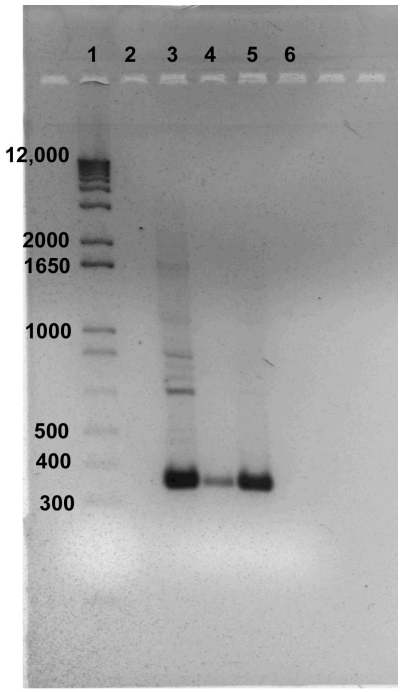

Figure 4.9 Confirmation PCR of Clone B5B-C12. DNA sequences identified as differentially expressed through Suppression Subtraction Hybridization and isolated for cloning were visually confirmed as differentially expressed through PCR in the original samples. The lanes are as follows: 1 – 1 KB+ ladder, 2 – Blank, 3 – 129 SvEv Stem Cells, 4 – Blastocyst, 5 – C57BL/6 Stem Cells, and 6 – Negative Control. The stem cell samples show a greater yield of product than the blastocyst sample, however a number of non-specific bands are also visible in the 129SvEv stem cell sample indicating a need to optimize the PCR reaction.

Table 4.1: GenBank Identities of Sequenced Clones

Source:	Identity:	Clone Number:	GenBank Accession Numbers for Matches:
Blastocyst vs Stem Cell (B5B vs.129-2)	Ribosomal	129-2-C11 129-2-C12 129-2-C13 129-2-C37 129-2-C38 129-2-C39 129-2-C40 129-2-C41 B5B-C12	BK000964 BC021595
	Tyrosine 3-monooxygenase/tryptophan 5-monooxygenase activation protein, zeta polypeptide (Ywhaz)	B5B-C8	BC05089 NM_011740
	Voltage-dependent anion channel 3 (Vdacs3)	B5B-C10	BC004743 MMU30839 NM_011696
	Mitochondrial	B5B-C14	AY339599
	Glucose related protein 78/ Heat shock 70kD protein 5	B5B-C15	MUSGRP78A BC050927 MUSGRP784 D78645
	GM2 activator protein (Gm2a)	B5B-C16	NM_010299 BC004651 MMU09816
	Ribonucleotide reductase M2 (Rrm2)	B5B-C17	NM_009104 MUSRNRM2A
	Peroxiredoxin1 (Prdx1)	B5B-C18 B5B-C19	AK008711 AK083243 AK010688 NM_011034
	RP515 Protein	B5B-C13	AK010652

Trophectoderm vs. Blastocysts (T vs B5A)	Unknown	T1-C1	
	Cleavage and polyadenylation specificity factor 3 (Cpsf3)	B5A-C2	BC006748, XW_358148, BC023297, NM_018813, AK045238, AK010566, AK004317
Stem Cell vs. Feeder Cell (129-1 vs. F1)	Proliferating cell nuclear antigen	129-1-C1 129-1-C2	BC005778
	Unknown	129-1-C3 129-1-C7 F1-C5	
	mKIAA1430 protein/4933411K20 gene	129-1-C4 129-1-C5	AK129358, BC058092, NM_025747
	Ribosomal	129-1-C6	AK088777
	Thromospondin 1	F1-C1	BC042422
	Cyclin G1	F1-C2	BC005534
	S100 calcium binding protein A11 (calizzarin)	F1-C3 F1-C6	BC021916, NM_016740
	Mitochondrial	F1-C4	BC020382

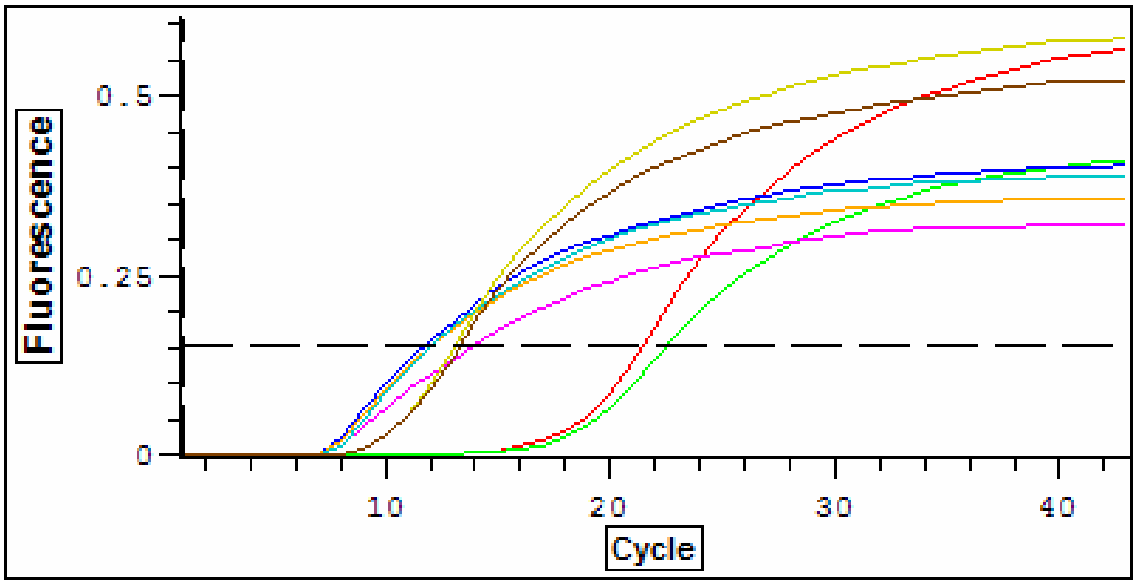

Figure 4.10 Real Time PCR Amplification Graph for Ribosomal 18s, Run 1. The graph demonstrates the amount of replicated r18s product with each amplification cycle in each of the three samples, murine blastocyst, 129SvEv murine embryonic stem cells, and C57Bl/6 murine embryonic stem cells, as determined by DyNAmo HS SYBR Green fluorescence. Each sample was tested twice in each run. Each run was repeated a second time for a total of four data sets for each gene in each sample. The second amplification graph for this gene is comparable to this graph and is not shown.

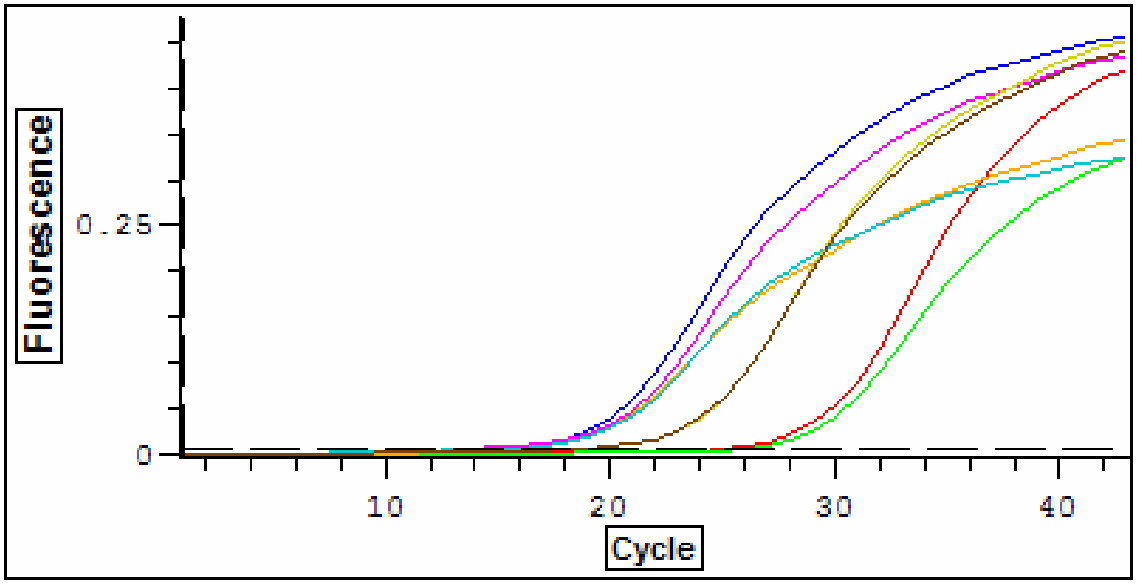

Figure 4.11 Real Time PCR Amplification Graph for Prdx1, Run 1. The graph demonstrates the amount of replicated Prdx1 product with each amplification cycle in each of the three samples, murine blastocyst, 129SvEv murine embryonic stem cells, and C57Bl/6 murine embryonic stem cells, as determined by DyNAmo HS SYBR Green fluorescence. Each sample was tested twice in each run. Each run was repeated a second time for a total of four data sets for each gene in each sample. The second amplification graph for this gene is comparable to this graph and is not shown.

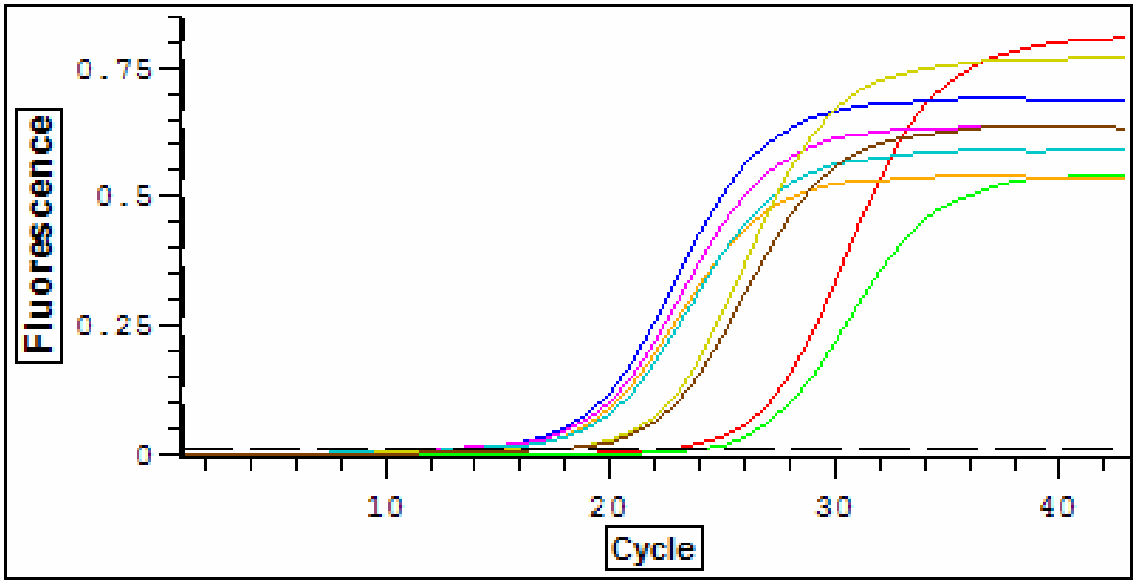

Figure 4.12 Real Time PCR Amplification Graph for Ywhaz, Run 1. The graph demonstrates the amount of replicated Ywhaz product with each amplification cycle in each of the three samples, murine blastocyst, 129SvEv murine embryonic stem cells, and C57Bl/6 murine embryonic stem cells, as determined by DyNAmo HS SYBR Green fluorescence. Each sample was tested twice in each run. Each run was repeated a second time for a total of four data sets for each gene in each sample. The second amplification graph for this gene is comparable to this graph and is not shown.

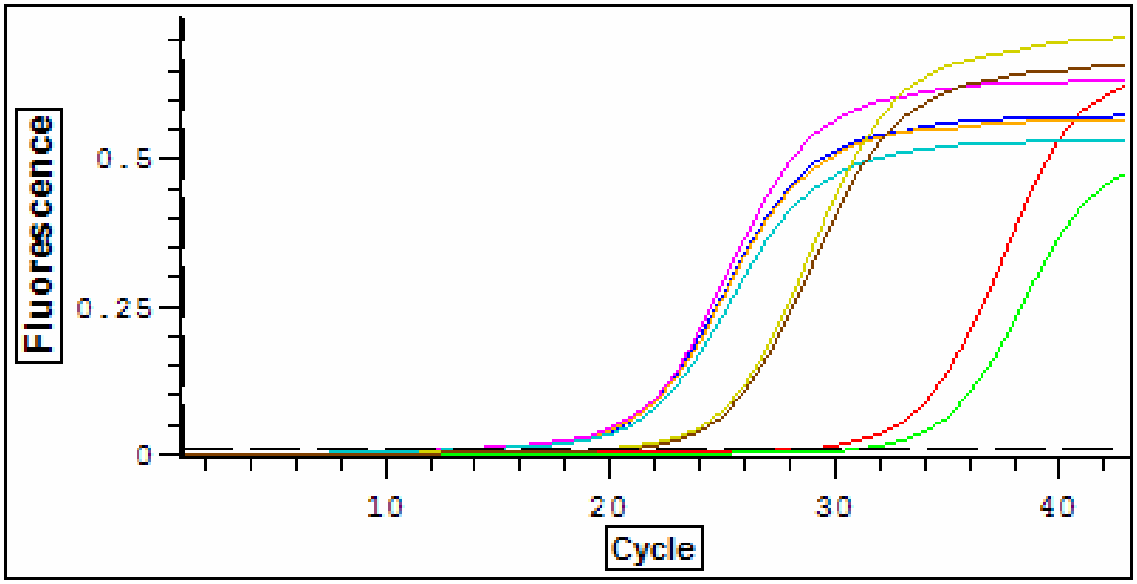

Figure 4.13 Real Time PCR Amplification Graph for Vdac3, Run 1. The graph demonstrates the amount of replicated Vdac3 product with each amplification cycle in each of the three samples, murine blastocyst, 129SvEv murine embryonic stem cells, and C57Bl/6 murine embryonic stem cells, as determined by DyNAmo HS SYBR Green fluorescence. Each sample was tested twice in each run. Each run was repeated a second time for a total of four data sets for each gene in each sample. The second amplification graph for this gene is comparable to this graph and is not shown.

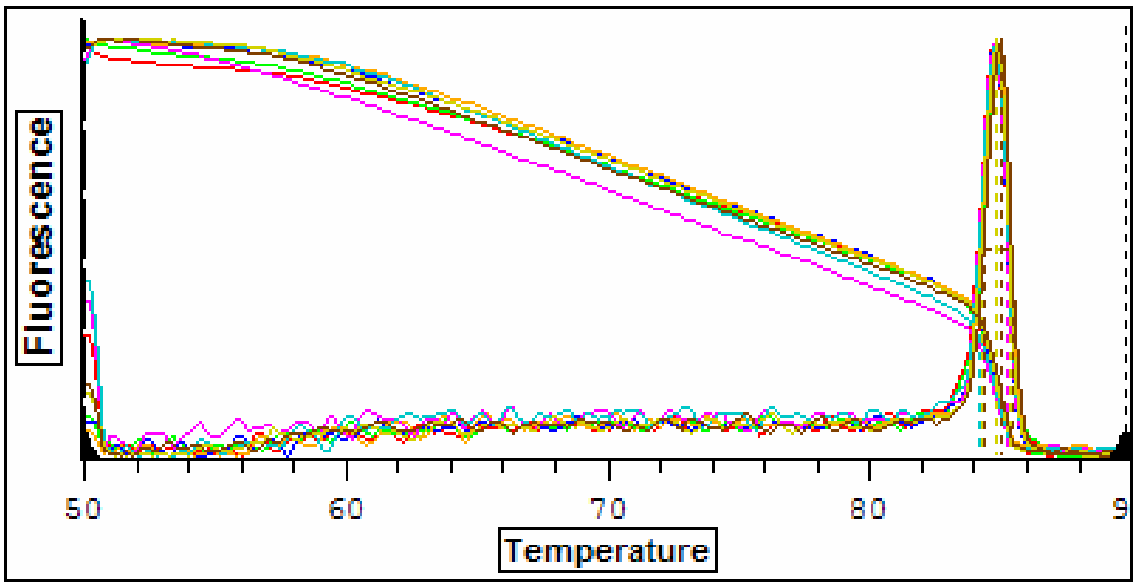

Figure 4.14 Melting Curve Analysis for Ribosomal 18s Amplification, Run 1. A melting curve analysis was done for each real time PCR run from 50°C to 90°C. The graph is of the rate of change of relative fluorescence with time and therefore peaks at the melting temperature of the product. This graph demonstrates a uniform peaking at the r18s melting point (84.4 °C) for all samples and confirms that fluorescence reading within those wells were only due to the presence of the desired amplicon and not primer dimers or random priming products. The melting curve for the second run is comparable to this graph and therefore is not shown.

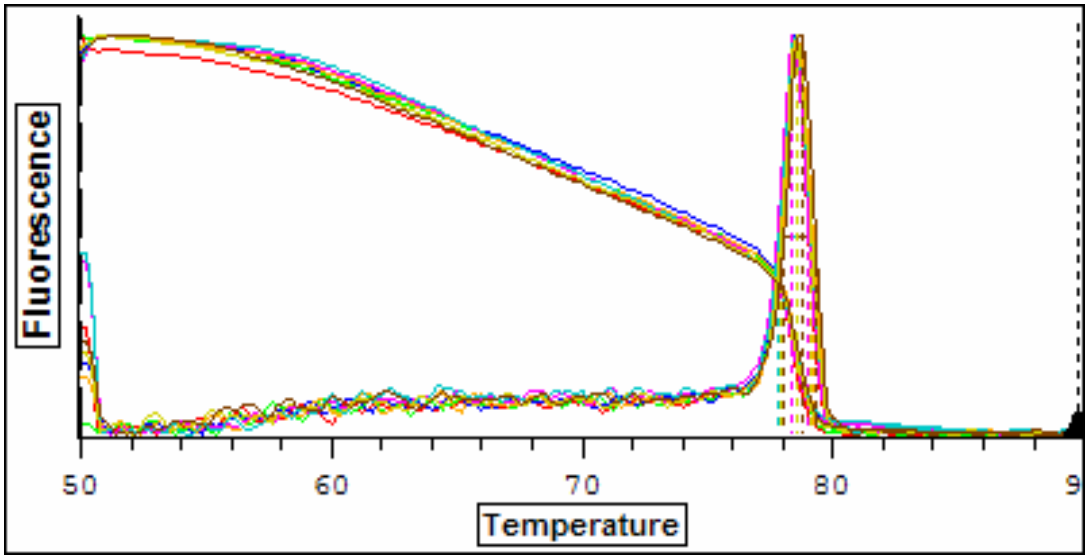

Figure 4.15 Melting Curve Analysis for Prdx1 Amplification, Run 1. A melting curve analysis was done for each real time PCR run from 50°C to 90°C. The graph is of the rate of change of relative fluorescence with time and therefore peaks at the melting temperature of the product. This graph demonstrates a uniform peaking at the Prdx1 melting point (78.8 °C) for all samples and confirms that fluorescence reading within those wells were only due to the presence of the desired amplicon and not primer dimers or random priming products. The melting curve for the second run is comparable to this graph and therefore is not shown.

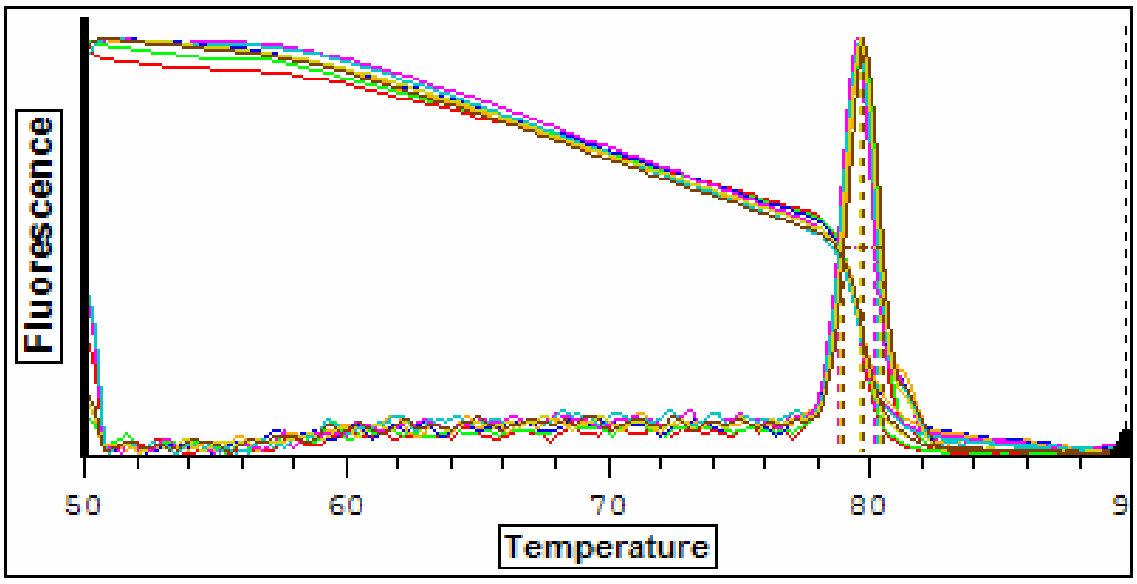

Figure 4.16 Melting Curve Analysis for Ywhaz Amplification, Run 1. A melting curve analysis was done for each real time PCR run from 50°C to 90°C. The graph is of the rate of change of relative fluorescence with time and therefore peaks at the melting temperature of the product. This graph demonstrates a uniform peaking at the Ywhaz melting point (79.6 °C) for all samples and confirms that fluorescence reading within those wells were only due to the presence of the desired amplicon and not primer dimers or random priming products. The melting curve for the second run is comparable to this graph and therefore is not shown.

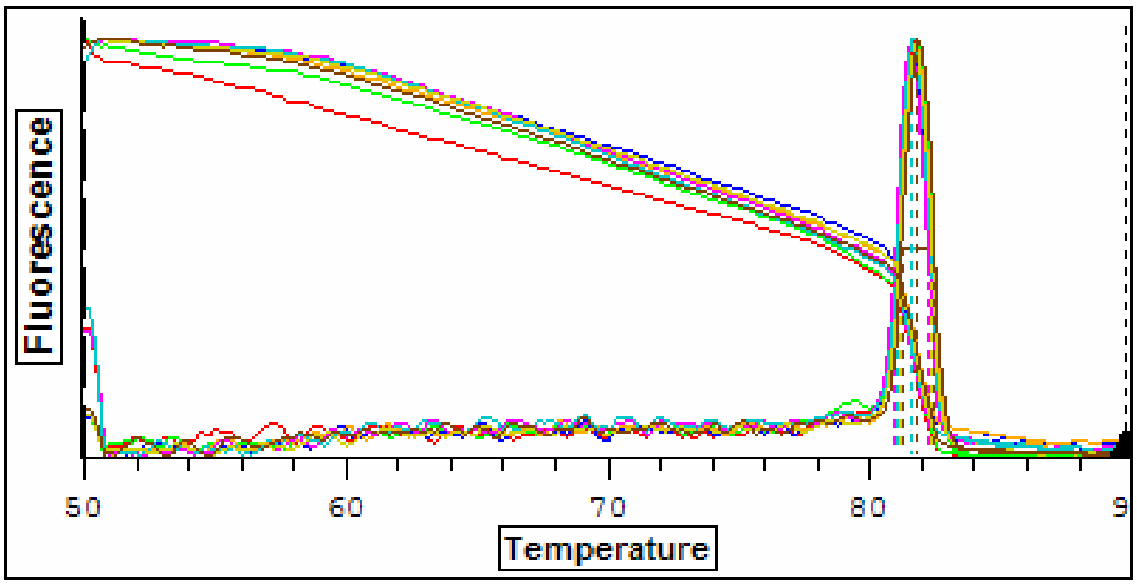

Figure 4.17 Melting Curve Analysis for Vdac3 Amplification, Run 1. A melting curve analysis was done for each real time PCR run from 50°C to 90°C. The graph is of the rate of change of relative fluorescence with time and therefore peaks at the melting temperature of the product. This graph demonstrates a uniform peaking at the Vdac3 melting point (81.6 °C) for all samples and confirms that fluorescence reading within those wells were only due to the presence of the desired amplicon and not primer dimers or random priming products. The melting curve for the second run is comparable to this graph and therefore is not shown.

Table 4.2: Real Time PCR Fold Difference Calculations.

Gene:	Samples:	Sample Avg. C_T[†]:	r18s Avg. C_T[†]:	ΔC_T[‡]:	$\Delta\Delta C_T$[§]:	Fold Difference[¶]:
Prdx1	Blastocyst	24.83 ± 1.41	22.21 ± 0.63	2.62	-2.27	4.81
	129 SvEv SC	13.83 ± 1.31	11.85 ± 0.29	1.98	-2.91	7.51
	C57BL/6 SC	12.91 ± 0.59	12.79 ± 0.87	0.12	-4.77	27.28
	Feeder Cells	18.21 ± 0.83	13.32 ± 0.26	4.89	0.00	1.00
Ywhaz	Blastocyst	23.13 ± 0.65	22.21 ± 0.63	0.92	-2.94	7.65
	129 SvEv SC	13.00 ± 0.61	11.85 ± 0.29	1.15	-2.70	6.49
	C57BL/6 SC	12.59 ± 0.77	12.79 ± 0.87	-0.20	-4.05	16.56
	Feeder Cells	17.17 ± 0.47	13.32 ± 0.26	3.85	0.00	1.00
Vdacs3	Blastocyst	29.52 ± 1.33	22.21 ± 0.63	7.31	0.00	1.00
	129 SvEv SC	13.07 ± 0.63	11.85 ± 0.29	1.22	-6.09	68.07
	C57BL/6 SC	12.77 ± 0.84	12.79 ± 0.87	-0.02	-7.33	161.04
	Feeder Cells	19.52 ± 0.77	13.32 ± 0.26	6.20	-1.11	2.16

Each average C_T value is from a total of 4 data points obtained from two runs with duplicates in each run.

[†] C_T = Cycle Threshold; Cycle number in which product amplification fluorescence reaches a set threshold. (Threshold is set to the beginning of the exponential amplification phase of the product.)

[‡] ΔC_T = Sample Avg. C_T – r18s Avg. C_T; Normalization in regards to the reference gene.

[§] $\Delta\Delta C_T$ = The largest ΔC_T from the data set for each gene is subtracted from the remaining ΔC_T values. The sample with the largest ΔC_T has the lowest target expression and is subtracted from all other samples.

[¶] Fold Difference is calculated using $2^{-\Delta\Delta C_T}$; Fold difference normalized to the reference gene and relative to the gene with the lowest expression.

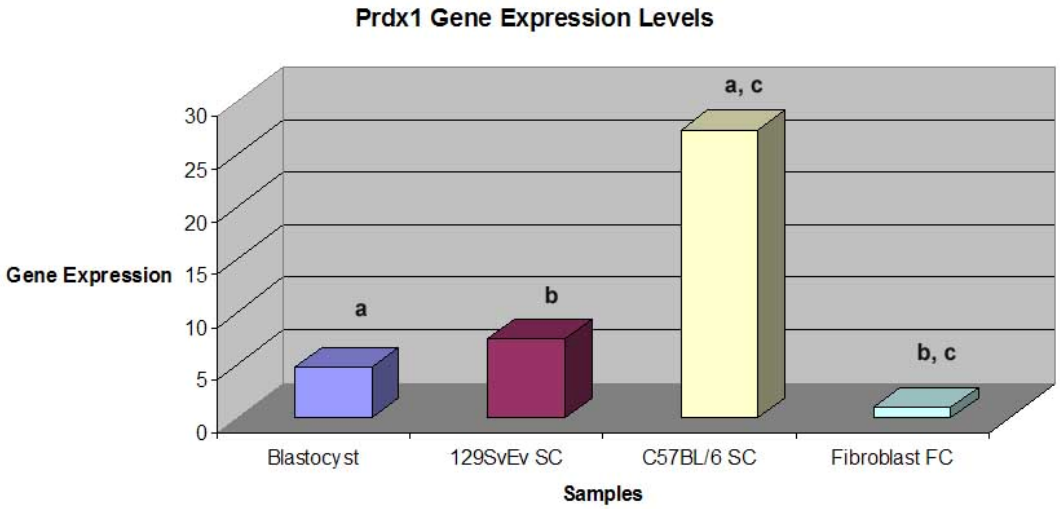

Figure 4.18 Fold Differences in Prdx1 Gene Expression Levels Based on Real Time PCR. Notations a-c indicate statistically significant comparisons as identified by Tukey's honestly significant difference analysis. For a, $p = 0.034$, for b, $p = 0.014$, and for c, $p = 0.000$.

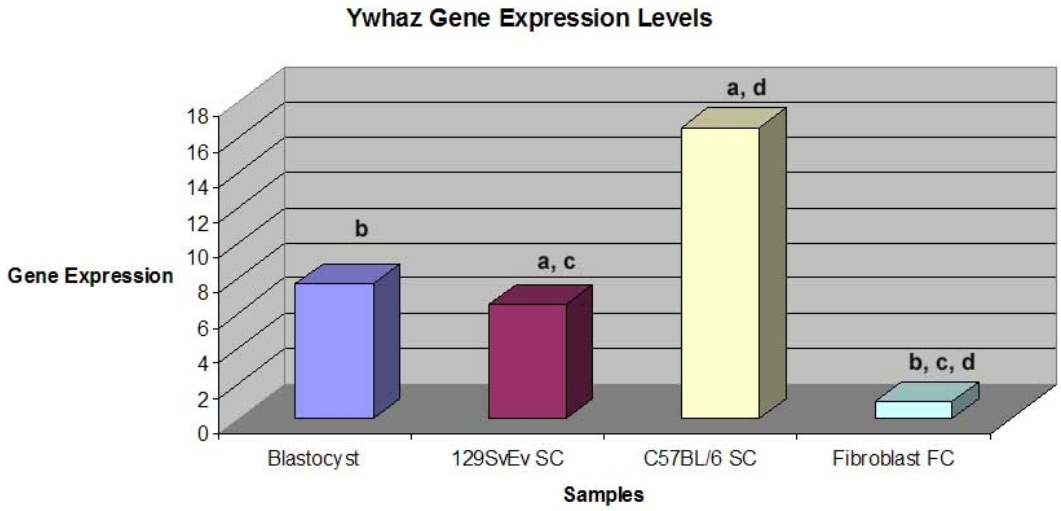

Figure 4.19 Fold Differences in Ywhaz Gene Expression Levels Based on Real Time PCR. Notations a-d indicate statistically significant comparisons as identified by Tukey's honestly significant difference analysis. For a, $p = 0.045$, for b, $p = 0.000$, for c, $p = 0.000$, and for d, $p = 0.000$.

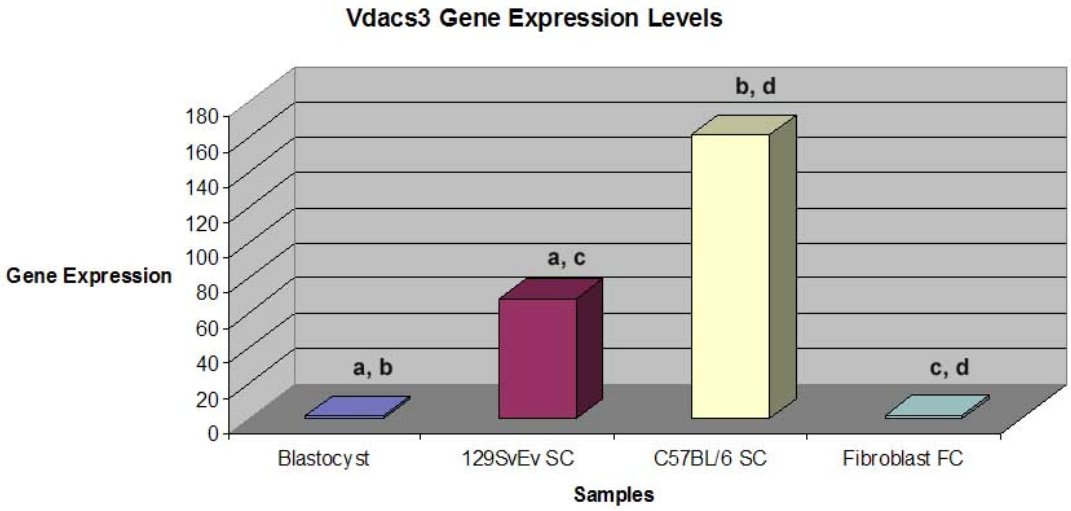

Figure 4.20 Fold Differences in Vdacs3 Gene Expression Levels Based on Real Time PCR. Notations a-d indicate statistically significant comparisons as identified by Tukey's honestly significant difference analysis. For all four comparisons, $p = 0.000$

Table 4.3: Levene's Test of Homogeneity of Variance for Quantitative PCR ΔC_T Values

Gene:	Significance:
Prdx 1	0.267
Ywhaz	0.715
Vdacs3	0.454

Table 4.4: ANOVA for Quantitative PCR ΔC_T Values. Comparison of the ΔC_T values for each sample within each gene analysis to look for statistical differences. ANOVA confirmed there were differences in the relative expression levels for all three genes between the 4 samples.

Gene:	Significance:
Prdx 1	0.001
Ywhaz	0.000
Vdacs3	0.000

Table 4.5: Tukey's HSD for Quantitative PCR ΔC_T Values

Gene:	Test Sample:	Test Sample:	Significance:	
Prdx 1	Blastocyst	129 SvEv ESC	0.843	
		C57BL/6 ESC	0.034	*
		Feeder Cells	0.058	
	129 Stem Cells	Blastocyst	0.843	
		C57BL/6 ESC	0.137	
		Feeder Cells	0.014	*
	C57 Stem Cells	Blastocyst	0.034	*
		129 SvEv ESC	0.137	
		Feeder Cells	0.000	*
	Feeder Cells	Blastocyst	0.058	
		129 SvEv ESC	0.014	*
		C57BL/6 ESC	0.000	*
Ywhaz	Blastocyst	129 SvEv ESC	0.950	
		C57BL/6 ESC	0.112	
		Feeder Cells	0.000	*
	129 Stem Cells	Blastocyst	0.950	
		C57BL/6 ESC	0.045	*
		Feeder Cells	0.000	*
	C57 Stem Cells	Blastocyst	0.112	
		129 SvEv ESC	0.045	*
		Feeder Cells	0.000	*
	Feeder Cells	Blastocyst	0.000	*
		129 SvEv ESC	0.000	*
		C57BL/6 ESC	0.000	*
Vdacs3	Blastocyst	129 SvEv ESC	0.000	*
		C57BL/6 ESC	0.000	*
		Feeder Cells	0.371	
	129 Stem Cells	Blastocyst	0.000	*
		C57BL/6 ESC	0.282	
		Feeder Cells	0.000	*
	C57 Stem Cells	Blastocyst	0.000	*
		129 SvEv ESC	0.282	
		Feeder Cells	0.000	*
	Feeder Cells	Blastocyst	0.371	
		129 SvEv ESC	0.000	*
		C57BL/6 ESC	0.000	*

* The mean difference is significant at the 0.05 level.

CHAPTER V

CONCLUSION

Potential applications of embryonic stem cells have been greatly discussed from advances in knowledge about embryonic development, to drug development and repair of damaged tissue. However, while a great amount of research has gone into understanding general stem cell characteristics, limited work had been done to characterize the developmental progression of embryonic stem cells from the blastocyst stage embryo.

The primary focus of this research was to utilize suppression subtraction hybridization to characterize the transcriptional differences between murine blastocyst stage embryos and murine embryonic stem cells. SSH was especially appropriate for this research due to its ability to begin with limited amounts of research material as well as its ability to amplify genes that are differentially expressed between two samples without prior gene specific knowledge.

From four SSH comparisons, blastocyst vs. blastocyst, trophectoderm vs. blastocyst, blastocyst vs. 129SvEv stem cells, and 129SvEv stem cells vs. fibroblast feeder cells, sequences were obtained for 33 clones of uniquely expressed transcripts. From this group, 10 clones were identified as having ribosomal homologies while 23 clones had either gene specific homologies or else were unknown. Three of the 23 genes, Prdx1, Ywahz, and Vdacs3, were selected for future quantitative analysis through

real time PCR in blastocyst, 129SvEv stem cell, C57BL/6 stem cells, and fibroblast feeder cell samples.

Peroxiredoxin 1

For Prdx1, in comparison to the fibroblast feeder cells which had the lowest expression level, the blastocyst had a 4.81 fold expression level difference, the 129SvEv stem cells had a 7.51 fold difference, and the C57BL/6 stem cells showed a 27.28 fold difference. Expression levels were significantly different between the blastocyst and C57BL/6 samples as well as the fibroblast feeder cells and both stem cell samples based on statistical analysis of the ΔC_T values. The significant difference in expression levels between the stem cells and the fibroblast verifies that the high rate of expression demonstrated within stem cells was not a false result created by the possibility of fibroblast contamination through routine cell culture conditions at the time of stem cell collection.

Peroxiredoxin 1 Overview

Peroxiredoxin-1 (Prdx1) is a cytoplasmic protein belonging to the peroxiredoxin family (Prdxs) which includes antioxidant proteins in organisms from all three kingdoms. Prdx1 is ubiquitously distributed throughout various types of mammalian tissue and is coded for by chromosome 4 in the mouse, producing a protein with a relative molecular mass of 23 kDa [47, 48]. The peroxiredoxins protect the cells from reactive oxygen

species (ROS) such as hydrogen peroxide (H_2O_2) by reduction through the thioredoxin (TRX) system [49].

Prdx1 exists within the cell as a homodimer consisting of two monomers arranged anti-parallel and is classified within the peroxiredoxin family based on its two conserved cysteine molecules, Cys^{52} and Cys^{173}. It functions to eliminate H_2O_2 by oxidizing a Cys^{52} residue to form cysteine sulfenic acid (Cys-SOH) which subsequently reacts with the Cys^{173} residue of the other monomer (Figure 5.1). This produces an intermolecular disulfide bond accompanied by the release of water. The disulfide bond is subsequently reduced by thioredoxin [50, 51].

Several mechanisms for the regulation of Prdx1 have been discovered. Prdx1 contains a phosphorylation site utilized by cyclin-dependent kinases (Cdk) which results in a decrease in peroxidase activity. Research of cells halted at varying stages of the cell cycle, demonstrated that Prdx1 was phosphorylated simultaneous to Cdc2 kinase activation [51]. In addition, nuclear factor (erythroid-derived-2)-related factor (Nrf2), has been shown to be an important transcription factor for Prdx1, especially in response to hypoxia and reoxygenation, a characteristic of a tumor microenvironment [50].

Peroxiredoxin 1 Cellular Implications

The ROS have long been considered to be toxic by-products of cellular activity (metabolism, etc.) and environmental factors (radiation, drugs, etc.) with the potential to cause great harm to the cell such as oxidation of proteins, lipid peroxidation, and DNA modification or breakage. Research has shown that mutant mice lacking the Prdx1 gene and therefore less able to eliminate ROS, develop hemolytic anemia and malignant

cancers resulting in shortened lifespans. The loss of Prdx1 expression in heterozygotes similarly saw an increase in these lymphomas, sarcomas, and carcinomas which also indicates a potential role for the protein in tumor suppression [47].

Other research however has linked ROS to a wider range of cellular regulatory activities in mammalian cells. For example, nitric oxide aids in immune system response in effector cells, such as the macrophages, when produced at high levels, but at lower levels is believed to function in signal transduction in a variety of cell types [51, 52]. Similarly, ROS have been found to be involved in transcription regulation in bacteria [53] as well as signal transduction in plants [54]. Other studies have shown that when various types of cells are stimulated by a variety of ligands such as cytokines and peptide growth factors, the intracellular levels of ROS increase, suggesting a role as a second messenger molecule [52]. For example, it has been demonstrated that hydrogen peroxide oxidizes protein tyrosine phosphatases (PTP) in response to stimulation by growth factors, resulting in PTP inactivation [51, 55].

This more complex understanding of the role of ROS in cellular activity also indicates a more complex involvement of Prdx1 in signaling cascades and redox regulation of the cell [49]. Research has shown Prdx1 transcription to increase in human mammary epithelial cell lines induced to proliferate by serum stimulation with a decrease in expression in subsequent differentiation [56]. Similarly, through use of a cDNA expression array, Prdx1 was found to be down-regulated during differentiation of a human embryonal carcinoma cell line used as a model for human neuronal differentiation [57].

Additional research has also indicated a role for peroxiredoxin 1 in enhancing cell survival. Prdx1 expression has been found to be upregulated in several types of cancer, including squamous cell lung carcinomas [50, 58] as well as in Alzheimer's disease and Down Syndrome [59]. In addition, research on embryonic interdigital cell death found Prdx1 downregulated at the time of commitment to programmed cell death, however normal levels of Prdx1 were maintained when the cultures were induced to survive. Interestingly though, silencing of Prdx1 though RNA interference treatment, failed to cause interdigital death, therefore indicating the required involvement of additional cellular components [60].

Other research using a proteomic approach, however, has shown Prdx1 to be upregulated during differentiation of a human fetal midbrain cell line [61] as well in the rat striatal progenitor model cell line ST14A transfected with glial cell line-derived neurotrophic factor (GDNF), an important neuronal differentiation factor. Interestingly, a Prdx1 expression change was not detected in untransfected ST14A within the 72 hours of the study [62]. Additionally, previous research by the group on a transcriptional level though use of microarrays, failed to reveal any differences in Prdx1 levels between transfected and untransfected ST14A cells [63].

Prdx1 has been shown to specifically interact with myelocytomatosis oncogene (c-Myc) , a transcription factor with roles in the cell cycle, differentiation, cell size, and apoptosis through its interaction with over 1000 different genes [64, 65]. Alterations in the expression of c-Myc have been documented in a large variety of cancers, including Burkitt's lymphoma, and prostate, breast, and colon cancers. [65]. Recent research by Egler, *et al*. in embryonic fibroblasts taken from a mutant prdx1 -/- mouse strain,

demonstrated increased levels of ROS in addition to signs of the deregulation of c-Myc, including decreased growth rates and altered c-Myc target gene expressions [65]. This interaction by Prdx1 further support its role as a tumor suppressor gene in addition to its role in eliminating ROS [64, 65].

Prdx1 has also been demonstrated to associate *in vivo* and *in vitro* with Abelson leukemia oncogene (c-Abl), a tyrosine-kinase with reported roles in inhibiting cell division, cellular response to stress, cell adhesion, and differentiation. c-Abl migrates between the cytoplasm and the nucleus and oxidative stress has been shown to activate c-Abl. Within the nucleus, c-Abl responds to DNA damage with apoptotic signaling [66]. Overexpression of Prdx1 inhibited c-Abl kinase activity [67]. This inhibition can have a significant impact on abnormal cell development as one of the normal functions of c-Abl is protector of p53, a well-studied tumor suppressor gene, by interactions with p53's inhibitors [68].

Peroxiredoxin 1 Research Significance

Overall, recent research points to the fundamental role of Prdx1 as one of promoting cell survival within the stem cell samples. As in the current research, a review of published supplemental data from research analyzing murine stem cells with microarrays also finds a high expression of Prdx1 within embryonic stem cells [69]. On the most basic level, Prdx1 protects cells from ROS and may play a role in various signaling cascades. In addition, genomic studies show increased levels of Prdx1 during proliferation with decreasing levels during differentiation. Conflicting proteomic studies indicating higher levels during differentiation still need to be resolved but may point to

alterations in the degradation rate of Prdx1. Prdx1's association with c-Myc and c-Abl, two molecules with roles in cell replication and apoptosis, as well as the experimental findings of Prdx1 being upregulated in various forms of cancer also support the role of Prdx1 as increasing cell survival and replication, essential characteristics for stem cells.

Tyrosine 3-Monooxygenase/Tryptophan 5-Monooygenase Activation Protein

Similar to Prdx1, the fibroblast feeder sample also showed the lowest expression level of Ywhaz. In comparison, the blastocyst sample showed a 7.65 fold difference of expression, the 129SvEv stem cells showed a 6.49 fold difference of expression, and the C57BL/6 stem cells showed a 16.56 fold difference of expression. In analysis of the ΔC_T values, the two stem cell sample values were significantly different from each other as was the fibroblast feeder cell value from all other samples; however the blastocyst sample was not significantly different from either stem cell sample.

Ywhaz Overview

Tyrosine 3-monooxygenase/tryptophan 5-monooygenase activation protein, zeta polypeptide (Ywhaz), also known as 14-3-3 zeta (14-3-3 ζ), is one of seven mammalian isoforms of the highly conserved 14-3-3 protein family. They were first described in 1967 as copious proteins found in the bovine brain and named 14-3-3 based on their isolation pattern [70]. Although there are seven known isotypes, a search of the human genome indicates a potential of three additional homologous transcripts to be discovered [71]. While their largest concentration is within the brain (1% of soluble proteins), most

isoforms have also been detected in lower levels within numerous other tissues. Despite specific knowledge about the roles of some mammalian isoforms, much of the functional differences between the various isoforms has yet to be determined [72]. As the expanded name would indicate, one of their first discovered roles, was as activators of tryptophan 5-monooxygenase and tyrosine 3-monooxygenase, therefore involved in the regulation of serotonin and noradrenalin production in the brain [73]. In general however, they have been found to interact with hundreds of other proteins with roles in cell signaling, cell cycle regulation, transcription, apoptosis, cytoskeletal structure, metabolism, oncogenesis, and intracellular trafficking/targeting [70, 74-76]. Their general mechanisms of action include altering target protein activity, altering target proteins interactions with other proteins, altering protein modifications, preventing degradation, and intracellular localization of target proteins [77, 78].

Ywhaz, like the other 14-3-3 proteins, consists of two 30 kDa acidic monomers, each with nine antiparallel α-helices organized with N-terminal and C-terminal domains, together forming a helical, dimeric protein with a large, negatively charged groove or channel (Figure 5.2). Within the channel are conserved regions that are common among all 14-3-3 proteins while the exterior portion of the protein has isoforms specific variations which most likely account for the variation in ligand binding activities between the different isoforms. In addition, conserved phosphorylation sites for each isoforms assist in the regulation of binding motifs. The phosphorylated form of 14-3-3 ζ was originally discovered separately and given the name 14-3-3 δ (delta) [70]. In addition to their homodimer formation, 14-3-3 isoforms have also been found in various heterodimer

arrangements including the binding of 14-3-3 ζ monomers with 14-3-3 ε monomers [79, 80].

In more recent years, the ubiquitous expression of Ywhaz has made it known as a housekeeping gene and it has been studied as a reference gene for use in real time PCR. In evaluation of appropriate reference genes in studies of dolphin skin biopsies [81], human placental tissue [82], and bovine preimplantation embryos [83], Ywhaz was among the three most stable reference genes from those studied. In another study however of prostate cancer tissue, Ywhaz rated only 10^{th} for expression stability among the sixteen genes studied [84].

Variations in Ywhaz expression, however, have been researched as potential sources for a number of diseases. A single nucleotide polymorphism (SNP) for Ywhaz was examined in an association study for paranoid schizophrenia and was found to occur significantly higher in patients than in matched controls [85]. In addition, 14-3-3 proteins are known to bind to α-synuclein, and Ywhaz, along with several other isoforms, is found to colocalize with Lewy bodies in Parkinson's disease [86]. Ywhaz expression is also found to peak during progression of chronic myeloid leukemia through the late chronic stage [87]. In Alzheimer's disease, neurofibrillary tangles composed of abnormally phosphorylated microtubule associated tau proteins are a key neuropathological characteristic. Ywhaz has been detected associated with tau within brain extracts and Ywhaz has been shown *in vitro* to stimulate tau's phosphorylation [88]. In addition, 14-3-3 proteins have been found in the cerebrospinal fluid in studies of over twenty-four different diseases [71].

Ywhaz Cellular Implications

One of the many actions of the 14-3-3 proteins, including Ywhaz, is binding to cruciform DNA. Cruciform DNA has been shown to form in both eukaryotic and prokaryotic organisms where inverted repeat sequences under constraints such as supercoiling, form non-B-DNA conformation through the formation of intra-strand base pairs. This transient cruciform formation has been shown to correlate with DNA replication and transcription and the 14-3-3 cruciform binding protein (CBP) activity is seen only in replicating cells. It is hypothesized that when this structural change occurs at origins of replication, it serves in the recruitment of initiator proteins and regulation of DNA replication. Hence, due to their CBP activity, 14-3-3 proteins are believed to be involved in regulating DNA replication [89].

Ywhaz also binds to a number of proteins and phosphorylation of both Ywhaz and the target proteins mediate this interaction. Most interactions depend on a target phosphorylated serine or threonine motif, RSXpSXP and RXXXpSXP (pS represents both phosphoserine and phosphothreonine) [77, 90]. For example, Ywhaz has been shown to bind to Raf proteins aiding in their activation [91]. The Raf proteins are a family of three serine/threonine kinases (A-Raf, B-Raf and C-Raf or Raf-1) that operate in a variety of cellular cascades. Raf-1 is ubiquitously expressed and functions in a signaling cascade downstream of Ras (Ras/Raf/MEK/ERK). For example, when the pathway is stimulated by the epidermal growth factor receptor, it leads to a variety of changes such as increased levels of anti-apoptotic proteins, Bcl2, and inhibition of Bad, a proapoptotic protein. In addition, Raf1 operates independently of the MEK/ERK pathway to activate Bcl2, inhibit proapoptotic proteins ASK1 and MST2, and promote

cell cycle continuation and differentiation [92, 93]. Phosphorylation of Ywhaz on Thr-233 by casein kinase Iα (CKIα) however, prevents its association with Raf-1 (also known as c-Raf) [91] as does *in vitro* treatment of Raf-1 by phosphatase [94].

Like many other target proteins, several proapoptotic proteins are also known to require phosphorylation for association with 14-3-3 proteins (including 14-3-3ζ), including Bad, FOXOa, cAbl, Yap, Nur77, and Bim. Bax, another proapoptotic protein, however does not require phosphorylation. These proteins have been shown to associate in the cytoplasm with the 14-3-3 proteins which maintains them in a sequestered, inactivated form away from the mitochondria and nucleus. Phosphorylation, however, of the 14-3-3 proteins (at Ser 184 for 14-3-3ζ) by c-Jun NH_2-terminal kinase (JNK) in response to DNA damage or dephosphorylation of the target proteins (minus Bax) cause their release and therefore results in apoptotic cellular signaling. (Foxo, Yap, Nur77, and cAbl function in the nucleus and Bad, Bim and Bax function in the mitochondria for their respective roles in apoptosis.) (Figure 5.3) In fact, low levels of 14-3-3 increase a cell's susceptibility to apoptotic signals and increased 14-3-3 levels makes a cell more resistant to apoptotic signaling [66, 72, 76, 95-98].

In addition to the regulation of 14-3-3 through the JNK phosphorylation at S184 previously described, additional kinases Sdk1 (Sphingosine-dependent kinase) and PKA type II (protein kinase A type II) have also been found to phosphorylate 14-3-3 at S58. This residue lies in the dimeric interface and its phosphorylation prevents dimeric formation. While the monomeric 14-3-3 may still be able to bind to some target proteins with a lower affinity, it would not be able to produce the conformational changes needed for the activation of some target proteins. In addition, a number of 14-3-3 target proteins

only interact with the dimeric form. The end result of this phosphorylation is the downregulation 14-3-3 activity [76, 77, 99, 100].

In addition to the previously mentioned proapoptotic proteins that interact with 14-3-3, numerous other target proteins have been identified, many that may directly or indirectly play a role in the cell survival/apoptosis balance. These proteins include the MAP3K stress response proteins, Ask1 (or Map3k5), Mekk1, Mekk2, and Mekk3; mitogenic promoters, Raf (previously detailed) and Mek; nutrient signaling protein Ampk; and survival regulators Igf1r and Pi3 kinase [76].

In contrast to the number of 14-3-3 interactions that support cell survival, 14-3-3 has also been found to bind to and stabilize E2f1, a proapoptotic transcription factor. The end result is the expression of proapoptotic target genes p73, Apaf-1, and caspases. Overall however, current research supports a greater role for 14-3-3 in normally promoting regulation of proapoptotic proteins and supporting cell survival [76].

14-3-3 proteins have also been shown to play a key role in cell cycle regulation (Figure 5.4; Table 5.1) and are believed to have roles in cancer formation [101]. Cell cycle progression is regulated by interactions among the cyclin-dependent kinases (CDKs) and additional regulator subunits. One important member of the CDK family is cell division cycle 2 (Cdc2; also known as Cdk1) whose activation is required for entry into mitosis. Cdc2 is suppressed following DNA damage and during interphase by phosphorylation, but Cdc25c phosphatase dephosphorylates Cdc2 to allow cell cycle progression. Cdc25c however can be regulated itself by phosphorylation by checkpoint 1 kinase (Chk1) and subsequent binding to 14-3-3 proteins during interphase and at cell cycle checkpoints, which results in inhibition of mitotic entry [78, 102-104].

Interestingly, once Cdc2 is activated by Cdc25, it phosphorylates Cdc25 at Ser 214 in a positive feedback loop blocking potential inhibitory phosphorylation at Ser 216 which would lead to a mid-mitotic checkpoint [105].

Chk1, the kinase that aids in the regulation of Cdc25, is also itself regulated by association with 14-3-3. Phosphorylation of Chk1 in response to DNA damage activates it and causes it to associate with 14-3-3 proteins [78, 106, 107].

Another cell cycle protein regulated through interactions with 14-3-3 ζ is Mdxd, a p53 regulator. Cellular DNA damage stimulates the phosphorylation of Mdxd leading to its binding to 14-3-3 proteins. Mdxd complexed with 14-3-3 leads to the ubiquitinylation of Mdxd by Mdm2 and its subsequent degradation. The reduction of Mdxd leads to the activation of p53 and cell cycle arrest or apoptosis [108].

One CDK inhibitor, p27, regulates the cell cycle through its interactions with cyclin-CDK complexes within the nucleus. p27 is regulated by its concentration and cellular localization and phosphorylation on one of numerous residues results in either its degradation or cytoplasmic localization. Phosphorylation by Akt at Thr-157 allows p27 to bind to 14-3-3 ζ which results in cell cycle progression [78, 109, 110].

The last group of cell cycle regulators shown to interact specifically with 14-3-3 ζ belongs to the Forkhead family of transcription factors (Foxo) which aid in cell cycle arrest. Phosphorylation of Foxo3a (also known as FKHRL1), Foxo1 (Fkhr), and Foxo4 (Afx) (the three major mammalian Foxo members) by Akt leads to their association with 14-3-3 ζ , cytoplasmic localization, and cell cycle progression [111-114].

While much research interest has centered on the role of the 14-3-3 proteins in cell cycle regulation and apoptosis, recent proteomic studies have greatly enlarged the

scope of understanding of the role of these proteins within the cell. In addition, while historical studies have not differentiated between the binding affinities of various isoforms, more recent research is beginning to shed more light on potential isoforms differences. One recent research project by Meek *et al.* purified over 300 proteins (Appendix B) that were found to bind to 14-3-3ζ in HeLa cells during both interphase and mitosis. While some target proteins were cell cycle dependent, many were cycle independent. Roles of the target proteins within both phases included cell division, cell signaling (kinases, small GTPase related, misc.), nucleolar proteins, proteolysis/ubiquitination, stress or checkpoint response, apoptosis, nucleotide metabolism, chromatin structure/DNA binding, RNA binding, translation, cytoskeleton, metabolism, chaperones, nuclear transport, transcription, sugar binding, and vesicle trafficking/formation. One interesting note was that Yhwaz was found to bind to Prdx1, the first gene of interest in this study, in a cell cycle independent manner [74]. The great diversity of target proteins and associated functions indicate a role for the 14-3-3 proteins, especially 14-3-3ζ, in a wide range of cellular activities.

Ywhaz Research Significance

While the exact function of Ywhaz within the cell is unclear, the diversity of its known interactions with over 300 other proteins signifies important roles in cell division and cell regulation. In general, Ywhaz is believed to support cell growth proteins and repress proapoptotic genes [101]. This is supported by the research finding that increased Ywhaz levels increases a cell's resistance to proapoptotic signaling. The need for continued cell division is an established need for maintenance of a stem cell line and

therefore it is not difficult to understand the need to upregulate Ywhaz in stem cells. Continued cell division however is also a key characteristic of early developing embryos so it is not surprising that a greater fold difference of expression was not found. While Tukey's HSD statistical analysis of the real time data did not reveal statistical differences between the blastocyst and stem cell samples for Ywhaz, the alternative LSD analysis did find statistical differences between the C57BL/6 sample and blastocyst sample (data not shown) and therefore should be included for analysis in further research studies.

Voltage-dependent Anion Channel 3

In contrast to Prdx1 and Ywhaz, the blastocyst sample had the lowest level of expression for Vdacs3. The fibroblast feeder cells had a 2.16 fold difference of expression, the 129SvEv stem cells had a 68.07 fold difference of expression, and the C57BL/6 stem cells had a 161.04 fold difference of expression. When comparing the ΔC_T values, the blastocyst sample was statically different from both of the stem cell samples. In addition, the fibroblast sample was also significantly different from either stem cell sample.

Vdac3 Overview

The voltage-dependent anion channel (Vdac) family (also called mitochondrial porins) in mammals consists of three proteins, Vdac1, Vdac2, and Vdac3, which form pores within the outer mitochondrial membrane (OMM). In addition to the majority of research focused on their role in mitochondria, further research has found Vdac within

other cellular compartments (Table 5.2) including the sarcoplasmic reticulum (SR), endoplasmic reticulum, endocytotoic vesicles, and the plasma membrane [115-117]. In addition, Vdac1 was co-purified in rats with the $GABA_A$ receptor complex obtained from neuronal plasma membranes [118].

Mitochondria, once understood only as cellular energy producers, have been linked to a much broader role, including responsibilities controlling redox reactions, osmosis, pH, calcium levels, cell signaling, stress response, proliferation, intercellular communication, and apoptosis [116]. As the major OMM pore forming protein in addition to serving as a binding site for several cytosolic proteins, the Vdac proteins play important roles in these various functions[116, 119].

Vdac proteins have been found within all eukaryotic species however more complex organisms have been shown to have more isoforms (3) than the more simplistic species (1). Within mice, the three isoforms are 65-70% identical and Vdac3, the isoforms of interest, is a 30 kDa protein coded by chromosome 8 [116, 119, 120]. Vdac3 has also been shown to have an alternative splicing site in mice that adds a single methionine and is specifically expressed within the brain, heart, and skeletal muscle [121].

The Vdac pore is generally formed from a single peptide consisting of one α-helix and several (13-19) amphipathic β-strands. Together, it forms a transmembrane voltage-gated pore (Figure 5.5) which serves to transport anions, cations, ATP, Ca2+, and other metabolites at low transmembrane potentials with reduced conductivity at high transmembrane potentials [115, 116, 122]. In mice, Vdac3 has also been shown to contain an additional leucine zipper motif in the portion of the peptide that is believed to

form the cytoplasmic loop [119, 123]. While most research has found the Vdac pore to be formed from a single peptide, recent research has also shown the ability of Vdac to join in dimers or tetramers within cellular membranes [124, 125].

When cellular extracts of Vdac is reformed within planar lipid bilayers, the pore routinely fails to completely close, however numerous other proteins and inhibitors (Table 5.3) have been able to invoke closure or modify channel activity under experimental conditions, leading to the belief that Vdac has a complex regulation mechanism [115].

The three Vdac isoforms have great structural homology and cellular differences between them have not been greatly defined, however they have been shown to display some functional differences. In one experiment, each of the three murine isoforms was individually expressed in mutant yeast lacking the endogenous Vdac gene. Both Vdac1 and Vdac2 were able to complement the deficiency to restore normal growth potential, but Vdac3 was only able to partially complete the mutation [119]. Other researchers also expressed each of the isoforms individually in mutant yeast lacking Vdac and found that the expression of each isoforms resulted in varying degrees of mitochondrial membrane permeability. In addition, while Vdac3 could be inserted into liposomes, it had difficulty inserting into planar membrane, especially in the presence of an ion gradient, and when inserted, did not respond like Vdac1 or Vdac2 to changes in the membrane potential [126].

In another experiment, knockout murine embryonic stem cell lines for each of the isoforms were generated and examined. While there were no statistically significant differences in growth rates for the cell lines with single mutations, double mutant cell

lines could not be generated. In addition, the singularly mutant cell lines all demonstrated a 30% decrease in oxygen consumption, and while Vdac1 -/- and Vdac2 -/- lines also showed a decrease in cytochrome c oxidase activity, Vdac3 -/- showed normal activity. In Vdac1 -/- cell lines, an increase of citrate synthase was detected, indicating an increase in mitochondria, however in Vdac 2-/- and Vdac3 -/- lines, an increase in Vdac1 expression was detected by Western blot [127]. (Isoform specific antibodies were not available for Vdac2 or Vdac3 and therefore were not tested.) So while any individual isoforms appears to be dispensable, at least two are required by the cell for survival and each of the three isoforms appear to have overlapping, but different mechanisms of operation.

Subsequent research in the same laboratory generated mice deficient in Vdac3 from heterozygous mice in normal Mendelian ratios, indicating no lethal effect in embryogenesis. While the resulting mice appeared overall healthy, the males showed significant decreases in sperm motility (17% versus wild type 70%) and proved infertile. Further examination revealed 68% of Vdac3 knockout sperm have abnormal axonemes structure while tracheal epithelial had normal cilia, but fewer ciliated cells. Mitochondria within testicular spermatids and skeletal muscles were found to be enlarged and abnormally shaped. Respiratory chain activity was also decreased with skeletal mitochondria [128]. More recent research in bovine, localized Vdac2 and Vdac3 to the cytoskeletal outer dense fibers of the sperm flagellum [129].

Vdac3 Cellular Implications

Research is still needed to fully define the physiological roles of the Vdac isoforms within the mitochondria and other cellular compartments. Within muscle cells, the sarcoplasmic reticulum stores Ca^{2+} and aids in the regulation of muscle contractions. Control of the calcium levels within the SR involves numerous proteins that are themselves regulated by phosphorylation [115]. It has been proposed that Vdac functions within the SR to both transport the ATP required for phosphorylation and to allow the transfer of cations and anions in order to prevent osmotic and potential changes when Ca^{2+} levels fluctuate [130].

Within the cell membrane, Vdac has been proposed to function within a large multicomponent chloride channel such as the outwardly rectifying chloride channel (ORCC) complex with the ability to function based upon environmental changes and regulation as a maxi-, midi-, or a mini-chloride channel [117]. The cystic fibrosis transmembrane conductance regulator (CFTR) regulates ORCC by inducing cellular release of ATP [131].

Additional research has also linked Vdac located within the cell membrane to ATP release and cell volume regulation of murine cells [132] as well as brain tissue volume regulation in bovine [133]. Research on superoxide anion localization with rat heart mitochondria has also suggested a role for Vdac in transporting the superoxide anion out of the mitochondria [134].

The Vdac isoforms have also been linked to roles in apoptosis through several different proposed models. In apoptosis, mitochondria play an important role in releasing apoptogenic proteins such as cytochrome *c* and apoptosis inducing factor (AIF) into the

cytoplasm as the outer mitochondrial membrane increases permeability in response to cellular signaling. Vdac alone however, normally forms a pore too small for the transmission of proteins as large as cytochrome *c* [116].

One model proposes that stimulated Vdac closure within the mitochondrial membrane prevents ATP-ADP exchange across the membrane which results in rupturing of the membrane, cytochrome *c* release, and apoptosis [135]. Other research however has found that cytochrome *c* can be released from the mitochondria without disturbing the OMM integrity therefore lending support to alternative models [136, 137].

In a second model, Vdac functions as part of the permeability transition pore (PTP) that in response to cellular pro-apoptotic signaling, increases its permeability. The PTP crosses both mitochondrial membranes and includes Vdac in the OMM, cyclophilin-D in the mitochondrial matrix, and adenine nucleotide translocase (ANT) in the IMM [116, 138, 139]. Additional research has specifically linked the blockage of the mitochondrial membrane permeability transition (MPT) which plays a role in necrosis and possibly apoptosis to Vdac regulation by the Bcl-2 family. Bcl-2 and Bcl-x likely block MPT by inhibiting Vdac activity while Bax is proposed to interact with Vdac to cause cytochome *c* permeation [116, 140, 141].

The recent discovery of the variable existence of Vdac in dimers, trimers, and tetramers also suggests the possibility of oligomeric Vdac functioning in apoptosis to increase mitochondrial membrane permeability. Cellular proapoptotic stimulation may induce oligomeric formation allowing for the formation of pores large enough to allow molecules like cytochrome *c* to pass without disrupting membrane integrity. In fact,

purified Vdac reconstituted into liposomes was stimulated to form oligomeric structures when stimulated by cytochrome *c* [124].

Interestingly, research utilizing several different cell and Vdac sources found that overexpression of Vdac induced apoptosis [116, 142, 143]. However, overexpression of hexokinase isoforms I (HK-I), known to reduce Vdac conductance, in cells with an overexpression of Vdac, were found to be resistant to the induction of apoptosis [142]. Proposed mechanisms of apoptosis induction from increased levels of Vdac include an increase in OMM leakage followed by decreased cell viability as well as possible increase in Vdac oligomerization followed by release of apoptotic proteins [116].

In contrast to normal cells which undergo apoptosis when Vdac is overexpressed, analysis of AH130, a malignant cell line, found all three Vdac isoforms (1-3) to be overexpressed when compared to normal liver cells [144]. Since previous research had shown more than 100 fold increased mitochondrial binding of hexokinase in tumor cells than in normal cells [145], the three isoforms were cloned and sequenced. Their primary sequences were found to be identical to Vdacs expressed in normal liver cells, therefore suggesting that the binding difference was the result of transcript differences rather than structural differences [144]. While increased hexokinase activity in tumor cells has been tied to tumor cells increased need for energy and anabolic precursors [144, 145], it has also been found that the binding of hexokinase to Vdac with the OMM induces channel closure and prevents PTP opening for cytochrome c release. Glucose 6-phosphate, a hexokinase product and a regulator of hexokinase activity, was able to re-open both Vdac and PTP [146]. The deducing of the mechanisms behind the dual role of hexokinase in increasing glycolysis and decreasing mitochondrial permeability in cancer cells as well as

ways to target it for cancer therapy is the subject of much current cancer thought and research [147-149].

Vdac3 Research Significance

While interest in Vdac has generated a great deal of research within the past two decades, its complex role within the cell, especially differentiating between isoforms, has yet to be fully defined. Like Prdx1, previous microarray research has also found Vdac to be highly expressed in murine embryonic stem cells [69]. Of the three genes studied by real time PCR in this current research, Vdac3 showed the greatest fold difference between the blastocyst sample and the embryonic stem cell samples and there are several possible explanations for its increased expression. Vdac could be playing an important role in cell volume regulation in the rapidly dividing cells. Future research characterizing the cellular localization of Vdac between the blastocyst sample and the ESC samples could provide useful information for this model.

Increased levels of Vdac within the cell could also simply provide a greater abundance of the various metabolites known to pass through its pore as energy needs of the cell increases in response to continual cell division. Similar to cancer cells, embryonic stem cells have a great need both for increased energy and increased metabolic components to allow for continual cell division. This common characteristic is reflected in the large fold difference of expression between both stem cell samples and the blastocyst sample. While the precise mechanism by which Vdac increases a cell's viability is still being investigated, it is believed to be significant that Vdac is upregulated in both cancer cells and embryonic stem cells, in contrast to other cell lines that were

found to undergo apoptosis when Vdac was overexpressed. Future research examining hexokinase levels between the blastocyst sample and the ESC samples could provide useful information for comparing the Vdac mechanism between cancer cell lines and ESC samples and confirming if hexokinase also serves as a protective anti-apoptotic mechanism in ESC.

General Discussion and Conclusion

While previous research characterized embryonic development or embryonic stem cells, the current work focused on characterizing the genomic changes in the development of murine embryonic stem cells from blastocyst stage embryos. A review of research literature for the three genes identified through SSH and specifically studied through real time PCR, Prdx1, Ywhaz, and Vdac3, suggests important roles in promoting cell survival and continued cell division. Alterations of expression levels of all three genes have been found in cancer lines which have similar characteristics of continued cell division without normal occurrence of differentiation. In addition, all three genes have been suggested as direct or downstream targets of Oct4, an essential gene known for its role in maintaining stem cell pluripotency [2]. While further studies remain to fully understand the actions of each of these genes within the cell, especially in distinguishing isoforms differences for each gene, the overall focus on allowing continued stem cell growth is clear.

One matter that remains for consideration concerns the different rates of expression between the two different ESC lines. The focus of the research was to identify key overall differences in the progression from blastocyst to ESC. By comparing

multiple strains, strain specific differences could hopefully be eliminated. It is possible that the difference observed are strain related or they could be normal fluctuations that occur through the progression of the cell cycle. It is also possible that the variation could also be passage related. The ESC samples were generously donated by Dr. Hochgeschwender from OMRF and at the time of original sample collection, it was noted that the 129SvEv sample was from passage 10 and the C57BL/6 sample was from passage 2. It would be ideal to try to eliminate this variable in future research. However, since the real time PCR analysis was designed to quantitatively confirm the results achieved through SSH, the overall statistically significant trend towards upregulation for Prdx1 and Vdac3 in ESC still provides valuable information on the differences between blastocyst stage embryos and embryonic stem cells.

Future research could take several directions. Ideally, additional differentially expressed gene would be identified through SSH and quantified through real time PCR to provide a more complete profile of the genetic transition occurring during the formation of ESC. In addition, the other 20 genes already identified in this study should also be analyzed through real time PCR within the same samples to look for additional statistically significant differences. For the three genes analyzed in this work, additional research measuring their expression across timelines within embryos, as stem cells are developed from those same embryos, and as the stem cell colonies continue to replicate could provide useful information on their role over time within each sample. The varying results found for Prdx1 between genomic and proteomic studies also encourage inclusion of proteomic analysis.

While this current work identifies a small sample of the potential genes involved in the transition from blastocyst stage embryo to embryonic stem cell line, it offers a valuable first step in understanding the molecular alterations that occur during this essential time period. Peroxiredoxin 1 and Voltage dependent anion channel 3 both demonstrated significant upregulation in the comparison between blastocyst stage embryos and ESC and function to enhance cell survival and continued cell reproduction. It is the author's hope that future research will continue to expand our understanding of this transitional period in order to identify key markers of stem cell development in embryonic sources with potential applications in the development of future alternative sources.

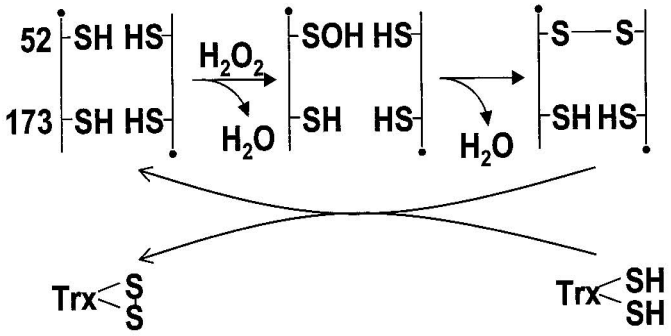

Figure 5.1 Reduction of Hydrogen Peroxide by Peroxiredoxin. [51]

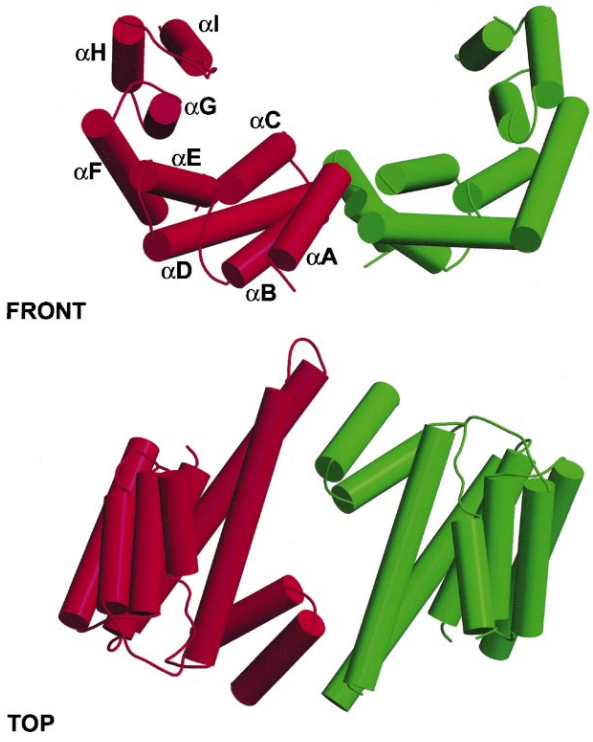

Figure 5.2 14-3-3 Dimeric Structure. The nine alpha helices are shown as cylinders and notated as αA – αI. [77]

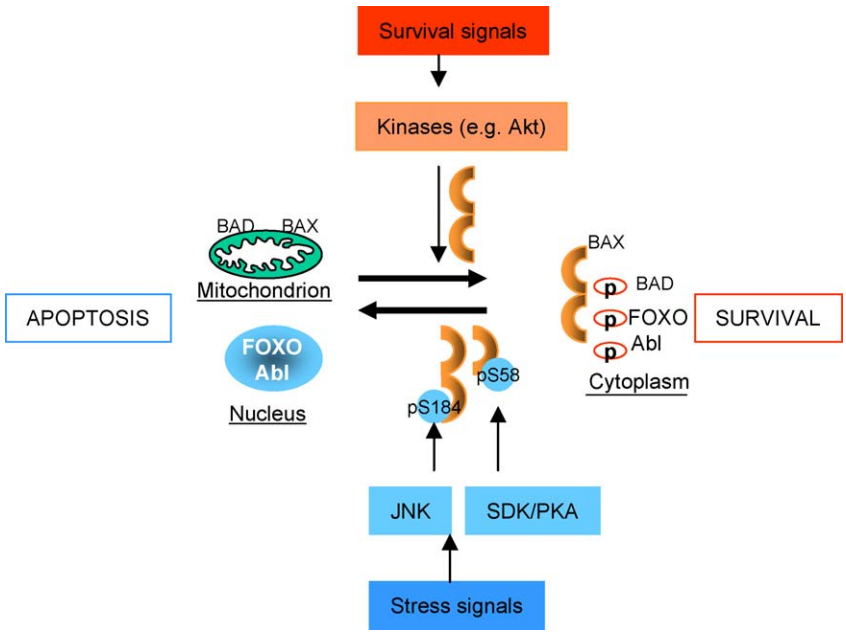

Figure 5.3 14-3-3 Apoptosis Regulation. 14-3-3 proteins, indicated by the copper colored dimeric loops, sequester proapoptotic proteins in the cytoplasm as a result of cellular survival signals. JNK phosphorylation of 14-3-3 dimers at Ser 184 or the formation of 14-3-3 monomers by the phosphorylation at S58 by SDK/PKA in response to cellular damage or stress signals causes the release of these proapoptotic proteins and their subsequent migration to the mitochondria or nucleus. [76]

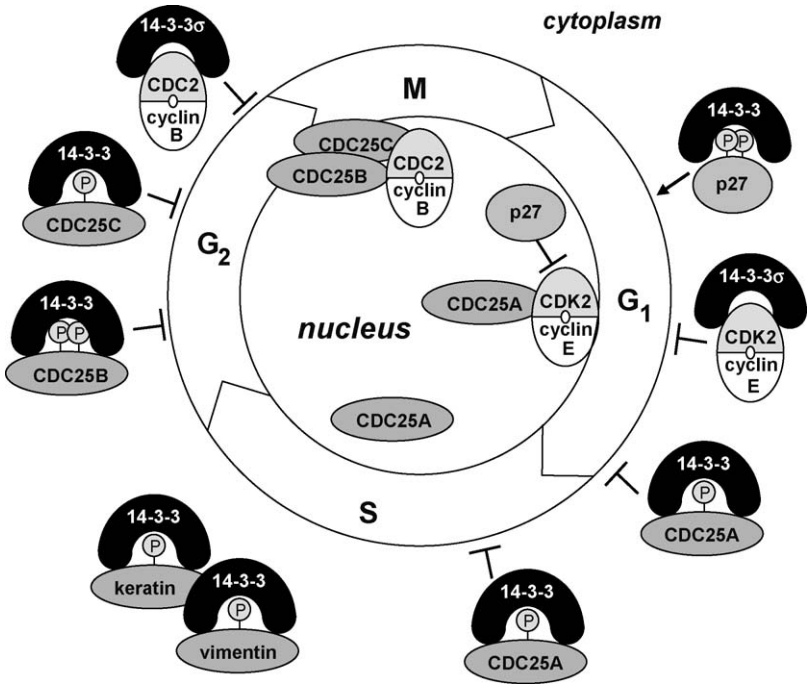

Figure 5.4 Summary of 14-3-3 protein interactions during the cell cycle. Taken from Hermeking and Benzinger [78].

Table 5.1 Cell cycle regulators affected by 14-3-3 binding. Adapted from Hermeking and Benzinger [78].

Cell cycle phase	Cell cycle regulator	14-3-3 isoform	Phosphorylation site	Kinase	Effect of association	Reference
G1–S	CDK2	σ	n.d.	n.d.	Cytoplasmic sequestration	[150]
	CDK4	σ	n.d.	n.d.	Cytoplasmic sequestration	[150]
	CDC25A	ε	S178, T507	CHK1	Cytoplasmic sequestration	[151]
	p27	ε, η, τ	T198	AKT	Cytoplasmic sequestration	[110]
	p27	ε, η, σ, τ	T198	RSK	Cytoplasmic sequestration	[152]
	p27	β, ε, γ, τ, ζ	T157	AKT	Cytoplasmic sequestration	[109]
	FOXO1	β, γ, η, τ, ζ	T24, S256	AKT	Cytoplasmic sequestration	[112, 113]
	FOXO3a	ζ	T32, S253	AKT	Cytoplasmic sequestration	[114]
	FOXO4	ζ	T28, S193	AKT	Cytoplasmic sequestration	[111]
	MIZ1	η, (γ,τ,σ)	S428, T291	AKT, n.d.	Inhibition of DNA-binding	[153]
G2–M	CDC2	σ	n.d.	n.d.	Cytoplasmic sequestration	[150, 154]
	CDC25B	β, ε	S309	CHK1, p38	Cytoplasmic sequestration	[155-157]
	CDC25B	σ	S216	CHK1	Unclear	[157]
	CDC25C	ε, γ, ζ	S216	CHK1, CHK2, c-TAK1	Cytoplasmic sequestration	[104, 158-160]
	WEE1	β, σ	S642	CHK1	Increase of kinase activity	[161-163]
	WEE1	τ	S642	AKT	Cytoplasmic sequestration	[164]
	CHK1	β, ζ	S345	(ATR)	Nuclear retention	[106, 107]
	p53	γ, ε, τ	S378	PKC	Increase in DNA-binding	[165, 166]
	p53	σ	n.d.	n.d.	Increase in DNA-binding	[167]
	MDMX	β, γ, ε, η, τ, ζ	S367	n.d.	Degradation	[108]

n.d. – not determined

Table 5.2 Cellular Localization of Vdac. Adapted from Reyman, et. al [117] and Shoshan-Barmatz and Israelson [115].

Cell Component	Cell Source	Vdac Isoform (if known)	Reference
Sarcoplasmic reticulum	Cane toad, *Bufo marinus*		[168]
	Rabbit skeletal muscle	Vdac1 + Vdac?	[130, 169]
Endoplasmic reticulum	Rat cerebellum		[125]
Plasma membrane	Bovine astrocytes	Vdac1	[133]
	Human lymphocytes	Vdac1	[117, 170]
	Rat neurons	Vdac1	[118]
	Synaptosomes of Torpedo Electric Organ, *Torpedo marmorata* and *Torpedo oscellata*	Multiple versions – closest matches to Vdac1 and Vdac3	[171]
	Caveolae and caveolae like domains from rat heart, bovine brain, dog lung, and human lymph-ocytes, megakaryocytes, promyelocytes, monocytes	Vdac1	[172]
	Mouse lung caveolae	Vdac1 per [172]	[173]
Endocytotic vesicles	Rat renal cortex	Vdac1	[174]

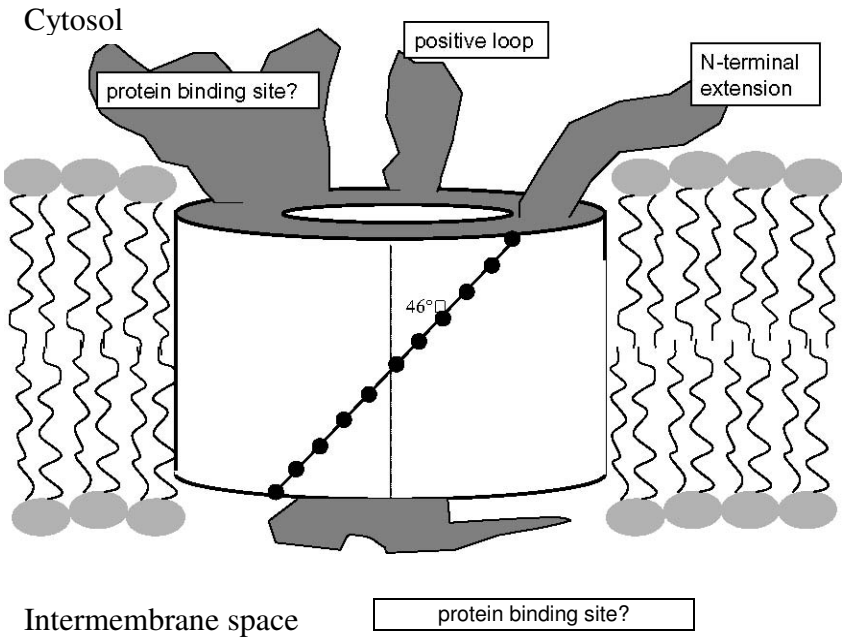

Figure 5.5 Model of VDAC in the Mitochondrial Membrane. [122]

Table 5.3 Modifiers of Vdac channel activity. Adapted from Shoshan-Barmatz and Israelson [115].

Molecule	Reference
Ruthenium red (RuR)	[115, 138, 175]
Ruthenium amine binuclear complex (Ru360)	[115, 138, 176]
Dicyclohexylcarbodiimide (DCCD)	[130, 169]
4,4'-diisothiocyanostilbene-2,2'-disulfide acid (DIDS)	[115, 130]
Soluble protein	[177, 178]
Hexokinase (HK-1)	[115, 146]
NADH	[179]
$LaCl_3$	[115, 175, 176]
Glutamate	[115, 138, 176, 180, 181]
Polyamines	[182]
Polyanions	[183]

REFERENCES

1. Sharov, A.A., et al., *Transcriptome analysis of mouse stem cells and early embryos.* Plos Biology, 2003. **1**(3).
2. Matoba, R., et al., *Dissecting Oct3/4-Regulated Gene Networks in Embryonic Stem Cells by Expression Profiling.* PLoS ONE, 2006. **1**(1): p. e26.
3. Biswas, A. and R. Hutchins, *Embryonic Stem Cells.* Stem Cells and Development, 2007. **16**(2): p. 213-222.
4. Donovan, P.J. and J. Gearhart, *The end of the beginning for pluripotent stem cells.* Nature, 2001. **414**: p. 92-97.
5. Lovell-Badge, R., *The future for stem cell research.* Nature., 2001. **414(6859)**: p. 88-91.
6. Pera, M.F., B. Reubinoff, and A. Trounson, *Human embryonic stem cells.* Journal of Cell Science, 2000. **113**(Pt 1): p. 5-10.
7. Evans, M.J. and M.H. Kaufman, *Establishment in culture of pluripotential cells from mouse embryos.* Nature, 1981. **292**(5819): p. 154-6.
8. Martin, G.R., *Isolation of a pluripotent cell line from early mouse embryos cultured in medium conditioned by teratocarcinoma stem cells.* Proceedings of the National Academy of Sciences of the United States of America, 1981. **78**(12): p. 7634-8.
9. Bongso, A., et al., *Isolation and culture of inner cell mass cells from human blastocysts.* Human Reproduction, 1994. **9**(11): p. 2110-7.
10. Thomson, J.A., et al., *Embryonic stem cell lines derived from human blastocysts.* Science, 1998. **282**(5391): p. 1145-7.
11. Shamblott, M.J., et al., *Derivation of pluripotent stem cells from cultured human primordial germ cells.* Proceedings of the National Academy of Sciences of the United States of America, 1998. **95**(23): p. 13726-31.
12. *NIH Human Embryonic Stem Cell Registry*, in *Stem Cell Information [World Wide Web site]*, National Institute of Health. U.S. Department of Health and Human Services.
13. Anonymous, *Burning bridges.* Nature Biotechnology, 2007. **25**(1).
14. *Stem Cells: Scientific Progress and Future Directions*. 2001, National Institutes of Health. p. 106+.
15. Anderson, K.N., ed. *Mosby's Medical, Nursing, and Allied Health Dictionary*. 5th ed. 1998, Mosby: St. Louis. 2042.
16. Larsen, W.J., *Human Embryology*. 2nd ed. 1997, New York: Churchill Livingstone. 512.
17. Hogan, B., F. Costantini, and E. Lacy, *Manipulating the Mouse Embryo: A Laboratory Manual*. 1986, Cold Springs Harbor: Cold Springs Harbor Laboratory. 332.
18. Guan, K., et al., *Pluripotency of spermatogonial stem cells from adult mouse testis.* Nature, 2006. **440**(7088): p. 1199-1203.

19. Jiang, Y., et al., *Pluripotency of mesenchymal stem cells derived from adult marrow.* Nature, 2002. **418**(6893): p. 41-49.
20. De Coppi, P., et al., *Isolation of amniotic stem cell lines with potential for therapy.* Nature Biotechnology, 2007. **25**(1): p. 100-106.
21. Trounson, A., *A fluid means of stem cell generation.* Nature Biotechnology, 2007. **25**(1): p. 62-63.
22. Goldsby, R.A., et al., *Immunology*. 5th ed. 2003, New York: W.H. Freeman and Company. 551+.
23. Kim, S.J., et al., *Human Placenta-Derived Feeders Support Prolonged Undifferentiated Propagation of a Human Embryonic Stem Cell Line, SNUhES3: Comparison with Human Bone Marrow-Derived Feeders.* Stem Cells and Development, 2007. **16**(3): p. 421-428.
24. Ozolek, J.A., et al., *Human Embryonic Stem Cells (HSF-6) Show Greater Proliferation and Apoptoses When Grown on Glioblastoma Cells Than Mouse Embryonic Fibroblasts at Day 19 in Culture: Comparison of Proliferation, Survival, and Neural Differentiation on Two Different Feeder Cell Types.* Stem Cells and Development, 2007. **16**(3): p. 403-412.
25. Lodish, H., et al., *Molecular Cell Biology*. 4th ed. 2000, Basingstroke, England: W. H. Freeman and Company. 1084+.
26. Koestenbauer, S., et al., *Embryonic stem cells: similarities and differences between human and murine embryonic stem cells.* American Journal of Reproductive Immunology, 2006. **55**(3): p. 169-80.
27. Bortvin, A., et al., *Incomplete reactivation of Oct4-related genes in mouse embryos cloned from somatic nuclei.* Development, 2003. **130**(8): p. 1673-80.
28. Zangrossi, S., et al., *Oct-4 Expression in Adult Human Differentiated Cells Challenges Its Role as a Pure Stem Cell Marker.* Stem Cells, 2007. **25**(7): p. 1675-1680.
29. Gurdon, J.B. and A. Colman, *The future of cloning.* Nature, 1999. **402**(6763): p. 743-6.
30. Cyranoski, D., *Activated eggs offer route to stem cells.* Nature, 2007. **448**(7150): p. 116.
31. Revazova, E.S., et al., *Patient-Specific Stem Cell Lines Derived from Human Parthenogenetic Blastocysts.* Cloning Stem Cells, 2007.
32. Shamblott, M.J., et al., *Human embryonic germ cell derivatives express a broad range of developmentally distinct markers and proliferate extensively in vitro.* Proceedings of the National Academy of Sciences of the United States of America, 2001. **98**(1): p. 113-8.
33. Carter, M.G., et al., *The NIA cDNA project in mouse stem cells and early embryos.* Comptes Rendus Biologies, 2003. **326**(10-11): p. 931-40.
34. Diatchenko, L., et al., *Suppression subtractive hybridization: a method for generating differentially regulated or tissue-specific cDNA probes and libraries.* Proceedings of the National Academy of Sciences of the United States of America, 1996. **93**(12): p. 6025-30.
35. Lee, K.F., K.L. Kwok, and W.S. Yeung, *Suppression subtractive hybridization identifies genes expressed in oviduct during mouse preimplantation period.* Biochemical & Biophysical Research Communications, 2000. **277**(3): p. 680-5.

36. Robert, C., et al., *Subtractive hybridization used to identify mRNA associated with the maturation of bovine oocytes.* Molecular Reproduction & Development, 2000. **57**(2): p. 167-75.
37. Zeng, F. and R.M. Schultz, *Gene expression in mouse oocytes and preimplantation embryos: use of suppression subtractive hybridization to identify oocyte- and embryo-specific genes.* Biol Reprod, 2003. **68**(1): p. 31-9.
38. Yao, Y.Q., et al., *Identification of mRNAs that are up-regulated after fertilization in the murine zygote by suppression subtractive hybridization.* Biochem Biophys Res Commun, 2003. **304**(1): p. 60-6.
39. Du, Z., H. Cong, and Z. Yao, *Identification of putative downstream genes of Oct-4 by suppression-subtractive hybridization.* Biochem Biophys Res Commun, 2001. **282**(3): p. 701-6.
40. *Super SMART TM PCR cDNA Synthesis Kit User Manual*. 2002, Mountain View, CA: CLONTECH Laboratories, Inc. 39.
41. *SMART TM PCR cDNA Synthesis Kit User Manual*. 2001: CLONTECH Laboratories, Inc. 1-39.
42. *CLONTECH PCR-Select TM cDNA Substraction Kit User Manual*. 2000: CLONTECH Laboratories, Inc. 1-47.
43. Diatchenko, L., A. Chenchik, and P.D. Siebert, *Suppression Subtractive Hybridization: A Method for Generating Subtracted cDNA Libraries Starting from Poly(A+) or Total RNA*, in *Gene Cloning and Analysis by RT-PCR*, P.D. Siebert and J. Larrick, Editors. 1998, BioTechniques Books: Natick, MD. p. 213-237.
44. Hall, T., *BioEdit: a user-friendly biological sequence alignment editor and analysis*. 1999: Raleigh.
45. *Lasergene*. 2001, DNASTAR, Inc: Madison.
46. Marino, J.H., P. Cook, and K.S. Miller, *Accurate and statistically verified quantification of relative mRNA abundances using SYBR Green I and real-time RT-PCR.* Journal of Immunological Methods, 2003. **283**(1-2): p. 291-306.
47. Neumann, C.A., et al., *Essential role for the peroxiredoxin Prdx1 in erythrocyte antioxidant defence and tumour suppression.* Nature, 2003. **424**(6948): p. 561-5.
48. Lyu, M.S., et al., *Genetic mapping of six mouse peroxiredoxin genes and fourteen peroxiredoxin related sequences.* Mammalian Genome, 1999. **10**(10): p. 1017-9.
49. Kang, S.W., et al., *Mammalian peroxiredoxin isoforms can reduce hydrogen peroxide generated in response to growth factors and tumor necrosis factor-alpha.* Journal of Biological Chemistry, 1998. **273**(11): p. 6297-302.
50. Kim, Y.J., et al., *Human prx1 gene is a target of Nrf2 and is up-regulated by hypoxia/reoxygenation: implication to tumor biology.* Cancer Research, 2007. **67**(2): p. 546-54.
51. Rhee, S.G., et al., *Cellular regulation by hydrogen peroxide.* Journal of the American Society of Nephrology, 2003. **14**(8 Suppl 3).
52. Finkel, T., *Oxygen radicals and signaling.* Current Opinion in Cell Biology, 1998. **10**(2): p. 248-53.
53. Demple, B., *Study of redox-regulated transcription factors in prokaryotes.* Methods, 1997. **11**(3): p. 267-78.

54. Shirasu, K., R.A. Dixon, and C. Lamb, *Signal transduction in plant immunity.* Current Opinion in Immunology, 1996. **8**(1): p. 3-7.
55. Rhee, S.G., et al., *Hydrogen peroxide: a key messenger that modulates protein phosphorylation through cysteine oxidation.* Science's Stke [Electronic Resource]: Signal Transduction Knowledge Environment, 2000. **53**: p. 10.
56. Prosperi, M.T., et al., *A human cDNA corresponding to a gene overexpressed during cell proliferation encodes a product sharing homology with amoebic and bacterial proteins.* Journal of Biological Chemistry, 1993. **268**(15): p. 11050-6.
57. Satoh, J. and Y. Kuroda, *Differential gene expression between human neurons and neuronal progenitor cells in culture: an analysis of arrayed cDNA clones in NTera2 human embryonal carcinoma cell line as a model system.* Journal of Neuroscience Methods, 2000. **94**(2): p. 155-64.
58. Deng, B., et al., *Proteomics analysis of stage-specific proteins expressed in human squamous cell lung carcinoma tissues.* Disease Markers Section a Cancer Biomarkers, 2005. **1**(6): p. 279-86.
59. Kim, S.H., et al., *Protein levels of human peroxiredoxin subtypes in brains of patients with Alzheimer's disease and Down syndrome.* Journal of Neural Transmission. Supplementum, 2001. **61**: p. 223-35.
60. Shan, S.W., et al., *Comparative proteomic analysis identifies protein disulfide isomerase and peroxiredoxin 1 as new players involved in embryonic interdigital cell death.* Developmental Dynamics, 2005. **233**(2): p. 266-81.
61. Hoffrogge, R., et al., *2-DE proteome analysis of a proliferating and differentiating human neuronal stem cell line (ReNcell VM).* Proteomics, 2006. **6**(6): p. 1833-47.
62. Hoffrogge, R., et al., *2-DE profiling of GDNF overexpression-related proteome changes in differentiating ST14A rat progenitor cells.* Proteomics, 2007. **7**(1): p. 33-46.
63. Pahnke, J., et al., *Overexpression of glial cell line-derived neurotrophic factor induces genes regulating migration and differentiation of neuronal progenitor cells.* Experimental Cell Research, 2004. **297**(2): p. 484-94.
64. Mu, Z.M., X.Y. Yin, and E.V. Prochownik, *Pag, a putative tumor suppressor, interacts with the Myc Box II domain of c-Myc and selectively alters its biological function and target gene expression.* Journal of Biological Chemistry, 2002. **277**(45): p. 43175-84.
65. Egler, R.A., et al., *Regulation of reactive oxygen species, DNA damage, and c-Myc function by peroxiredoxin 1.* Oncogene, 2005. **24**(54): p. 8038-50.
66. Yoshida, K., et al., *JNK phosphorylation of 14-3-3 proteins regulates nuclear targeting of c-Abl in the apoptotic response to DNA damage.* Nature Cell Biology, 2005. **7**(3): p. 278-85.
67. Wen, S.T. and R.A. Van Etten, *The PAG gene product, a stress-induced protein with antioxidant properties, is an Abl SH3-binding protein and a physiological inhibitor of c-Abl tyrosine kinase activity.* Genes & Development, 1997. **11**(19): p. 2456-67.
68. Levav-Cohen, Y., et al., *C-Abl as a modulator of p53.* Biochemical & Biophysical Research Communications, 2005. **331**(3): p. 737-49.

69. Tanaka, T.S., et al., *Gene Expression Profiling of Embryo-Derived Stem Cells Reveals Candidate Genes Associated With Pluripotency and Lineage Specificity.* Genome Res., 2002. **12**(12): p. 1921-1928.
70. Aitken, A., *14-3-3 proteins: a historic overview.* Seminars in Cancer Biology, 2006. **16**(3): p. 162-72.
71. Berg, D., C. Holzmann, and O. Riess, *14-3-3 proteins in the nervous system.* Nature Reviews Neuroscience, 2003. **4**(9): p. 752-62.
72. Kjarland, E., T.J. Keen, and R. Kleppe, *Does isoform diversity explain functional differences in the 14-3-3 protein family?* Current Pharmaceutical Biotechnology, 2006. **7**(3): p. 217-23.
73. Ichimura, T., et al., *Brain 14-3-3 protein is an activator protein that activates tryptophan 5-monooxygenase and tyrosine 3-monooxygenase in the presence of Ca2+,calmodulin-dependent protein kinase II.* FEBS Letters, 1987. **219**(1): p. 79-82.
74. Meek, S.E., W.S. Lane, and H. Piwnica-Worms, *Comprehensive proteomic analysis of interphase and mitotic 14-3-3-binding proteins.* Journal of Biological Chemistry, 2004. **279**(31): p. 32046-54.
75. Hermeking, H., *14-3-3 proteins and cancer biology.* Seminars in Cancer Biology, 2006. **16**(3): p. 161.
76. Porter, G.W., F.R. Khuri, and H. Fu, *Dynamic 14-3-3/client protein interactions integrate survival and apoptotic pathways.* Seminars in Cancer Biology, 2006. **16**(3): p. 193-202.
77. Yaffe, M.B., *How do 14-3-3 proteins work?-- Gatekeeper phosphorylation and the molecular anvil hypothesis.* FEBS Letters, 2002. **513**(1): p. 53-7.
78. Hermeking, H. and A. Benzinger, *14-3-3 proteins in cell cycle regulation.* Seminars in Cancer Biology, 2006. **16**(3): p. 183-92.
79. Jones, D.H., S. Ley, and A. Aitken, *Isoforms of 14-3-3 protein can form homo- and heterodimers in vivo and in vitro: implications for function as adapter proteins.* FEBS Letters, 1995. **368**(1): p. 55-8.
80. Chaudhri, M., M. Scarabel, and A. Aitken, *Mammalian and yeast 14-3-3 isoforms form distinct patterns of dimers in vivo.* Biochemical & Biophysical Research Communications, 2003. **300**(3): p. 679-85.
81. Spinsanti, G., et al., *Selection of reference genes for quantitative RT-PCR studies in striped dolphin (Stenella coeruleoalba) skin biopsies.* BMC Molecular Biology, 2006. **7**(32).
82. Meller, M., et al., *Evaluation of housekeeping genes in placental comparative expression studies.* Placenta, 2005. **26**(8-9): p. 601-7.
83. Goossens, K., et al., *Selection of reference genes for quantitative real-time PCR in bovine preimplantation embryos.* BMC Developmental Biology, 2005. **5**(27).
84. Ohl, F., et al., *Gene expression studies in prostate cancer tissue: which reference gene should be selected for normalization?* Journal of Molecular Medicine, 2005. **83**(12): p. 1014-24.
85. Jia, Y., et al., *An association study between polymorphisms in three genes of 14-3-3 (tyrosine 3-monooxygenase/tryptophan 5-monooxygenase activation protein) family and paranoid schizophrenia in northern Chinese population.* European

Psychiatry: the Journal of the Association of European Psychiatrists, 2004. **19**(6): p. 377-9.
86. Berg, D., O. Riess, and A. Bornemann, *Specification of 14-3-3 proteins in Lewy bodies.* Annals of Neurology, 2003. **54**(1).
87. Janssen, J.J., et al., *Identification of genes potentially involved in disease transformation of CML.* Leukemia, 2005. **19**(6): p. 998-1004.
88. Hashiguchi, M., K. Sobue, and H.K. Paudel, *14-3-3zeta is an effector of tau protein phosphorylation.* Journal of Biological Chemistry, 2000. **275**(33): p. 25247-54.
89. Zannis-Hadjopoulos, M., et al., *14-3-3s are DNA-replication proteins.* Biochemical Society Transactions, 2002. **30**(4): p. 397-401.
90. Yaffe, M.B., et al., *The structural basis for 14-3-3:phosphopeptide binding specificity.* Cell, 1997. **91**(7): p. 961-71.
91. Dubois, T., et al., *14-3-3 is phosphorylated by casein kinase I on residue 233. Phosphorylation at this site in vivo regulates Raf/14-3-3 interaction.* Journal of Biological Chemistry, 1997. **272**(46): p. 28882-8.
92. Shah, B.H. and K.J. Catt, *Protein phosphatase 5 as a negative key regulator of Raf-1 activation.* Trends in Endocrinology & Metabolism, 2006. **17**(10): p. 382-4.
93. Daum, G., et al., *The ins and outs of Raf kinases.* Trends in Biochemical Sciences, 1994. **19**(11): p. 474-80.
94. Michaud, N.R., et al., *14-3-3 is not essential for Raf-1 function: identification of Raf-1 proteins that are biologically activated in a 14-3-3- and Ras-independent manner.* Molecular & Cellular Biology, 1995. **15**(6): p. 3390-7.
95. Sunayama, J., et al., *JNK antagonizes Akt-mediated survival signals by phosphorylating 14-3-3.* Journal of Cell Biology, 2005. **170**(2): p. 295-304.
96. Tsuruta, F., et al., *JNK promotes Bax translocation to mitochondria through phosphorylation of 14-3-3 proteins.* EMBO Journal, 2004. **23**(8): p. 1889-99.
97. Wang, H.G., et al., *Ca2+-induced apoptosis through calcineurin dephosphorylation of BAD.* Science, 1999. **284**(5412): p. 339-43.
98. Qi, X.J., G.M. Wildey, and P.H. Howe, *Evidence that Ser87 of BimEL is phosphorylated by Akt and regulates BimEL apoptotic function.* Journal of Biological Chemistry, 2006. **281**(2): p. 813-23.
99. Shen, Y.H., et al., *Significance of 14-3-3 self-dimerization for phosphorylation-dependent target binding.* Molecular Biology of the Cell, 2003. **14**(11): p. 4721-33.
100. Woodcock, J.M., et al., *The dimeric versus monomeric status of 14-3-3zeta is controlled by phosphorylation of Ser58 at the dimer interface.* Journal of Biological Chemistry, 2003. **278**(38): p. 36323-7.
101. Tzivion, G., et al., *14-3-3 proteins as potential oncogenes.* Seminars in Cancer Biology, 2006. **16**(3): p. 203-13.
102. Graves, P.R., et al., *Localization of human Cdc25C is regulated both by nuclear export and 14-3-3 protein binding.* Oncogene, 2001. **20**(15): p. 1839-51.
103. Kumagai, A. and W.G. Dunphy, *Binding of 14-3-3 proteins and nuclear export control the intracellular localization of the mitotic inducer Cdc25.* Genes & Development, 1999. **13**(9): p. 1067-72.

104. Peng, C.Y., et al., *C-TAK1 protein kinase phosphorylates human Cdc25C on serine 216 and promotes 14-3-3 protein binding.* Cell Growth & Differentiation, 1998. **9**(3): p. 197-208.
105. Bulavin, D.V., et al., *Phosphorylation of Xenopus Cdc25C at Ser285 interferes with ability to activate a DNA damage replication checkpoint in pre-midblastula embryos.[see comment].* Cell Cycle, 2003. **2**(3): p. 263-6.
106. Liu, Q., et al., *Chk1 is an essential kinase that is regulated by Atr and required for the G(2)/M DNA damage checkpoint.* Genes & Development, 2000. **14**(12): p. 1448-59.
107. Jiang, K., et al., *Regulation of Chk1 includes chromatin association and 14-3-3 binding following phosphorylation on Ser-345.* Journal of Biological Chemistry, 2003. **278**(27): p. 25207-17.
108. Okamoto, K., et al., *DNA damage-induced phosphorylation of MdmX at serine 367 activates p53 by targeting MdmX for Mdm2-dependent degradation.* Molecular & Cellular Biology, 2005. **25**(21): p. 9608-20.
109. Sekimoto, T., M. Fukumoto, and Y. Yoneda, *14-3-3 suppresses the nuclear localization of threonine 157-phosphorylated p27(Kip1).* EMBO Journal, 2004. **23**(9): p. 1934-42.
110. Fujita, N., et al., *Akt-dependent phosphorylation of p27Kip1 promotes binding to 14-3-3 and cytoplasmic localization.* Journal of Biological Chemistry, 2002. **277**(32): p. 28706-13.
111. Obsil, T., et al., *Two 14-3-3 binding motifs are required for stable association of Forkhead transcription factor FOXO4 with 14-3-3 proteins and inhibition of DNA binding.* Biochemistry, 2003. **42**(51): p. 15264-72.
112. Zhao, X., et al., *Multiple elements regulate nuclear/cytoplasmic shuttling of FOXO1: characterization of phosphorylation- and 14-3-3-dependent and -independent mechanisms.* Biochemical Journal, 2004. **378**(Pt 3): p. 839-49.
113. Rena, G., et al., *Roles of the forkhead in rhabdomyosarcoma (FKHR) phosphorylation sites in regulating 14-3-3 binding, transactivation and nuclear targetting.* Biochemical Journal, 2001. **354**(Pt 3): p. 605-12.
114. Brunet, A., et al., *Akt promotes cell survival by phosphorylating and inhibiting a Forkhead transcription factor.* Cell, 1999. **96**(6): p. 857-68.
115. Shoshan-Barmatz, V. and A. Israelson, *The voltage-dependent anion channel in endoplasmic/sarcoplasmic reticulum: characterization, modulation and possible function.* Journal of Membrane Biology, 2005. **204**(2): p. 57-66.
116. Shoshan-Barmatz, V., et al., *The voltage-dependent anion channel (VDAC): function in intracellular signalling, cell life and cell death.* Current Pharmaceutical Design, 2006. **12**(18): p. 2249-70.
117. Reymann, S., et al., *Further evidence for multitopological localization of mammalian porin (VDAC) in the plasmalemma forming part of a chloride channel complex affected in cystic fibrosis and encephalomyopathy.* Biochemical & Molecular Medicine, 1995. **54**(2): p. 75-87.
118. Bureau, M.H., et al., *Isolation and cloning of a voltage-dependent anion channel-like Mr 36,000 polypeptide from mammalian brain.* Journal of Biological Chemistry, 1992. **267**(12): p. 8679-84.

119. Sampson, M.J., R.S. Lovell, and W.J. Craigen, *The murine voltage-dependent anion channel gene family. Conserved structure and function.* Journal of Biological Chemistry, 1997. **272**(30): p. 18966-73.
120. Sampson, M.J., et al., *A novel mouse mitochondrial voltage-dependent anion channel gene localizes to chromosome 8.* Genomics, 1996. **36**(1): p. 192-6.
121. Sampson, M.J., et al., *A novel isoform of the mitochondrial outer membrane protein VDAC3 via alternative splicing of a 3-base exon. Functional characteristics and subcellular localization.* Journal of Biological Chemistry, 1998. **273**(46): p. 30482-6.
122. Colombini, M., *VDAC: the channel at the interface between mitochondria and the cytosol.* Molecular & Cellular Biochemistry, 2004. **257**(1-2): p. 107-15.
123. De Pinto, V.D. and F. Palmieri, *Transmembrane arrangement of mitochondrial porin or voltage-dependent anion channel (VDAC).* Journal of Bioenergetics & Biomembranes, 1992. **24**(1): p. 21-6.
124. Zalk, R., et al., *Oligomeric states of the voltage-dependent anion channel and cytochrome c release from mitochondria.* Biochemical Journal, 2005. **386**(Pt 1): p. 73-83.
125. Shoshan-Barmatz, V., et al., *Subcellular localization of VDAC in mitochondria and ER in the cerebellum.* Biochimica et Biophysica Acta, 2004. **1657**(2-3): p. 105-14.
126. Xu, X., et al., *Mouse VDAC isoforms expressed in yeast: channel properties and their roles in mitochondrial outer membrane permeability.* Journal of Membrane Biology, 1999. **170**(2): p. 89-102.
127. Wu, S., et al., *Each mammalian mitochondrial outer membrane porin protein is dispensable: effects on cellular respiration.* Biochimica et Biophysica Acta, 1999. **1**: p. 68-78.
128. Sampson, M.J., et al., *Immotile sperm and infertility in mice lacking mitochondrial voltage-dependent anion channel type 3.* Journal of Biological Chemistry, 2001. **276**(42): p. 39206-12.
129. Hinsch, K.D., et al., *Voltage-dependent anion-selective channels VDAC2 and VDAC3 are abundant proteins in bovine outer dense fibers, a cytoskeletal component of the sperm flagellum.* Journal of Biological Chemistry, 2004. **279**(15): p. 15281-8.
130. Shoshan-Barmatz, V., et al., *VDAC/porin is present in sarcoplasmic reticulum from skeletal muscle.* FEBS Letters, 1996. **386**(2-3): p. 205-10.
131. Schwiebert, E.M., et al., *CFTR regulates outwardly rectifying chloride channels through an autocrine mechanism involving ATP.* Cell, 1995. **81**(7): p. 1063-73.
132. Okada, S.F., et al., *Voltage-dependent anion channel-1 (VDAC-1) contributes to ATP release and cell volume regulation in murine cells.* Journal of General Physiology, 2004. **124**(5): p. 513-26.
133. Dermietzel, R., et al., *Cloning and in situ localization of a brain-derived porin that constitutes a large-conductance anion channel in astrocytic plasma membranes.* Proceedings of the National Academy of Sciences of the United States of America, 1994. **91**(2): p. 499-503.

134. Han, D., et al., *Voltage-dependent anion channels control the release of the superoxide anion from mitochondria to cytosol.* Journal of Biological Chemistry, 2003. **278**(8): p. 5557-63.
135. Vander Heiden, M.G., et al., *Outer mitochondrial membrane permeability can regulate coupled respiration and cell survival.* Proceedings of the National Academy of Sciences of the United States of America, 2000. **97**(9): p. 4666-71.
136. Doran, E. and A.P. Halestrap, *Cytochrome c release from isolated rat liver mitochondria can occur independently of outer-membrane rupture: possible role of contact sites.* Biochemical Journal, 2000. **2**: p. 343-50.
137. Von Ahsen, O., et al., *Preservation of mitochondrial structure and function after Bid- or Bax-mediated cytochrome c release.* Journal of Cell Biology, 2000. **150**(5): p. 1027-36.
138. Shoshan-Barmatz, V. and D. Gincel, *The voltage-dependent anion channel: characterization, modulation, and role in mitochondrial function in cell life and death.* Cell Biochemistry & Biophysics, 2003. **39**(3): p. 279-92.
139. Crompton, M., *The mitochondrial permeability transition pore and its role in cell death.* Biochemical Journal, 1999. **341**(Pt 2): p. 233-49.
140. Tsujimoto, Y., T. Nakagawa, and S. Shimizu, *Mitochondrial membrane permeability transition and cell death.* Biochimica et Biophysica Acta, 2006: p. Sep-Oct.
141. Shimizu, S., et al., *Essential role of voltage-dependent anion channel in various forms of apoptosis in mammalian cells.* Journal of Cell Biology, 2001. **152**(2): p. 237-50.
142. Zaid, H., et al., *The voltage-dependent anion channel-1 modulates apoptotic cell death.* Cell Death & Differentiation, 2005. **12**(7): p. 751-60.
143. Godbole, A., et al., *VDAC is a conserved element of death pathways in plant and animal systems.* Biochimica et Biophysica Acta, 2003. **1642**(1-2): p. 87-96.
144. Shinohara, Y., et al., *Characterization of porin isoforms expressed in tumor cells.* European Journal of Biochemistry, 2000. **267**(19): p. 6067-73.
145. Nakashima, R.A., et al., *Purification and characterization of a bindable form of mitochondrial bound hexokinase from the highly glycolytic AS-30D rat hepatoma cell line.* Cancer Research, 1988. **48**(4): p. 913-9.
146. Azoulay-Zohar, H., et al., *In self-defence: hexokinase promotes voltage-dependent anion channel closure and prevents mitochondria-mediated apoptotic cell death.* Biochemical Journal, 2004. **377**(Pt 2): p. 347-55.
147. Kroemer, G., *Mitochondria in cancer.* Oncogene, 2006. **25**(34): p. 4630-2.
148. Robey, R.B. and N. Hay, *Mitochondrial hexokinases, novel mediators of the antiapoptotic effects of growth factors and Akt.* Oncogene, 2006. **25**(34): p. 4683-96.
149. Mathupala, S.P., Y.H. Ko, and P.L. Pedersen, *Hexokinase II: cancer's double-edged sword acting as both facilitator and gatekeeper of malignancy when bound to mitochondria.* Oncogene, 2006. **25**(34): p. 4777-86.
150. Laronga, C., et al., *Association of the cyclin-dependent kinases and 14-3-3 sigma negatively regulates cell cycle progression.* Journal of Biological Chemistry, 2000. **275**(30): p. 23106-12.

151. Chen, M.S., C.E. Ryan, and H. Piwnica-Worms, *Chk1 kinase negatively regulates mitotic function of Cdc25A phosphatase through 14-3-3 binding.* Molecular & Cellular Biology, 2003. **23**(21): p. 7488-97.
152. Fujita, N., S. Sato, and T. Tsuruo, *Phosphorylation of p27Kip1 at threonine 198 by p90 ribosomal protein S6 kinases promotes its binding to 14-3-3 and cytoplasmic localization.* Journal of Biological Chemistry, 2003. **278**(49): p. 49254-60.
153. Wanzel, M., et al., *Akt and 14-3-3eta regulate Miz1 to control cell-cycle arrest after DNA damage.* Nature Cell Biology, 2005. **7**(1): p. 30-41.
154. Chan, T.A., et al., *14-3-3Sigma is required to prevent mitotic catastrophe after DNA damage.[see comment].* Nature, 1999. **401**(6753): p. 616-20.
155. Forrest, A. and B. Gabrielli, *Cdc25B activity is regulated by 14-3-3.* Oncogene, 2001. **20**(32): p. 4393-401.
156. Bulavin, D.V., et al., *Initiation of a G2/M checkpoint after ultraviolet radiation requires p38 kinase.* Nature, 2001. **411**(6833): p. 102-7.
157. Uchida, S., et al., *Binding of 14-3-3beta but not 14-3-3sigma controls the cytoplasmic localization of CDC25B: binding site preferences of 14-3-3 subtypes and the subcellular localization of CDC25B.* Journal of Cell Science, 2004. **117**(Pt 14): p. 3011-20.
158. Peng, C.Y., et al., *Mitotic and G2 checkpoint control: regulation of 14-3-3 protein binding by phosphorylation of Cdc25C on serine-216.[see comment].* Science, 1997. **277**(5331): p. 1501-5.
159. Chaturvedi, P., et al., *Mammalian Chk2 is a downstream effector of the ATM-dependent DNA damage checkpoint pathway.* Oncogene, 1999. **18**(28): p. 4047-54.
160. Dalal, S.N., M.B. Yaffe, and J.A. DeCaprio, *14-3-3 family members act coordinately to regulate mitotic progression.* Cell Cycle, 2004. **3**(5): p. 672-7.
161. Wang, Y., et al., *Binding of 14-3-3beta to the carboxyl terminus of Wee1 increases Wee1 stability, kinase activity, and G2-M cell population.* Cell Growth & Differentiation, 2000. **11**(4): p. 211-9.
162. Rothblum-Oviatt, C.J., C.E. Ryan, and H. Piwnica-Worms, *14-3-3 binding regulates catalytic activity of human Wee1 kinase.* Cell Growth & Differentiation, 2001. **12**(12): p. 581-9.
163. Lee, J., A. Kumagai, and W.G. Dunphy, *Positive regulation of Wee1 by Chk1 and 14-3-3 proteins.* Molecular Biology of the Cell, 2001. **12**(3): p. 551-63.
164. Katayama, K., N. Fujita, and T. Tsuruo, *Akt/protein kinase B-dependent phosphorylation and inactivation of WEE1Hu promote cell cycle progression at G2/M transition.* Molecular & Cellular Biology, 2005. **25**(13): p. 5725-37.
165. Stavridi, E.S., et al., *Substitutions that compromise the ionizing radiation-induced association of p53 with 14-3-3 proteins also compromise the ability of p53 to induce cell cycle arrest.* Cancer Research, 2001. **61**(19): p. 7030-3.
166. Baudier, J., et al., *Characterization of the tumor suppressor protein p53 as a protein kinase C substrate and a S100b-binding protein.* Proceedings of the National Academy of Sciences of the United States of America, 1992. **89**(23): p. 11627-31.

167. Yang, H.Y., et al., *14-3-3 sigma positively regulates p53 and suppresses tumor growth.* Molecular & Cellular Biology, 2003. **23**(20): p. 7096-107.
168. Lewis, T.M., M.L. Roberts, and A.H. Bretag, *Immunolabelling for VDAC, the mitochondrial voltage-dependent anion channel, on sarcoplasmic reticulum from amphibian skeletal muscle.* Neuroscience Letters, 1994. **181**(1-2): p. 83-6.
169. Shafir, I., W. Feng, and V. Shoshan-Barmatz, *Dicyclohexylcarbodiimide interaction with the voltage-dependent anion channel from sarcoplasmic reticulum.* European Journal of Biochemistry, 1998. **253**(3): p. 627-36.
170. Thinnes, F.P., *Evidence for extra-mitochondrial localization of the VDAC/porin channel in eucaryotic cells.* Journal of Bioenergetics & Biomembranes, 1992. **24**(1): p. 71-5.
171. Shafir, I., W. Feng, and V. Shoshan-Barmataz, *Voltage-dependent anion channel proteins in synaptosomes of the torpedo electric organ: immunolocalization, purification, and characterization.* Journal of Bioenergetics & Biomembranes, 1998. **30**(5): p. 499-510.
172. Bathori, G., et al., *Porin is present in the plasma membrane where it is concentrated in caveolae and caveolae-related domains.* Journal of Biological Chemistry, 1999. **274**(42): p. 29607-12.
173. Lisanti, M.P., et al., *Characterization of caveolin-rich membrane domains isolated from an endothelial-rich source: implications for human disease.* Journal of Cell Biology, 1994. **126**(1): p. 111-26.
174. Reymann, S., et al., *Endosomes: another extra-mitochondrial location of type-1 porin/voltage-dependent anion-selective channels.* Pflugers Archiv European Journal of Physiology, 1998. **436**(3): p. 478-80.
175. Gincel, D., H. Zaid, and V. Shoshan-Barmatz, *Calcium binding and translocation by the voltage-dependent anion channel: a possible regulatory mechanism in mitochondrial function.* Biochemical Journal, 2001. **358**(Pt 1): p. 147-55.
176. Gincel, D., N. Vardi, and V. Shoshan-Barmatz, *Retinal voltage-dependent anion channel: characterization and cellular localization.* Investigative Ophthalmology & Visual Science, 2002. **43**(7): p. 2097-104.
177. Holden, M.J. and M. Colombini, *The mitochondrial outer membrane channel, VDAC, is modulated by a soluble protein.* FEBS Letters, 1988. **241**(1-2): p. 105-9.
178. Liu, M.Y., A. Torgrimson, and M. Colombini, *Characterization and partial purification of the VDAC-channel-modulating protein from calf liver mitochondria.* Biochimica et Biophysica Acta, 1994. **1185**(2): p. 203-12.
179. Zizi, M., et al., *NADH regulates the gating of VDAC, the mitochondrial outer membrane channel.* Journal of Biological Chemistry, 1994. **269**(3): p. 1614-6.
180. Gincel, D., S.D. Silberberg, and V. Shoshan-Barmataz, *Modulation of the Voltage-Dependent Anion Channel (VDAC) by Glutamate.* Journal of Bioenergetics & Biomembranes, 2000. **32**(6): p. 571-583.
181. Gincel, D. and V. Shoshan-Barmatz, *Glutamate interacts with VDAC and modulates opening of the mitochondrial permeability transition pore.* Journal of Bioenergetics & Biomembranes, 2004. **36**(2): p. 179-86.
182. Horn, A., S. Reymann, and F.P. Thinnes, *Studies on human porin. XVI: Polyamines reduce the voltage dependence of human VDAC in planar lipid*

bilayers--spermine and spermidine inducing asymmetric voltage gating on the channel. Molecular Genetics & Metabolism, 1998. **63**(3): p. 239-42.
183. Bathori, G., et al., *Novel aspects of the electrophysiology of mitochondrial porin.[erratum appears in Biochem Biophys Res Commun 1998 May 8;246(1):299].* Biochemical & Biophysical Research Communications, 1998. **243**(1): p. 258-63.
184. Rhee, S.G., H.Z. Chae, and K. Kim, *Peroxiredoxins: a historical overview and speculative preview of novel mechanisms and emerging concepts in cell signaling.* Free Radical Biology & Medicine, 2005. **38**(12): p. 1543-52.
185. Ishii, T., et al., *Cloning and characterization of a 23-kDa stress-induced mouse peritoneal macrophage protein.* Journal of Biological Chemistry, 1993. **268**(25): p. 18633-6.
186. Li, B., et al., *Pathways of induction of peroxiredoxin I expression in osteoblasts: roles of p38 mitogen-activated protein kinase and protein kinase C.* Journal of Biological Chemistry, 2002. **277**(14): p. 12418-22.
187. Kawai, S., et al., *Cloning and characterization of OSF-3, a new member of the MER5 family, expressed in mouse osteoblastic cells.* Journal of Biochemistry, 1994. **115**(4): p. 641-3.
188. Immenschuh, S., et al., *Expression of the mRNA of heme-binding protein 23 is coordinated with that of heme oxygenase-1 by heme and heavy metals in primary rat hepatocytes and hepatoma cells.* Biochemistry, 1995. **34**(41): p. 13407-11.
189. Shau, H. and A. Kim, *Identification of natural killer enhancing factor as a major antioxidant in human red blood cells.* Biochemical & Biophysical Research Communications, 1994. **199**(1): p. 83-8.

APPENDICES

Appendix A

Alternative Gene Names

Prdx1	Prdx1	Peroxiredoxin 1
	Prx1	Peroxiredoxin 1 [184]
	MSP23	Macrophage 23-kDa stress protein (mouse) [185, 186]
	OSF-3	Osteoblast specific factor 3 (mouse) [186, 187]
	PAG	Proliferation associated gene (human) [56, 186]
	HBP23	Heme-binding protein 23 kDa (rat) [186, 188]
	NKEF-A/NKEFA	Natural killer enhancing factor A [184, 189]
Ywhaz	Ywhaz	Tyrosine 3-monooxygenase/tryptophan -5-monooxygenase activation protein, zeta peptide
	14-3-3 ζ	Named based on its isolation pattern via (DEAE)-cellulose chromatography and starch-gel electrophoresis [71]
Vdac3		Mitochondrial porins [119]

Appendix B

Known Ywhaz Target Proteins [74]

Supplementary Table 1
(A) Mitosis

Function	Matched protein	Matched unique peptides	GenBank accession number (gi)
Cell division	NuMA	9, 2	35119
	Pericentriolar material 1 (PCM1)	3, 25	5453856
	NUDE (nuclear distribution gene E homolog)	1	8923110
	Replication factor C (RFC) 37 kDa subunit	1	4506491
	Rec 14	1	13376840
	Wee1 *	1	1085293
Signaling - Kinases	PCTAIRE-3	2	20178302
	PCTAIRE-2	4	266426|
	EMK / Par1B*	6, 11, 2	11067437
	C-TAK / Par1A*	15, 4	3089349
	B-raf *	12	213599
Signaling – Small GTPase related	Rho-interacting protein 3 (RIP3)	5, 2	21740322
	GEF-H1	1	19744759
	RhoGAP10	15, 10	25535866
	IQGAP1	3, 1	1170586
	KIAA1521	14	20521930
	ARHGEF 16	4	30353993
	ARL6-interacting protein 2	4	11641303
Signaling - Misc.	Liprin beta 1	25, 15	29294627
	LL5 beta	9, 2, 7	21955172
	Insulin receptor substrate 2 (IRS2) *	3, 2, 37, 23	14537854
	Phosphodiesterase (PDE) 3A *	3, 10	20070127
	Yes-associated protein (YAP)	2	1363003
	Epithelial protein lost in neoplasia B (EPLINb) / Sterol regulatory element binding protein 3 (SREBP3)	2	7705373
	calmodulin*	4	multiple
	PAR3 / ASIP*	2	11275612
	BA416N2.2, FISH-like	2, 3, 1	10334638
	signal-induced proliferation-associated 1 like 3	2	42661622
	Arg/Abl interacting protein 2	7, 8	10947118
	A kinase anchoring protein (AKAP)	42	21493029
	APC (adenomatous polyposis coli)	3	4557319
Nucleolar proteins	NOLC1 (nucleolar phosphoprotein p130)	54, 64, 5, 27, 20, 14, 32, 23, 11, 6	434765
	Nucleolin/C23	2	21750187
	Nucleophosmin / B23	4	10835063

Proteolysis/ ubiquitination	Ki Antigen / proteasome activator subunit	7	2135531
	26S proteasome regulatory subunit	1	6174930
	COP 9 subunit 4	1	7022321
Stress or checkpoint responses	Thioredoxin	2, 2, 1	10120659
	Peroxiredoxin 1	14	4505591
	KARP-1-binding protein (KAB1)	11	7662142
	KARP-1-binding protein 2 (KAB2)	4	5734603
Apoptosis	PCD6 (programmed cell death 6) / alg2	1	12230420
Nucleotide metabolism	CTP synthase	4	14495609
	Carbamoyl-phosphate synthase 1 (CPS1)	6	21361331
	Poly(p)/ATP NAD kinase	11, 5	8480400
	Nucleoside diphosphate kinase	3	1421609
	Thymidine kinase	1	225602
	UMP-CMP kinase	1	2497487
Chromatin structure, DNA binding	HDAC4 *	23, 8, 11, 18	5174481
	HDAC7A*	2, 15, 2, 7	30913097
	Y-box binding protein 1	5	181468
	mitochondrial ssDNA-binding protein	3	2624694
	Histone acetyltransferase B subunit 2	2	3334209
	Histone H4	7	122098
	Histone H2 B	5	10800138
	Histone 1 (histone 2A G)	4	10800130
	SUPT6H	6, 9	1136404
	DNA methyltransferase 1	1	20137608
	CGI-46 / DNA helicase	5	4929561
	RuvB-like (ATP helicase)	1	28201891
RNA binding	hnRNP F	2	16876910
	hnRNP H2	1	9624998
	hnRNP K	4	585911
	hnRNP X	13, 5	5453854
	hnRNP C	9	13097279
	hnRNP A1	4	133254
	LRPPRC (LRP130, GP130, Leucine-rich PPR motif containing protein)	3	1730078
	Dead-box RNA binding protein 1 (DDX1)	3, 4	6919862
	Dead-box RNA binding protein 3 (DDX3)	1	3023628
	DKFZP434I116 protein isoform 1	2	10434568
	Unnamed	3	21750187

	La autoantigen	2	10835067
	Angiogenin 2 (RNase)	1	2500561
Translation	Ribosomal protein S3 / UV endonuclease	5	12848978
	Ribosomal protein P0	14	12654583
	Ribosomal protein L19	2	4506609
	Ribosomal protein L5	4	1173054
	Ribosomal protein P2	6	133061
	Ribosomal protein S7	4	134000
	Glutamyl-tRNA synthetase *	1	4758294
	Poly(A) binding protein * 2 (PABP2)	3, 5	12229876
	Poly(A) binding protein* 4 (PABP4)	5	4504715
	Glycyl-tRNA synthetase	2	21264523
	HsGCN1	1	2282576
	eIF 4G I	3	21634449
	eIF3-epsilon	2	4503519
	eEF 2	9	4503483
	eEF 1 alpha 1	14	4503471
	eEF 1B	2	119163
	Elongation factor Ts	2	12644268
	Mitochondrial ribosomal protein S27	2	13129094
Cytoskeleton	Kinesin heavy chain*	63	4758648
	Kinesin 2	27, 23	14250822
	Kinesin light chain 2	8, 2	10433849
	mitotic kinesin-like protein 1	3	20143967
	Dynein heavy chain	6	30581065
	Tubulin, alpha, beta	14, 4	multiple
	Vimentin*	28, 21	2119204
	Lamin A/C	56, 14	27436946
	Lamin B1	7	5031877
	Annexin A2	16	18645167
	Annexin I	4	4502101
	Talin 1	2	14916725
	Actin	10, 13	multiple
	Fascin 1	2	13623415
	E-cadherin binding protein E7	6	13376204
	Profilin 1	3	30584265
	Cofilin 1 *	1	5031635
Metabolism	Phosphofructokinase, platelet type	5	11321601
	Phosphofructokinase heart isoform*	17	11933149
	Fatty acid synthase	8	21618359
	Long-chain fatty acid coenzyme A ligase 4 (LACS4)	2	12669909
	Enoly CoA hydratase	2	12707570
	Glyceraldehyde-3-phosphate	12	31645

	dehydrogenase (GAPDH) *		
	creatine kinase	8	180570
	Lactate dehydrogenase (heart type)	11, 4	13786847
	Lactate dehydrogenase (muscle type)	7	13786849
	Sepiapterin reductase	2	3885362
	H^+-ATP synthase alpha subunit*	2	15030240
	H^+-ATP synthase beta subunit	3	114562
	Pyruvate kinase, M2 *	23	125604
	Adenosylhomocysteinase (AdoHcyase)	1	9951915
	Transketolase	5	14250367
	Aldolase	6	229674
	Enolase	20	30583767
	Pyridoxal kinase	1	13543317
	Triose phosphate isomerase	3	17389815
Chaperones	Chaperonin containing t complex (CCT) theta	12	1136741
	Chaperonin containing t complex (CCT) zeta	10	4502643
	Chaperonin containing t complex (CCT) eta	8	5453607
	Chaperonin containing t complex (CCT) beta	4	5453603
	Chaperonin containing t complex (CCT) gamma	3	2136253
	Chaperonin containing t complex (CCT) alpha	1	135538
	Chaperonin (HSP 60)	41, 3	306890
	Heat shock protein 70 kDa (BiP)	41, 42, 10, 3	16507237
	Heat shock protein 90 kDa alpha	5	123678
	Heat shock protein 90 kDa beta	29, 25	20149594
	heat shock 105kDa protein	2	42544159
	Heat shock protein 27 kDa	10	4504517
	Calreticulin	4	30583735
	Cyclophilin A	5	1633054
	Mitochondrial heat shock protein 75 (MTHSP75)	27, 21	292059
	DnaK-type chaperone	49	2119712
Nuclear transport	Importin 7	2	11544639
	Importin beta 1	11	20981701
	Importin beta 2	7	1613834
	Importin alpha re-exporter (Cellular apoptosis susceptibility protein)	3	20141403
Transcription	KRAB-associated protein KAP1	2	1699027
	Human capicua	3, 9	16507208
Sugar-binding	Homolog of bovine peptidoglycan	17	27808640

	recognition protein		
	Beta galactoside soluble lectin	4	227920
Unknown		42, 22, 36, 54, 68,	17225574
	LMO7 (Lim-domain only 7)	13	
	KIAA1429 (viriliser-related)	81, 9, 23	7243239
	Wilms tumor 1 associating protein 1 (WTAP)	22, 4, 3	21361159
	FLJ34154	2	21749840
	Unnamed	3	10434568
	Unnamed	26, 23, 48, 6	27477667
	KIAA1458	9	14722175
	KIAA0853	20, 3, 6, 3	31982941
	TRIM28	2	33873597
	sterol regulatory element binding protein 3	2	7705373
	trinucleotide repeat containing 15; Grb10 interacting GYF protein 2	8	42476299
	dJ469A13.1	3	14717080
	KIAA1458	7	14722175
	FLJ38426	2	27734703
	Unnamed	2	23468240
	KIAA0642	4	20521117
	Unnamed	8	21740322
	KIAA0731	4	3882183
	KIAA0456	2	25535897
	FLJ10211	4	37551910
	Valosin-containing protein (VCP), transitional ER ATPase	5	2984586
	FLJ38426	3	27734703
	CGI-99	4	7706322
	N8, long isoform	2	1488414
	Polyposis locus protein 1 – like 1	1	14198280
	Protein associated with myc, PAM	49	7662380
Vesicle trafficking / formation	Clathrin heavy chain*	63, 7, 13	4758648

(B) Interphase

Function	Matched protein	Matched unique peptides	GenBank accession number (gi)
Cell division	MCM3	1	6631095
	NUDE (nuclear distribution gene E homolog)	2	8923110
	Apoptosis stimulating of p53 protein 2 (ASPP2) / p53-binding protein 2 (53BP2)	1	16197705
Signalling - kinases	PI3 kinase C2 beta	2, 3, 6	13632400
	FRAP2 (MTOR2)	9	3282239
	C-TAK / Par1A*	3	3089349
	B-raf *	3	213599
	PCTAIRE 3	16	16160923
	DNA-PK, catalytic subunit	4	13606056
	PAK 4 (p21-activated kinase 4)	2	12585288
Signalling – small GTPase related	PDZ-containing GEF1	3	7657261
	ARHGEF16	8	30353993
	RhoGAP10	4, 3	20977541
	IQGAP1 (Ras GTPase-activating-like protein)	5	1170586
	Rap1GAP	2	106198
	Rho-interacting protein 3 (RIP3)	11, 3, 2	21740322
	Unnamed, similar to ADP-ribosylation factor-like 6 interacting protein 2)	3	10435296
	G protein coupled receptor 69A	21	5174445
	SRGAP1	2	31753111
	AF-6	3, 2	12644018
	Lbc (a GEF)	3, 3	15207794
	Rab GDP dissociation inhibitor	1	15290266
	ARL6-interacting protein	8	14424435
Signalling - misc.	liprin beta 1	14, 4, 3	3309539
	Tuberin / Tuberous sclerosis complex 2 (TSC2) *	6	3522922
	Insulin receptor substrate 2 (IRS2) *	7, 10, 13, 6, 2, 2, 3, 7, 6	14537854
	Proline-rich AKT substrate *	5	14150199
	Protein tyrosine phosphatase PTPH1*	1	131530
	Yes-associated protein (YAP)-like protein, 65 kDa	8, 12, 12	23398532
	A kinase anchoring protein (AKAP)	61	15986729

	BA416N2.2, FISH-like	2	10334638
	SH3 domain binding protein 4	1	7657562
Nucleolar proteins	NOLC1 (nucleolar phosphoprotein p130)	22, 15, 10, 4	434765
	Nucleolin / C23	16, 7	21750187
	Nucleophosmin / B23	6	10835063
Proteolysis/ ubiquitination	26S proteasome regulatory subunit	3	25777600
	Ki antigen, proteasome activator subunit 3	4	30410796
	Proteasome theta chain	2	22538465
	NEDD4-like ubiquitin ligase	9	21361472
	NAP1	2	4758754
	Deubiquitinating enzyme 8 (USP8)	3	731046
	TIP120	2	21361794
	Ubiquitin-activating enzyme E1	7	23510338
Stress or checkpoint responses	DNA damage-binding protein 1	3	12643730
	Hus1	8	4758576
	Thioredoxin	2, 3, 2, 3, 2, 6, 2	10120659
	Peroxiredoxin 1	10	4505591
Apoptosis	B-cell receptor-associated protein 31 (BAP31) / CDM protein	2	1705725
	BH3-only domain protein 3	1	21361979
Nucleotide metabolism	CAD trifunctional protein	3, 14, 30	18105007
	CTP synthase	2, 11	14495609
	UMP-CMP kinase	1	2497487
	NAD kinase	11, 5	12804579
Chromatin structure, DNA binding	Histone deacetylase 4 *	24, 5	5174481
	Histone deacetylase 5 *	2	30353988
	Histone deacetylase 7A *	15	13259522
	Histone acetyltransferase B subunit 2	2	3334209
	Y-box binding protein 1	9	181468
	mitochondrial ssDNA-binding protein	4	2624694
	DNA primase large subunit	1	510408
RNA binding	LRPPRC (leucine-rich PPR motif containing protein)	12	31621305
	hnRNP X	4	14141166
	hnRNP I	2	14165464
	hnRNP U	2	14044052
	Decapping protein Dcp1a	1	8923767
	Regulator of nonsense transcript stability	2	1575536
	Dead-box RNA binding protein (DDX) 9	2	13514822
Translation	Ribosomal protein L10a	8	22002029

	Ribosomal protein P0	9	12654583
	Splicing factor 3B, subunit 3	3	11034823
	Splicing coactivator Srm300	13, 4, 2	19923466
	Ribosomal protein S3 / UV endonuclease	15, 6	13097759
	Poly(A) binding protein 4 (PABP4)	8	4504715
	Poly(A) binding protein 2 (PABP2)	11, 27, 32	12229876
	Valyl tRNA synthetase	2	15215421
	Isoleucyl tRNA synthetase	2, 5	31873360
	Leucyl tRNA synthetase	8	24496789
	Alanyl tRNA synthetase	3	15079238
	Mitochondrial ribosomal protein S27	2	13129094
	HsGCN1	4, 3	20521848
	eIF 4E type 3	4	29839292
	eIF 3 theta	1	4503509
	eIF 4A	7	4503529
	eEF2	34	4503483
	eEF 1 alpha 1	10	4503471
	eEF 1 B	2	
Cytoskeleton	Kinesin heavy chain*	5, 8, 102	4758648
	Kinesin-like protein 5	3	20143967
	Kinesin 2	29, 16	14250822
	Kinesin light chain 2	33	13878553
	Kinesin light chain 3	4, 6	13878563
	Tubulin, alpha, beta	6, 8, 2, 11, 14, 4	multiple
	Dynein heavy chain	4	30581065
	Hornerin	1	28557150
	Filamin	2, 7	1203969
	Talin 1	2	14916725
	Vimentin*	52, 11, 8	2119204
	Annexin A2	13	16306978
	Annexin I	3	4502101
	Cofilin*	3	116850
	Profilin	3	30584265
	Cingulin	6	16262452
	Desmoyokin	7, 4	627367
	Desmoplakin I	3	2134996
	Ezrin	1	119717
	Spectrin alpha II	3, 4	1805280
	Spectrin beta 2	2	30315658
	Actin	24, 8, 21	multiple
	Vinculin	3, 1	4507877
	Alpha actinin 4	5	12025678
Metabolism	Phosphofructokinase heart isoform (PFK2) *	22, 3, 32	11933149
	Phosphoglucose isomerase	4, 3	14488680

	Phosphoglycerate mutase 1	5	130348
	Phosphoglycerate kinase 1	10	4505763
	Fatty acid synthase	2, 22	21618359
	Very long-chain acyl coA synthetase (VLCS)	1	4503653
	creatine kinase	8, 3	180570
	Glyceraldehyde-3-phosphate dehydrogenase (GAPDH)	16	31645
	Lactate dehydrogenase (heart type)	16	13786847
	Lactate dehydrogenase (muscle type)	8	13786849
	Pyruvate kinase M2-type *	4, 9, 8	125604
	Panthothenate kinase	1	27805667
	Panthothenate kinase 2	1	27805667
	Adenosylhomocysteinase, AdoHcyase	1	9951915
	Arginosuccinate synthase	2	16950633
	Adenylosuccinate synthase	1	1172749
	Cystathionase	1	345809
	Enolase	28	30583767
	Aldolase	8	229674
	Transketolase	12	14250367
	Triose phosphate isomerase	9	17389815
	Transferrin receptor	4	4507457
Chaperones	Chaperonin containing t complex (CCT) delta	19	2559008
	Chaperonin containing t complex (CCT) eta	15	5453607
	Chaperonin containing t complex (CCT) theta	3	1136741
	Chaperonin / HSP 60	9, 7	306890
	Calreticulin	4	30583735
	cyclophilin A	7	1633054
	Heat shock protein 70 kDa (BiP)	12	16507237
	Heat shock 70kDa 9B / mortalin	9, 8	12653415
	Heat shock 70kDa 8	40	27805925
	Heat shock protein 90 kDa alpha	6	123678
	Heat shock protein 27	6	19855073
	Protein disulphide isomerase (PDI)	2	2507460
	FK506 binding protein 4	1	12804069
	Heat shock protein A4	7	20547107
	heat shock 105kDa protein	2	42544159
	ER heat shock protein 90 (gp96)	7	15010550
	HSP 90 related	30	11277141
Nuclear transport	Importin 7	4, 3	11544639
	CRM1/exportin		
	Importin alpha 1	9	13543657

	Importin beta 2	3, 3, 5	1613834
	Importin alpha re-exporter (Cellular apoptosis susceptibility protein)	5	20141403
Transcription	NFAT2	1	1082855
	Human capicua	4	16507208
Sugar-binding	Homolog of bovine peptidoglycan recognition protein	16, 3	27808640
Unknown	LMO7 (Lim-domain only 7)	6, 13, 5, 6	17225574
	Wilms tumor 1 associating protein 1 (WTAP)	21	21361159
	cytoplasmic FMRP (fragile X mental retardation protein) interacting protein 1	13	24307969
	Valosin-containing protein (VCP), transitional ER ATPase	9	2984586
	S100A6 / calcyclin binding protein	4	7656952
	Copine 1	1	12231878
	SET	2, 2	21618461
	HSPC117	5	12652799
	KIAA0264	2	1665795
	Protein associated with myc, PAM	28	7662380
	Unnamed	33, 5, 9, 9, 11, 9	27477667
	TBC1 (Tre2, Bub2, CDC16) domain protein 4 (TBC4)	30, 9, 6, 3, 4, 53	7662198
	KIBRA	4, 4	24307969
	Retinoic acid induced 14	2	13470086
	Major vault protein (MVP)	1	19913412
	Neoplasm-related C140 product	1	546831
	Epithelial cell marker protein 1	8	631131
	Polyposis locus protein 1 – like 1	1	14198280
		53, 30, 3, 2, 24, 53,	3882183
	KIAA0731	7	
	KIAA0456	22, 3	25535897
	KIAA0747	7	14149680
	KIAA1401	2	7243183
	KIAA1720	5	12697985
	FLJ34154	2	21749840
	FLJ1128	6	10437164
	Unnamed	2	27469519
Vesicle trafficking / formation	Clathrin heavy chain*	7, 26	1705916
	Fer1-like protein 3	4, 7	10834587
	secretory carrier membrane protein 2	1	5730031

VITA

Sarah Elizabeth Myer

Candidate for the Degree of

Doctor of Philosophy

Thesis: DIFFERENTIAL GENE EXPRESSION OF MURINE BLASTOCYST STAGE EMBRYOS AND MURINE EMBRYONIC STEM CELLS

Major Field: Biomedical Sciences

Biographical:

Personal Data: Born in North Carolina, the daughter of G. Edward Lowder and Pamela A. Lowder. Married to Brian J. Myer. Mother of two daughters, Hannah E. Myer and Maggie S. Myer.

Education: Graduated from North Carolina School of Science and Mathematics, Durham, NC, in 1990; received Bachelor of Arts in Biology from Oral Roberts University, Tulsa, Oklahoma, in 1994; received Masters in Education from Oral Roberts University, Tulsa, Oklahoma, in 1995. Completed the requirements for the Doctor of Philosophy degree at Oklahoma State University Center for Health Sciences, Tulsa, Oklahoma in December 2007.

Experience: Instructor of Biology at Oral Roberts University, 1999-present. Instructor of 7th grade Life Science at Sapulpa Middle School, Oklahoma, 1995-1999.

Professional Memberships:
Oklahoma Academy of Science

Name: Sarah E. Myer Date of Degree: December, 2007

Institution: Oklahoma State University Location: Tulsa, Oklahoma

Title of Study: DIFFERENTIAL GENE EXPRESSION OF MURINE BLASTOCYST STAGE EMBRYOS AND MURINE EMBRYONIC STEM CELLS

Pages in Study: 148 Candidate for the Degree of Doctor of Philosophy

Major Field: Biomedical Sciences

Scope and Method of Study: Embryonic stem cells (ESC), derived from cultured blastocyst embryos, have the potential to provide insight into developmental and medical issues. The cellular transition, however, from blastocyst to ESC has not been well characterized. The purpose of this study was to identify transcriptional differences between blastocysts and ESC through use of suppression subtraction hybridization (SSH) in murine CD1 blastocyst and 129SvEv ESC. Comparisons between the following groups: blastocyst - blastocyst, trophectoderm - blastocyst, blastocyst - ESC, and ESC – fibroblast feeder cell, resulted in the cloning, sequencing, and identification of uniquely expressed sequences. The second objective was to compare expression levels of three selected transcripts through real time PCR in blastocysts, 129SvEv ESC, C57BL/6 ESC, and fibroblast feeder cells.

Findings and Conclusions: Using SSH, 33 unique clones were identified and 10 had strong ribosomal homologies while 23 had either gene specific homologies or else were unknown. Prdx1, Ywahz, and Vdacs3 were analyzed through real time PCR. For Prdx1, fibroblast feeder cells had the lowest expression level, blastocysts had a 4.81 fold increase, 129SvEv ESC had a 7.51 fold increase, and the C57BL/6 ESC showed a 27.28 fold increase. Expression levels were significantly different between the blastocyst and C57BL/6 samples as well as the fibroblast feeder cells and both ESC samples based on ΔC_T statistical analysis. For Ywhaz, the fibroblast feeder sample showed the lowest expression level, blastocysts had a 7.65 fold increase, 129SvEv ESC showed a 6.49 fold increase, and C57BL/6 ESC showed a 16.56 fold difference. The two ESC values were significantly different as was the fibroblast feeder cell value from all other samples. For Vdacs3, the blastocyst sample had the lowest level of expression, fibroblast feeder cells had a 2.16 fold difference, 129SvEv ESC had a 68.07 fold difference, and C57BL/6 ESC had a 161.04 fold difference. Statistically, the blastocyst sample was different from both of the ESC samples and the fibroblast sample from either ESC sample. Prdx1 and Vdacs3 both demonstrated significant upregulation in comparison between blastocyst stage embryos and ESC and function to enhance cell survival and continued cell reproduction.

ADVISER'S APPROVAL: Dr. Lee F. Rickords